THE ELECTRICAL PROPERTIES OF IRON RICH SILICATES

MASS. INST. OF TECHNOLOGY
FEB 23 1961
LIBRARY

by

DUANE CHRISTIAN UHRI

B. S., Michigan State University

(1953)

M. S., Michigan State University

(1954)

SUBMITTED IN PARTIAL FULFILLMENT

OF THE REQUIREMENTS FOR THE

DEGREE OF DOCTOR OF

PHILOSOPHY

at the

MASSACHUSETTS INSTITUTE OF TECHNOLOGY

February, 1961

Signature of Author .....
Department of Geology and Geophysics,
January 23, 1961

Certified by .....
Thesis Supervisor

Accepted by .....
Chairman, Departmental Committee
on Graduate Students

ABSTRACT

Title: The Electrical Properties of Iron Rich Silicates

Author: Duane Christian Uhri

Submitted to the Department of Geology and Geophysics on January 23, 1961 in partial fulfillment of the requirements for the degree of Doctor of Philosophy at Massachusetts Institute of Technology.

The electrical conductivities of a number of minerals (primarily garnets, but also enstatite, hypersthene, hornblende, olivine, and quartz) are measured in a controlled atmosphere as a function of the temperature. The design of the apparatus is applicable to the measurement of A.C. and D.C. conductivities at elevated temperatures and the atmosphere is efficiently regulated by a wustite buffer so as to prevent alteration of the iron contents of the specimens.

Although the majority of specimens measured exhibit a conductivity peak (as great as 3 orders of magnitude) or a suggestion of a peak in the plots of the logarithm of the conductivity versus the temperature, garnets are the only specimens investigated in detail. Experimentation with garnets indicates that conductivity curves obtained from heating and cooling measurements do not coincide, but a given set of curves may be reproduced exactly providing another sample from the same specimen is measured under identical conditions. The presence of an aqueous vapor phase tends to eliminate the electrical conductivity peak and suggests that the water vapor in the laboratory air may be responsible for the absence of the conductivity peak associated with a sample run in air. Oxidation of the sample appears to increase the overall conductivity. Therefore, a buffered atmosphere is an absolute necessity in measuring rock-forming minerals containing ferrous iron.

For those garnets run in a dry buffered atmosphere, a possible dependence of the electrical conductivity upon chemical composition is demonstrated. It appears that the lower temperature conductivities depend upon the concentrations of FeO and Fe_2O_3, the highest temperature conductivities upon "MgO" (CaO plus MgO as equibalent MgO), and the intermediate temperature conductivities possibly upon "MgO" and/or "MgO"/MnO.

Polarization and/or thermo-electric effects become predominant in the higher temperature regions for many of the minerals investigated, especially quartz and enstatite. However, as the iron contents of the minerals increase, these

effects become suppressed to the point of being unobservable. Corrections are attempted where polarization and thermoelectric effects occur and the accuracies of all the measurements are estimated to be within 10% of the actual values.

The majority of the curves obtained for log σ vs 1/T are quite different from those obtained by other investigators and this may be due to the following: 1) a dry silicate run in air produces no conductivity peak; 2) a dry silicate run in a dry buffered atmosphere yields a conductivity peak; and 3) a dry silicate run in an aqueous buffered atmosphere gives no conductivity peak.

If the conductivity peaks observed in this investigation occur in nature, they may possess considerable geophysical significance.

Until the presence or absence of a conductivity peak is verified for the minerals at depth, a maximum for the iron content in the upper portion of the mantle may not be determined from geomagnetic field observations or magnetotelluric sounding techniques.

Finally, on the basis of the magnitudes of the electrical parameters and the shapes of the curves for log σ vs 1/T, the following processes probably determine the electrical conductivity in the outer portion of the earth: 1) in the near surface region of the crust - ionic conductivity determined by abundant pore fluids; 2) in the lower portion of the crust - impurity and intrinsic semi-conduction; 3) in the basal portion of the crust or upper mantle - intrinsic semi-conduction and ionic conduction together (peak conductivity region); and 4) in the deeper mantle - intrinsic semi-conduction giving way to ionic conductivity with depth.

ACKNOWLEDGEMENTS

The author wishes to express his gratitude for the interest and counsel of Professor Harry Hughes during this investigation. Professor Hughes suggested this problem which resulted in many enjoyable discussions.

The advice of Professor W. H. Dennen and others of the Cabot Spectrographic Laboratory and of Professor W. H. Pinson and Mr. C. Schnetzler of the Geochemical Laboratory is gratefully acknowledged. The author wishes to express his appreciation also to Mrs. Barbara A. Uhri for her assistance in many of the chemical analyses.

During his graduate studies at M.I.T., the author was supported by a generous fellowship from the Magnolia Petroleum Company (Socony - Mobil Oil Company) and is indebted to this industrial organization for their sponsorship.

Finally, he gratefully acknowledges the efforts of Miss Delores Suter, who has performed all of the secretarial work in this thesis.

TABLE OF CONTENTS

TABLE OF CONTENTS (Continued)

TABLE OF CONTENTS (Continued)

TABLE OF CONTENTS (Continued)

TABLE OF TABLES

TABLE OF FIGURES

PART I

INTRODUCTION - In recent years, many of the investigations into the nature of the interior of the earth have been concerned, directly or indirectly, with the electrical conductivity of the earth's crust, mantle, and core. It is well known to geophysicists that the numerous laws of chemistry and physics defining the earth's internal constitution and behavior are inter-related in such a manner that a discussion of a particular phenomenon is difficult or even impossible without reference to other contemporary phenomena. Such is the case of the evaluation of the electrical conduction properties of the interior of the earth which requires a knowledge of the temperatures at depth, the chemical composition, data obtained from geomagnetic field observations, and laboratory measurements of pertinent compounds at high temperatures and pressures. Also, further theory is required to extrapolate the measurements to the temperatures and pressures within the earth. This extrapolation demands some knowledge of the conduction mechanism, which, in turn, requires further measurements for elucidation.

A detailed discussion of the preceding relationships would be rather voluminous and the reader is referred to Birch's (1952) work for one of the best discussions and an extensive bibliography.

Previous investigations by others have indicated that increasing the proportion of iron in a mineral specimen greatly increases the electrical conductivity. For example, the

curves of the logarithm of the conductivity as a function of the temperature of Coster (1948) show increasing conductivity for increasing iron content. However, as pertains to minerals containing ferrous iron, many measurements have been imprecise due to the reduction or further oxidation of the iron content as the sample is heated to elevated temperatures. Theoretically, this difficulty may be avoided in most instances by controlling the partial pressure of the oxygen in the vapor phase in the vicinity of the sample with a suitable buffer mixture. The first objective here, then, was to develop such a buffer mixture by a consideration of the oxidation-reduction phenomena associated with gas-solid equilibria of the sample and its vapor and, secondly, to design apparatus applicable to the measurement of the electrical conductivity in a controlled atmosphere at elevated temperatures.

Experimental difficulty has been encountered in the past due to polarization possibly arising from minor constituents or impurities in certain minerals. However, the high conductivity of iron-rich minerals tends to minimize this effect. Therefore, many of the mineral specimens selected for the measurement of electrical conductivity as a function of temperature in this investigation were iron-rich.

By comparing the measured conductivities of silicates of increasing iron content with the conductivity observed in the

the upper part of the earth's mantle, an upper limit to the iron content there should be determinable. The possibility of such application of the data is examined.

Finally, the results of the conductivity measurements are discussed in terms of solid-state physics in order to gain insight into probable conduction mechanisms in operation throughout the various temperature intervals.

REDUCTION-OXIDATION CONSIDERATIONS - Geologically, the most important elements in the crust are O, Si, Al, Fe, Ca, Na, K, and Mg since these constitute approximately 99% of the total composition and, in the earth as a whole, Fe, O, Si, Mg, Ni, Ca, and Al (Mason, 1952). In the majority of minerals formed from these, all of the elements exist in their highest oxidation states except for iron, which is either in the ferrous or ferric form, or both, Depending upon the partial pressure of the oxygen but not otherwise upon the chemical composition (or total pressure, if small) of the vapor phase, when a representative mineral containing ferrous iron is heated over a wide temperature range, the iron may be oxidized or reduced unless its relationship to the vapor is such that chemical stability exists over the entire temperature interval. If the ferrous-ferric ratio can be held constant in the sample throughout an experiment involving large temperature variations, chemical stability should exist for all components of the common igneous or metamorphic rock-forming minerals except except those containing Ni, Co, etc., in which case, oxides of these would be reduced.

Theoretically, this ratio can be controlled by buffering the system so as to give the proper partial pressure of oxygen versus temperature relationship. Considerable work has been done on the action of buffers and the criteria for stability of a number of minerals by Eugster (1957, 1959) and data for numerous metal-oxide systems have been compiled by Darken, Gurry, Muan, Richardson, Jeffes, Kelley, and others. Calculations utilizing these data and considerations of pertinent free energy relationships demonstrate that a buffer of wustite (FeO) composition will prevent alteration of ferrous silicates by regulating the partial pressure of the oxygen so as to maintain a chemical potential of insufficient magnitude to drive the related silicate reaction.

Since wustite does not exist below approximately 570° C, the buffer was prepared as a mixture of metallic iron and magnetite to produce an oxygen content equal to 23.26% by weight (see Darken and Gurry, 1953, Fig. 14-5). It should be mentioned here that stoichiometric FeO is thermodynamically unstable at all temperatures and that the maximum iron content corresponds to $Fe_{0.953}O$ (Darken and Gurry, 1946). Finally, further calculations demonstrate that 0.2 gm of buffer mixture is sufficient to control the vapor in a system with dimensions comparable to those of the apparatus in this investigation.

INSTRUMENTATION - Two experimental arrangements were employed in this investigation. Apparatus I provided only D.C. measurements while Apparatus II allowed both A.C. and D.C. measurements and minimized a few of the disadvantages and probable sources of error inherent in Apparatus I. Of considerable concern was the condensation of water vapor in Apparatus I during the measurement procedure.

The overall arrangements for Apparatus I and Apparatus II are illustrated in Figure 1 (Figure III-1 in Part II) and the furnace for Apparatus II in Figure 2 (Figure III-5 in Part II). The furnace winding consists of 23 feet of 0.01 inch platinum wire wound externally and non-inductively on a cylindrical alundum core with inside and outside diameters of 7/8 and 1 1/8 inches respectively and a length of 8 1/2 inches. The heater core is enclosed by a concentric alundum cylinder with inside and outside diameters of 1 3/8 and 1 3/4 inches respectively. Both tubes lie along the axis of a 6 inch diameter steel tube and the space between is filled with high temperature insulation material. The steel cylinder (1) is capped at both ends with 3/8 inch thick "Transite" discs (2) and brass rods (3) hold these in position. The stand (9) for the furnace also supports 2 clamps (8) which stabilize a recrystallized alumina tube (4). This impervious high-vacuum tube of interlocking corundum crystals passes through the center of the furnace and is sealed at both ends with universal compression seals (5). A combination of glass T's, rubber tubing, and clamps permit thermocouple entries (7) and gas flow (6).

The sample holder in the furnace tube is constructed of high temperature ceramic tubes and tool steel stabilizers (the stabilizers do not experience temperatures greater than approximately 150° C when the center of the furnace is about 1200° C). Set screws in the steel stabilizers hold the ceramic tubes in position. Thermocouple rods, pushed together by a spring arrangement, position the sample and allow for expansions and contractions of the sample and equipment during the temperature cycle. A platinum buffer container is supported by one of the thermocouple rods and is located approximately 1/2 cm from the end of the sample.

PROCEDURE - After numerous mineral specimens (primarily garnets, but also enstatite, hypersthene, olivine, quartz, and hornblende) were collected, 2 or 3 cores were extracted from each with the aid of a diamond core drill. The cores obtained had diameters on the order of 0.115 inch, varied in length, and were squared at the ends with a diamond saw. After the diameters and lengths of the cores were measured and prior to being installed in the furnace, each sample was coated on the end faces with a platinum paste (#758) made by Johnson-Matthey & Company of London, England. Considerable care was taken in the application of this paste to completely coat the ends of the sample and only these faces. At relatively low temperatures, the volatile component is driven off, leaving behind a thin film of platinum bonded to the surface of the sample and to the thermocouples, thereby insuring good electrical contacts.

Each of the samples was then placed into the furnace and the furnace was partially sealed. After flushing the furnace tube with argon gas for approximately 10 minutes, the system was sealed completely for the measurements of the electrical properties as a function of the temperature.

Utilizing a 1.5 volt battery, D.C. values were obtained for currents through the sample in the forward and reverse directions. 1.5 volt r.m.s. A.C. measurements were also made in order to observe the effects of polarization and thermo-electric processes on the conductivity.

CHEMICAL ANALYSES - Chemical analyses of the minerals to be measured were accomplished by following the procedure of Shapiro and Brannock (1956) for the "rapid analysis of silicate rocks". Using this technique, FeO, total iron as Fe_2O_3, MnO, and CaO plus MgO as equivalent MgO were determined for many of the samples. The two silicates, G-1 and W-1 (see Fairbairn, 1951) were run along with the samples as a check on the technique of the analyst and the accuracy of the results.

GARNET MEASUREMENTS - Since one of the goals of this investigation is to obtain data applicable to the study of the earth's interior, the choice of garnets for study is evident. These, with pyroxenes in eclogite, may well be the principal constituents of the upper mantle [Turner and Verhoogen (1951); Lovering (1957, 1958)] and, furthermore, extremely little has been published on their electrical behavior.

Garnets were chosen on the basis of color and specific gravity to give a range of values for the iron contents. After the specimens were examined macroscopically for twinning, fractures, homogeneity, and massiveness or crystallinity, the electrical conductivities were obtained for the specimens at temperatures up to their melting points and under various conditions (see Table 1). Typical conductivity data are illustrated by plots of the logarithm of the conductivity versus the reciprocal absolute temperature in Figures 3 through 15 (Figures A-20, A-21, A-18, A-19, A-11 through A-17, A-24, and A-25 respectively in Part II) ($\sigma = [\text{ohm-cm}]^{-1}$).

Inspection of these graphs and the corresponding compositions of the various garnets shows that similar compositions result in similar conductivity plots, providing that the measurements were carried out under the same conditions. All garnets measured in an atmosphere controlled by the wustite buffer in Apparatus II exhibit an electrical discontinuity at approximately 570° C (this is represented by a line on the graphs at $[1/T] \times 10^3 = 1.186$) and a conductivity peak or a suggestion of a conductivity peak at approximately 800° C. The values of the conductivities decrease for a short range of temperatures after the conductivity peak temperature, then increase, apparently asymptotic to a line determined by extremely large values for σ_o and E for the conductivity σ given by $\sigma = \sigma_o \exp[-E/kT]$ where σ_o is a constant and E is the excitation energy required to place a charge carrier into a mobile state. The cooling curves in each

case tend to be straight lines as well as the heating curves in the region below 570° C. Upon reheating, both the heating and cooling curves coincide and correspond rather closely to the initial cooling curve providing the maximum temperature of the initial run has not been exceeded.

As parameters of value in the interpretation of the data, the following quantities have been extracted from the graphs: 1) the excitation energy E and the constant σ_o as determined from the slopes and intercepts of the straight line segments; 2) the peak conductivities of certain curved portions and the associated temperatures; and 3) the differences in conductivity values as determined by passing current through the sample in the forward and reverse directions (see Table 2).

It was noted that there was considerable condensation of water upon termination of the measurements in Apparatus I. In order to investigate the effect of water vapor in the system on the values obtained for the electrical conductivities, a sample from garnet #106 was prepared and placed into the furnace of Apparatus II as in previous measurements, but, in this case, the buffer was saturated with water and approximately 2 ml of water was introduced into the ends of the gas-tight tube. The tube was partially sealed, flushed with argon gas for 10 minutes, and then completely sealed for conductivity measurements. Due to failure of the furnace coil at the maximum temperatures in this run, a second sample was

measured in order to determine the nature of the cooling curve. The results of these runs are plotted in Figures 3 and 4 (Figures A-20 and A-21 in Part II). It is to be noted that the aqueous runs give almost identical curves and that the conductivity in the peak area is less by approximately one order of magnitude than that of the normal run in Figure 5 (Figure A-18 in Part II). Aqueous run #2 agrees well with the normal run in the temperature region above the peak area but does not show the same separation of points at a given temperature. Therefore, water vapor reduces the conductivity in the conductivity peak region and prevents the separation of points (from measurements in the forward and reverse directions) in the high temperature region. Furthermore, there is little difference between the initial slopes of the dry and aqueous runs in the region below 570° C, illustrating that an aqueous vapor has little effect in this region.

A large sample from garnet #106 and approximately 0.2 gm of buffer mixture were placed into the furnace, which was then flushed with argon gas for 15 minutes. The furnace tube was sealed and heated to 800° C in 1.3 hours. The temperature was maintained between 800° and 826° C for 5 hours, whereupon, it was gradually decreased, the entire heating and cooling process requiring about 8 hours. Subsequent wet-chemical analyses demonstrated the ferrous iron content to be very close to those values obtained originally for garnet #106, thereby confirming the fact that the buffer is efficient in preventing significant oxidation or reduction of the ferrous

iron content in this garnet for periods of time of at least 8 hours (the approximate length of time required for a run) at elevated temperatures.

An initial run and a rerun, under conditions of a buffered atmosphere, were made on garnet #104 (see Figures 7 through 9)(Figures A-11 through A-13 in Part II). Following these, a third run was made with air passing through the furnace at a rate of approximately 100 cc per minute (see Figures 10 and 11)(Figures A-14 and A-15 in Part II). The most striking difference between these curves is the increase in the conductivity upon cooling for the oxidized sample. Furthermore, the conductivity as a whole for both heating and cooling curves is greater when the specimen is run in air. Therefore, we see that a buffered atmosphere is an absolute necessity in measuring conductivities of rock-forming minerals containing ferrous iron.

For all the garnet specimens as a group which were run in an atmosphere buffered with wustite in Apparatus II, the slopes of the initial heating curves in the region below 570° C do not appear to depend on the abundance of any particular element that was considered in the chemical analyses (e.g.- there are no trends in the magnitudes of the excitation energies (E) or the constants (σ_o) with the percent by weight of ferrous iron oxide). However, with the exception of garnet #112, the magnitudes of the excitation energies suggest that the ratio of total iron as ferric oxide to ferrous oxide may be important since these increase with this ratio. In this

case, the comparison of the garnet specimens should probably be made only on the basis of those garnets with similar physical properties (#103 through #107) since we do not know the effects of twinning, the degree of crystallinity, and other differences noted in the macroscopic examination of the specimens. Using these specimens only, E and σ_o increase with increasing FeO and Fe_2O_3 (actual) contents respectively. Other chemical oxides or ratios show no trends. The other temperature regions were examined in an analogous manner and it appears that the lower temperature conductivities depend upon the concentrations of FeO and Fe_2O_3 (actual), the highest temperature conductivities upon the "MgO" (equivalent MgO) content, and the intermediate temperature conductivities possibly upon "MgO" and/or "MgO"/MnO.

ENSTATITE-HYPERSTHENE MEASUREMENTS - Since enstatite and hypersthene may be representative of portions of the earth's mantle, the electrical conductivities of these minerals were measured. The pyroxenes, enstatite and hypersthene, are part of a continuous isomorphous series, which has the general formula: $(Mg,Fe)_2(SiO_3)_2$; those specimens containing less than 15% FeO are termed enstatite and those with a greater concentration, hypersthene (Dana, 1951). The enstatite specimen used in this investigation was cored from a lamellar, homogeneous mass and the hypersthene specimen from a homogeneous, cleavable aggregate. Data pertinent to the measurement of these specimens may be examined in Tables 1 and 2.

The curve for enstatite in Figure 16 (Figure A-39 in Part II) demonstrates a shape similar to the majority of minerals measured in this investigation. Polarization is considerable to extreme in the temperature region above 570° C and "corrections" made for this effect result in the solid black points as being comparable with the A.C. conductivity. The vertical line at the left side of Figure 16 is located at 1140° C, the temperature for the transition of enstatite to clino-enstatite. On the basis of the magnitudes of the parameters in Table 2, it appears that it is in this temperature region that the conductivity changes from intrinsic semiconduction to predominantly ionic conduction. The small circles represent points of the cooling curve and demonstrate that the heating and cooling curves do not coincide.

The conductivity plot for hypersthene in Figure 17 (Figure A-40 in Part II) possesses the same general shape as that for enstatite and yields comparable values for the excitation energies, but this is where the similarity ends. The most striking difference is the absence of polarization in the hypersthene measurements. Although not as obvious, another important factor is the overall increase in conductivity by approximately one order of magnitude.

HORNBLENDE MEASUREMENTS - When it became evident that water vapor in the furnace system affects the values of the conductivities in the intermediate temperature region, it was decided that hornblende conductivity measurements might help to determine more facts concerning this effect. This assumption

was made not only due to the fact that hornblende contains an $(OH)^-$ radical, but also due to the possibility of excess water having been trapped in the interstices of the crystal at the time of formation.

Since the D.C. equipment was not designed to handle such large conductivities as were observed here, only A.C. measurements are illustrated. In the lower temperature regions where D.C. conductivity measurements were possible, polarization was not evident. This specimen exhibits a conductivity plot (see Figure 18 [Figure A-42 in Part II]) unlike the majority of specimens in that a straight line may be passed through all of the low temperature points on the graph on into the temperature region of the conductivity peak illustrated by other curves. It is difficult to state with certainty whether or not a conductivity peak occurs here since the conductivity decreases with extreme rapidity on the high temperature side of this region. Upon completion of the run, it was observed that the sample had decreased in length and bulged slightly at the sides, thereby indicating that partial melting had taken place. It should be mentioned here that well-bonded electrode contacts were maintained throughout the run.

OLIVINE MEASUREMENTS - The possibility that olivine $[(Mg,Fe)_2SiO_4]$ may be a major constituent of the earth's mantle is generally agreed upon by most geophysicists and it is because of this that a number of investigations into the electrical properties of members of the olivine series have been

carried on in the past (see Hughes [1953, 1955], Balchan and Drickamer [1959], and Runcorn and Tozer [1955]). In many of these measurement sequences, there existed the possibility of alteration of the ferrous iron content in the specimen. Therefore, it seemed worthwhile to determine whether or not the data obtained previously would correspond to measurements performed in a buffered atmosphere.

Although a number of samples of dunite (in this case polycrystalline aggregates containing approximately 90% olivine) were cored, analyzed, and measured as in the previous sections, the conductivity data for #Gf 1 (Figures 19 and 20 [Figures A-36 and A-37 in Part II]) are, perhaps, the only data indicative of the conduction properties of dunites here for comparison purposes since this is the only dunite specimen that was measured in approximately the same manner as the other specimens. (This sample was measured in a vapor controlled by a wustite buffer, but in Apparatus I, and it is not known how efficiently this system operated.)

The initial heating curve for dunite #Gf 1 exhibits a conductivity peak similar to those of the other minerals measured in this investigation and a suggestion of a second conductivity peak. The rerun reproduces the high temperature results well with little polarization, but the separation of points is extreme at lower temperatures.

QUARTZ - Since SiO_2 is a constituent of many eclogites, the electrical conductivity of a specimen cored from a single quartz crystal was measured in a controlled atmosphere in

order that the experimental conditions would be similar to those in the preceding sections. The specimen was prepared in the same manner, but no chemical analyses were performed. The α and β quartz regions [regions (a) and (b) in Figure 21 (Figure A-41 in Part II)] demonstrate that polarization is all but absent and that the conductivity peak is as predominant as in many of the garnet curves. The tridymite region (c) is characterized by extreme polarization and a change in the conduction mechanism. On the basis of the "corrected" points, it appears that the highest temperature measurements may be located in another conductivity peak area. The cooling curve exhibits even greater polarization and the corrected values correspond rather well to the heating curve values in region (c). Upon termination of the run, it was observed that the specimen had not changed its appearance whatsoever.

DISCUSSION - Reproducibility of Measurements - In every specimen measured, there existed a distinct difference between the initial heating curve and the subsequent cooling curve, this difference being rather pronounced in the majority of runs. However, the two samples from garnet #106, which were measured in aqueous vapors, demonstrate that, although the cooling curve differs from the initial heating curve for a particular sample, both of these curves may be reproduced by measuring another sample from the same specimen under similar conditions. The values of the excitation energies for the two cases are observed to be in good

agreement. Furthermore, considerable extrapolation is necessary in order to determine the values of σ_o , a slight variation in the slope of the line resulting in a significant effect on the magnitude of σ_o . Therefore, it appears that the reproducibility of the measurement technique employed in this investigation is very satisfactory.

Differences between Initial Heating and Cooling Curves - For the minerals investigated, correspondence between the initial heating and cooling curves for a given sample should not be expected for at least two reasons: 1) the "freezing-in" of defects at elevated temperatures during cooling and 2) the separation of grain boundaries upon cooling during an experimental run.

Solid state theory suggests that conductivity in such crystals is due to the presence of lattice defects (i.e.-atomic displacements or irregularities involving an increase in internal energy, say E per defect, but a decrease in free energy because of the increased entropy). The equilibrium number of defects, and thus the conductivity, increases rapidly with the temperature as exp(-E/kT). Between the displaced atom and its regular position there will be an energy barrier, of magnitude say U, and if the temperature is reduced rapidly enough, the defect may be "frozen in". Quantitatively, this occurs when:

$$\nu \exp(-U/kT) << 1/t$$

where: ν is the frequency of atomic vibration

exp(-U/kT) represents the probability of the atom having sufficient energy to overcome the energy barrier

t is the time scale of the experiment

The rate of cooling in the experiment being many orders of magnitude higher than in nature, many more "frozen-in" defects may be present upon cooling than in the initial heating and the associated conductivity may be correspondingly higher.

The freezing-in of defects, like any other change in the conductivity mechanism, should be revealed by a kink in the log σ vs. 1/T curve. At low temperatures, the conductivity is proportional to:

$$n_o \exp(-E'/kT)$$

where n_o is the number of defects (fixed by the freezing-in in excess of the equilibrium number and independent of the temperature at low temperatures) and E' is some excitation energy. At higher temperatures, the conductivity is dependent upon:

$$n \exp(-E'/kT) = N \exp(-E/kT)\exp(-E'/kT)$$
$$= N \exp(-[E + E']/kT)$$

where: $n = N \exp(-E/kT)$ - the equilibrium number of defects

N - the number of atoms capabable of displacement

$\exp(-E/kT)$ - the probability of a displacement

In addition to the freezing-in of defects, we must also consider the effect of grain boundary separation. Separation of grain boundaries during heating and cooling, should, at first sight, reduce the conductivity by severing conduction paths. However, new surfaces may be created (e.g.-by the

spreading apart of internal fractures) and this may lead to an increasing conductivity from surface defects or along surface paths.

Therefore, in view of the above discussion, it is not to be expected that the heating and cooling curves will coincide.

Polarization and Thermo-electric Effects - In order to check for possible polarization, Coster (1948), employing D.C. techniques, measured the current, first in one direction, then in the reverse direction. He found that, in most cases, the measurements coincided, demonstrating that polarization was negligible. This process was followed in the present investigation and, in addition, thermo-electric effects were sought by allowing the sample itself to drive current through a galvanometer possessing high sensitivity. Furthermore, A.C. measurements were made at 30 c.p.s. and it was observed that the A.C. and D.C. measurements coincided in those temperature regions where the D.C. measurements indicated no polarization.

In certain instances, the D.C. points for a given temperature were so different that, in order to use the data, some form of polarization and/or thermo-electric correction had to be made. It was noted that, in most instances, the voltage produced by the sample itself was different before the measurement was performed than after and that it exhibited no signs of decay. This value was subtracted or added to the value for the sample, depending upon the direction of the current through the sample and whether this "correction" was

obtained before or after the measurement sequence. The "corrected" values coincided fairly well with each other and with the A.C. measurements. Therefore, the "corrected" values are indicative of the A.C. conductivity, the separation of the D.C. points representing the degree of polarization and thermoelectric effect. Then the A.C. and D.C. conductivities are represented by the same curve when all points coincide and, in the temperature regions where this is not true, there are three values for the conductivity: 1) the D.C. conductivity in the forward direction; 2) the D.C. conductivity in the reverse direction; and 3) the A.C. conductivity. The A.C. conductivity exhibited little frequency effect and, as was expected, the higher temperature regions demonstrated the greatest separation of D.C. values. Although, for the earth with its sinusoidal electrical variations, it is the A.C. conductivity that should be considered as representative of the actual electrical conductivity, D.C. values are applicable in many instances (e.g.-those temperature regions where A.C. and D.C. values coincide).

Sources of Error and Accuracy of Results - There are many sources of error inherent in this type of investigation and may be attributed to displacement currents or frequency effects, polarization, electrode phenomena and the associated voltage distribution across the sample, sensitivity limits of the meters utilized in the actual measurement circuit as well as those used to determine the values of circuit components, the accuracy of the measurements of the dimensions

of the specimens, contact and lead resistances, the accuracy of the graphical calibration curves for the A.C. measurements, etc.

Calculations demonstrate negligible displacement current for 30 c.p.s. A.C. measurements and no frequency dependence was observed as the frequency was varied from 30 to 300 to 3000 c.p.s. Polarization effects may be essentially "corrected" according to the procedure in the preceding section. The error introduced by the sensitivity limits of the meters, measurements of sample dimensions, etc. may be determined by the differential approach to error analysis. However, electrode phenomena and the associated voltage distribution across the sample may introduce greater uncertainty into the results than all other sources of error combined.

The voltage distribution across the sample was not considered in this investigation, but Cronemeyer (1952) made measurements of this for single crystals of rutile by placing probes at appropriate intervals across the specimen. He found that the field is markedly distorted near the electrodes so that the net field in the central portion of the crystal is appreciably smaller than the applied field strength. He shows further that the true conductivity may then be considerably different from the overall conductivity (by as much as 1 order of magnitude). This is in accordance with the theory concerning metal-semiconductor contacts as in Spenke (1958).

Therefore, without data pertaining to this phenomenon in the present investigation, the values obtained for the electrical conductivity data are estimated to be within approximately 10% of the actual values.

Comparison with Other Investigations - The majority of curves for the conductvitiy as a function of the temperature are quite different from those obtained by other investigators, however, Hughes (1953), Coster(1948), Cronemeyer (1952), and others observed a distinct difference between the heating and cooling curves, a phenomenon noted in this investigation and discussed above. Aside from this, Cronemeyer is the only one to illustrate a suggestion of a conductivity peak; all others found that the conductivity could be represented rather well by $\sigma = \sigma_1 \exp(-E_1/kT) + \sigma_2 \exp(-E_2/kT)$ for any particular temperature. The conductivity peak is the most striking difference between the present and previous investigations and, without a predominant conductivity peak, all the curves are quite similar in shape. The present research differs from the others in that the sample was not in contact with the laboratory atmosphere but utilized a buffer in a sealed system to control the partial pressure of the oxygen. Calculations demonstrated that the buffer was efficient in controlling the partial pressure of the oxygen so as to prevent alteration of the sample and wet-chemical analysis reinforced this argument.

If we generalize the data from this investigation, the facts are: 1) a dry silicate (i.e.-one containing no H_2O or

$[OH]^-$) run in air produces no conductivity peak; 2) a dry silicate run in a dry atmosphere buffered with wustite yields a conductivity peak; and 3) a dry silicate run in an aqueous buffered atmosphere gives no conductivity peak. One might expect, then, that a mineral containing H_2O or $(OH)^-$ and run in a dry buffered atmosphere would produce no conductivity peak, that the same mineral run in air would demonstrate a conductivity peak, and that the same mineral run in an aqueous buffered atmosphere would give a peak. It was pointed out that the curve for hornblende, measured in a dry buffered atmosphere, was a straight line and that the maximum temperature attained exceeded that of the melting point of the specimen.

It appears, then, that the presence of water vapor in the mineral or in the atmosphere surrounding it will greatly influence the shape of the log σ vs. 1/T curve and that dry silicates will not exhibit a conductivity peak if water vapor is present. Furthermore, it may be that the water content of the air in the laboratory is sufficient to eliminate the peak in the case of dry silicates.

The Electrical Conductivity of the Earth's Crust and Upper Mantle - The electrical conductivity of the upper portion of the earth's mantle may be estimated by analysis of transient variations in the geomagnetic field. Lahiri and Price (1939) employed this approach to obtain the electrical conductivity as a function of depth and suggest probable values for depths as great as 800 km. Some uncertainty in the shielding effect

of the oceans results in a corresponding uncertainty in the actual conductivity versus depth distribution. Furthermore, although several distributions are compatible with the observed geomagnetic variations, each curve demonstrates that the conductivity increases rapidly in the outer portion of the earth. Lahiri and Price conclude then that their interpretation has greater validity at depth than in the near surface region and, as Rikitake (1951), that the electrical conductivity rises sharply in the upper few kilometers of the earth.

More detailed information pertaining to the near surface region has been acquired by Cantwell (1960). Magneto-telluric sounding techniques were utilized in order to determine the electrical conductivity at depths on the order of 70 km. Cantwell states that, due to the measurement technique and the method of interpretation, this value may be stretched to 100 km. A discontinuity at these depths demonstrates an abrupt shift in conductivity from $1.25 \times 10^{-6}[\text{ohm-cm}]^{-1}$ to greater than $1.25 \times 10^{-4}[\text{ohm-cm}]^{-1}$ (the equipment will not permit a distinction between the latter value and infinite conductivity), a shift of at least 2 orders of magnitude.

Therefore, on the basis of the above and the data for near surface rocks, the electrical conductivity distribution in the outer portions of the earth may be represented by the following: 1) a shallow zone at the surface where the conductivity is predominantly ionic in nature and dependent upon intersticial connate water overlying 2) a zone exhibiting

conductivities on the order of $1.25 \times 10^{-6}[\text{ohm-cm}]^{-1}$ and extending to depths in the tens of kilometers (probably 30 to 70 km) where 3) an abrupt change demonstrates an electrical discontinuity of approximately 2 orders of magnitude to the vicinity of $1.25 \times 10^{-4}[\text{ohm-cm}]^{-1}$ or less.

Employing the data obtained from the measurements in this investigation in a similar manner to others (i.e.-assuming various temperature distributions and plotting the electrical conductivity as a function of depth), it may be shown that the conductivity peak areas in the curves of log σ vs. $1/T$ are of extreme importance in determining the conductivity distribution. At present, there are no laws or data which prohibit the occurrence of environmental conditions similar to the conditions under which the specimens were measured (except for the effect of pressure and possible surface effects introduced through coring the specimens). Therefore, it is conceivable that the partial pressure of the oxygen at depth may be comparable to a vapor pressure regulated by a wustite buffer. The plausibility of this is suggested by the occurrence of both ferrous and ferric iron in many rocks of deep-seated origin (e.g.-in garnets associated with eclogites). Furthermore, as pertains to the measurements in an aqueous buffered atmosphere, these conditions may be duplicated in the upper regions of the earth, beginning where insufficient water is present for ionic conductivity to predominate and penetrating to those depths where the water content is either essentially "squeezed out" due to the pressure

or excluded from the materials at depth as they undergo a phase transformation to higher pressure modifications.

Since the majority of minerals in this investigation exhibited a conductivity peak (even the transparent single crystal of quartz), the importance of this phenomenon is of a general nature rather than being confined to a specific mineral. In many instances, garnets demonstrated conductivity peaks of various magnitudes even though the chemical compositions were quite similar. Let us suppose that the curve for garnet #109 is representative of the conductivity of the minerals at depth, where the depth is such that essentially no water is present. In addition, let us assume a two layer model for the outer portion of the earth: one layer containing silicates in the presence of an aqueous buffered atmosphere; the other containing silicates in a dry buffered atmosphere. It is then possible to demonstrate conductivity discontinuities of various orders of magnitude and at a number of depths by assuming various temperature distributions and shifting from aqueous data curves to dry silicate curves.

It may be shown, then, that Cantwell's (1960) 70 km electrical discontinuity may or may not correspond to the Moho discontinuity, depending upon the temperatures with depth.

Therefore, if the conductivity peaks observed in this investigation occur in nature, they possess considerable geophysical significance.

A Maximum for the Iron Content in the Upper Mantle - It was mentioned earlier that a comparison of the measured

conductivities of increasing iron content with the conductivity observed in the upper part of the earth's mantle should result in an upper limit for the iron concentration. But, we have seen in the preceding section that, due to peaks in the conductivity curves, the conductivity in this region is not dependent upon the iron concentration even though the overall conductivity curve demonstrates higher values for greater iron concentrations. Therefore, until the presence or absence of a conductivity peak is verified for the minerals at depth, a maximum for the iron content in the upper portion of the mantle may not be determined from electrical conductivity data obtained from geomagnetic field observations or magneto-telluric sounding techniques.

Conductivity Mechanisms in the Upper Mantle - At present, there exists a fair amount of disagreement as to the exact mechanism of electrical conduction in the interior of the earth. Hughes (1959) attributes the conductivity of the mantle to ionic processes while Clark (1957) and Runcorn and Tozer (1955) suggest that intrinsic semi-conduction is the predominant mechanism. Coster (1948) found that the electrical conductivity of most rocks could be represented by two sets of parameters, one with an activation energy of about 0.7 ev, and the other, appearing at higher temperatures, with an activation energy on the order of 2 ev, where the associated constants in the conduction equation were 10^{-1} to 10^{-4} and approximately 10^{5} respectively. He suggests that the first set of parameters may be indicative of

impurity electronic semi-conduction. Hughes (1953) has associated σ_o - 10^{-4}- 10^{-6}[ohm-cm]$^{-1}$ and E - 0.5 - 1.0 ev with impurity semi-conduction, σ_o - 5 x 10^{1}- 10^{-1}[ohm-cm]$^{-1}$ and E - 2.0 - 3.0 ev with intrinsic semi-conduction, and σ_o - 10^{4}- 10^{10}[ohm-cm]$^{-1}$ and E - 2.8 - 4.0 with ionic conduction. In his work with crystals of TiO_2, Cronemeyer (1952) obtained the values σ_o - 2.76 x 10^{3} to 8.38 x 10^{4}[ohm-cm]$^{-1}$ and E - 3.05 - 3.67 ev and places these under the heading of electronic semi-conduction since passing current through the sample for appreciable lengths of time had no apparent destructive effect on the electrical properties of the crystal.

The magnitudes of the parameters obtained for the garnets measured in this investigation suggest that electronic semi-conduction predominates up to temperatures just below the melting point. Therefore, for an eclogitic upper mantle say, ionic conductivity will not become important as the major conduction mechanism until the temperatures at depth approach those of the melting point curve. However, the slopes of the curves in the conductivity peak region indicate that, upon initial heating, ionic conduction is also in operation for a small temperature range.

The question arises at this point, should the heating or cooling curves be taken as representative of the electrical conductivity in the earth? Possible reasons for differences in the heating and cooling curves in terms of "freezing-in" of defects were discussed above. If a phase change is in operation at the Moho, then one might expect that freezing-in

of defects might play an important part in the overall conductivity, depending upon whether the phase boundary is rising or falling. However, since this process occurs in geologic time, such considerations should be of little concern and the heating curves should be taken as representative of the actual electrical conductivity.

Therefore, for the outer portion of the earth, the following processes probably determine the electrical conductivity: 1) in the near surface region of the crust - ionic conductivity determined by abundant pore fluids; 2) in the lower portion of the crust - impurity and intrinsic semi-conduction; 3) in the basal portion of the crust or upper mantle - intrinsic semi-conduction and ionic conduction together (peak conductivity region); and 4) in the deeper mantle - intrinsic semi-conduction giving way to ionic conductivity with depth.

CONCLUSIONS - The design of Apparatus II is applicable to the measurement of A.C. and D.C. conductivities in a controlled atmosphere at elevated temperatures and, as was demonstrated on both a theoretical and chemical analysis basis, the atmosphere may be controlled efficiently by a wustite buffer.

Although the majority of specimens measured exhibited an electrical conductivity peak or a suggestion of a peak, garnets were the only specimens investigated in detail. Experimentation with garnets indicates that conductivity curves obtained from heating and cooling measurements do not coincide, but a given set of curves may be reproduced exactly providing another sample from the same specimen is measured

under identical conditions. The presence of an aqueous vapor phase tends to eliminate the electrical conductivity peak and suggests that the water vapor in the laboratory air may be responsible for the absence of the conductivity peak associated with a sample run in air. Oxidation of the sample appears to increase the overall conductivity. Therefore, a buffered atmosphere is an absolute necessity in measuring rock-forming minerals containing ferrous iron.

For those garnets run in a dry buffered atmosphere, a possible dependence of the electrical conductivity upon chemical composition is demonstrated. It appears that the lower temperature conductivities depend upon the concentrations of FeO and Fe_2O_3, the highest temperature conductivities upon "MgO" (CaO plus MgO as equivalent MgO), and the intermediate temperature conductivities possibly upon "MgO" and/or "MgO"/MnO.

Polarization and/or thermo-electric effects become predominant in the higher temperature regions for many of the minerals investigated, especially quartz and enstatite. However, as the iron contents of the minerals increase, these effects become suppressed to the point of being unobservable. Corrections were attempted where polarization and thermo-electric effects occurred and the accuracies of all the measurements are estimated to be within 10% of the actual values.

The majority of the curves obtained for log σ vs 1/T

are quite different from those obtained by other investigators and this may be due to the following: 1) a dry silicate run in air produces no conductivity peak; 2) a dry silicate run in a dry buffered atmosphere yields a conductivity peak; and 3) a dry silicate run in an aqueous buffered atmosphere gives no conductivity peak.

If the conductivity peaks observed in this investigation occur in nature, they may possess considerable geophysical significance .

Until the presence or absence of a conductivity peak is verified for the minerals at depth, a maximum for the iron content in the upper portion of the mantle may not be determined from geomagnetic field observations or magnetotelluric sounding techniques.

Finally, on the basis of the magnitudes of the electrical parameters and the shapes of the curves for log σ vs 1/T, the following processes probably determine the electrical conductivity in the outer portion of the earth: 1) in the near surface region of the crust - ionic conductivity determined by abundant pore fluids; 2) in the lower portion of the crust - impurity and intrinsic semi-conduction; 3) in the basal portion of the crust or upper mantle - intrinsic semi-conduction and ionic conduction together (peak conductivity region); and 4) in the deeper mantle - intrinsic semi-conduction giving way to ionic conductivity with depth.

TABLE 1. Experimental Conditions Existing During Conductivity Measurements

Specimen	Run or Rerun	D.C. and/or A.C.	T_{max} (°C)	Apparatus I or II	Buffer	Remarks
Garnet #104	Run 1	D.C. and A.C.	894	II	Wustite	Tube remained sealed between runs; buffer → hematite and magnetite; no apparent alteration.
	Rerun 1	D.C.	798	II	"	
Garnet #104 Air	Run 1	D.C.	877	II	None	Run in air.
Garnet #105	Run 1	D.C. and A.C.	1030	II	Wustite	
Garnet #106	Run 1	D.C. and A.C.	1042	II	Wustite	
Garnet #106 Aqueous 1	Run 1	D.C.	901	II	Wustite	Buffer saturated with H_2O and 2 ml at ends of tube; furnace coil failed at T_{max}.
Garnet #106 Aqueous 2	Run 1	D.C.	980	II	Wustite	H_2O as in Aqueous 1.
Garnet #109	Run 1	D.C. and A.C.	973	II	Wustite	
Hypersthene 1	Run 1	D.C.	1306	II	Wustite	

TABLE 1. (continued)

Specimen	Run or Rerun	D.C. and/or A.C.	T_{max}(°C)	Apparatus I or II	Buffer	Remarks
Enstatite 1	Run 1	D.C.	1308	II	Wustite	A.C. oscillator failed.
Quartz 1	Run 1	D.C.	1276	II	Wustite	Thermocouple failed.
Hornblende 1	Run 1	A.C.	1103	II	Wustite	Furnace coil failed. @ T_{max}; sample showed signs of melting.
Dunite #Gf1	Run 1	D.C.	1345	I	Fe & magnetite	Flushed with argon between runs.
	Rerun 1	D.C.	1333	I		

TABLE 2. Parameters Extracted from the Plots of Log σ vs. 1/T

E - electron volts [as in $\sigma = \sigma_o \exp(-E/kT)$]

σ_o - $(\text{ohm-centimeters})^{-1}$

[d] - difference in σ between forward and reverse measurements

Specimen	Run or Rerun	D.C. or A.C.	E	Line	σ_o	Peak	Remarks
Garnet #104	Run 1	D.C.	1.55 1.32 1.56	1 2 3	5.87×10^{3} 7.94×10^{1} 4.94×10^{3}	8.0×10^{-5} @ 0.955	[d] Very little.
Garnet #104	Run 1	A.C.	**		**		A.C. peak approx. same as D.C.
Garnet #104	Rerun 1	D.C.	1.02 1.12 0.875	1 2 3	2.82×10^{0} 9.89×10^{-1} 5.28×10^{0}	None	[d] Very little.
Garnet #104 Air	Run 1	D.C.	1.69 0.571 0.450	1 2 3	1.29×10^{5} 2.15×10^{-1} 4.20×10^{-2}	8.8×10^{-4} @0.900 & suggest. @lower T	[d] Very little.
Garnet #104 Air	Run 1	A.C.	**		**		A.C. values sli. higher than D.C. before peak; coincide thru cooling.

TABLE 2. (Continued)

Specimen	Run or Rerun	D.C. or A.C.	E	Line	σ_o	Peak	Remarks
Garnet #105	Run 1	D.C.	1.19 2.27 1.72 1.41	1 2 3 4	2.01×10^{1} 8.32×10^{4} 6.04×10^{2} 1.90×10^{1}	2.1×10^{-5} @ 0.963	[d] Very little.
Garnet #105	Run 1	A.C.	**		**		Lines thru A.C. points give same slopes but slightly higher σ_o .
Garnet #106	Run 1	D.C.	1.20 9.31 0.749	1 2 3	1.07×10^{1} 1.95×10^{32} 4.42×10^{-1}	6.9×10^{-6} @ 0.898	[d] fair in high T region.
Garnet #106	Run 1	A.C.	**		**		A.C. peak coincides with D.C. peak.
Garnet #106 Aqueous 1	Run 1	D.C.	1.09 1.31	1 2	2.24×10^{0} 4.90×10^{0}	suggest. of peak	[d] Very little.
Garnet #106 Aqueous 2	Run 1	D.C.	1.02 1.58 1.22 1.08	1 2 3 4	8.09×10^{-1} 6.43×10^{1} 1.59×10^{0} 3.07×10^{-1}	suggest. 8.3×10^{-6} @ 0.919	[d] Very little.

TABLE 2. (Continued)

Specimen	Run or Rerun	D.C. or A.C.	E	Line	σ_o	Peak	Remarks
Garnet #109	Run 1	D.C.	1.45 1.37 0.959 0.806	1 2 3 4	7.16×10^{3} 1.30×10^{2} 1.34×10^{0} 1.71×10^{-1}	6.6×10^{-3} @ 0.925	[d] Very little.
Garnet #109	Run 1	A.C.	**		**		A.C. peak approx. same as D.C. peak.
Dunite #Gf1	Run 1	D.C.				4.0×10^{-7} @ 1.185 & 8.4×10^{-8} @0.994	[d] extreme in peak area upon cooling.
Dunite #Gf1	Rerun 1	D.C.	2.58	1	1.09×10^{3}		[d] extreme except in high T region.
Enstatite #1	Run 1	D.C.	0.860 1.18 1.94	1 2 3	3.29×10^{-2} 3.90×10^{-1} 1.59×10^{2}	9.8×10^{-4} @ 0.978	[d] extreme above 570 ° C.
Quartz #1	Run 1	D.C.	0.430 4.62	1 2	4.99×10^{-5} 2.40×10^{10}		[d] extreme in high T region.
Hornblende #1	Run 1	A.C.	0.662	1	4.87×10^{1}		Essentially one straight line to melting point.

TABLE 2. (Continued)

Specimen	Run or Rerun	D.C. or A.C.	E	Line	σ_e	Peak	Remarks
Hypersthene	#1 Run 1	D.C.	1.15	1	1.50×10^{1}	1.0×10^{-3} [d] @ 0.925	Very little; equipment difficulties in high T region → ⊙ as approx. values.
			2.51	2	1.69×10^{9}		
			1.04	3	1.12×10^{1}		
			2.67	4	2.74×10^{6}		
			0.919	5	5.20×10^{-1}		
			1.25	6	6.67×10^{1}		

PART II

I INTRODUCTION

1.1 General

In recent years, many investigations into the nature of the interior of the earth have been concerned, directly or indirectly with the electrical conductivity of the earth's crust, mantle, and core. It is well known to geophysicists that the numerous laws of chemistry and physics defining the earth's internal constitution and behavior are inter-related in such a manner that a discussion of a particular phenomenon is difficult or even impossible without reference to other contemporary phenomena. Such is the case of the evaluation of the electrical conduction properties of the interior of the earth which requires a knowledge of the temperatures at depth, the chemical composition, data obtained from geomagnetic field observations, and laboratory measurements of pertinent compounds at high temperatures and pressures. Also, further theory is required to extrapolate the measurements to the temperatures and pressures within the earth. This extrapolation demands some knowledge of the conduction mechanism, which, in turn, requires further measurements for elucidation.

The temperature distribution within the earth is determined primarily by the intensity and distribution of heat sources and, possibly, the residual heat if the earth formed at high temperatures. Methods employed to obtain the temperatures at depth utilize data from surface heat flow measurements,

hypothetical distributions of radioactive materials and their relationships to the thermal history of the earth, melting-point relationships, seismic data and solid state theory, and observations of electric and magnetic phenomena (Verhoogen, 1956).

Temperature determination from electrical conductivity data, and vice-versa, is possible through the temperature dependence of the conductivity in the minerals comprising the earth, providing the electrical conductivity and chemical variation with depth are known and the electrical properties of the constituent minerals are at hand.

The electrical conductivity of certain portions of the mantle have been estimated from observed variations in the earth's magnetic field. Speculations on the chemical composition are based primarily upon estimates of elemental abundances in meteorites, the sun's atmosphere, stars, and dust clouds. The minerals possible at depth must satisfy density and seismic data, but these are rather insensitive to variations in chemical composition. Thermodynamic and solid state relationships limit the chemical composition even further. The electrical conductivities of a number of these minerals have been measured, but further work is necessary in order to compare these data efficiently with the variation of conductivity with depth.

A detailed discussion of the preceding relationships would be rather voluminous and the reader is referred to Birch's (1952) work for one of the best discussions and an extensive bibliography.

1.2 Previous Investigations

The earliest experimental data on the relationship between electrical conductivity and temperature for rocks at high temperatures were obtained by Coster (1948) and were used by Bullard (1950) to arrive at the first estimates of the electrical conductuvity of the lower mantle. A more detailed study was made by Hughes (1953), who measured the conductivities of the constituent minerals at temperatures up to their melting points and, by subsidiary experiments, sought to determine the nature of the conduction mechanism.

Hughes' experimentation indicated that the conductivity is given by:

(1.2-1) $$\sigma = \sum_n \sigma_{o_n} \exp(-B_n/T)$$

where σ_{o_n} and B_n are constants which depend upon the material and type of conduction mechanism in operation. Hughes suggested that these mechanisms are impurity conduction, intrinsic electronic conduction, and ionic conduction where:

(1.2-2) (a) $$\sigma_{\text{impurity}} = \sigma_o \exp(-E/2kT)$$

(b) $$\sigma_{\text{intrinsic}} = \sigma_o' \exp(-E'/2kT)$$

(c) $$\sigma_{\text{ionic}} = \sigma_o'' \exp(-E''/kT)$$

with:

$$\sigma_o < \sigma_o' < \sigma_o''$$

$$E < E' < 2E''$$

and where k = Boltzman's constant and the E's are the activation energies required to excite an electron or ion to a mobile

state. This accounts for the summation sign in equation (1.2-1) since all three mechanisms may be in operation at the same time. However, due to the exponential dependence of the conductivity on the temperature and the different excitation energies, a given small temperature interval will generally exhibit essentially one mechanism with the result that a plot of log σ vs. 1/T will usually give straight line segments corresponding to the regions in which different conductivity mechanisms predominate.

Hughes (1953) measured the electrical conductivity as a function of temperature for olivine (peridot-gem variety), dunite, synthetic forsterite, and the pyroxenes, enstatite and diopside. For the different conduction mechanisms, the values obtained for the constants and the activation energies are listed in Table I-1. Hughes suggests that the impurity conductivity in the minerals measured is not an important mechanism in the mantle since magnetic observations demand a much greater conductivity than can be supplied by such a process. Furthermore, in the vicinity of 900°- 1000°K, intrinsic electronic conductivity overshadows any contribution from the impurity conduction mechanism. At temperatures above 1400°- 1500°K (and at atmospheric pressure) ionic conductivity predominates.

About the same time as Hughes (1953) was conducting his experiments, Cronemeyer (1952) was investigating the electrical and optical properties of single crystals of rutile. While

TABLE I-1. Electrical Conductivity Constants and Excitation Energies (after Hughes, 1953)

Mechanism	Constant $(\Omega - cm)^{-1}$	Excitation Energy (ev)	Mineral or Series
impurity	σ_o - 10^{-4} - 10^{-6}	E - 0.5 - 1.0	Olivine series, Orthopyroxenes
intrinsic	σ_o' - 1 - 5	E'- 3.0	Magnesium-rich olivines
intrinsic	σ_o' - 10^{-1}	E'- 2.0	Enstatite and diopside
ionic	σ_o'' - 5×10^{6}	E"- 3.0	Magnesium-rich olivines
ionic	σ_o'' - 10^{4}	E"- 2.8	Enstatite
ionic	σ_o'' - 10^{10}	E"- 4.0	Diopside

Hughes' work was directed more along geophysical lines, Cronemeyer was concerned primarily with the semi-conduction properties of rutile as applied to the solid-state physics of semi-conducting materials.

Cronemeyer (1952) has made a number of studies of single crystals of rutile, which is the first member of the series TiO_2 -Ti_2O_3 - TiO - Ti, and the data obtained are important to the discussion of the present investigation. This series shows a progressive transition from an insulator to a metal as rutile is gradually reduced. Studies of clear synthetic rutile crystals indicate the possibility of correlating the high temperature conductivity (E' - 3.05 ev) with the threshold of optical absorption at low temperatures (E' - 3.03 ev) and with the maximum of the photoconductivity (3.03 - 3.06 ev), resulting in approximately 3.05 ev for the energy which corresponds to intrinsic electronic conduction as in equation (1.2-2). E' does not depend on the direction in which the current is passed through the crystal but the conductivity varies with the value of σ_o' , which changes as in Table I-2. For pure TiO_2 , log σ vs. 1/T plots as straight line segments for the heating curves (no cooling curves are shown).

Semi-conducting rutile, obtained through reduction with hydrogen at temperatures slightly under 800°C, exhibits a blue color from an optical maximum at approximately 1.7 (0.73 ev) and plots of log σ vs. 1/T result in approximately 0.68 ev for

TABLE I-2. Directional Dependence of σ_o' and E'
(after Cronemeyer, 1952)

Direction	σ_o' $(\Omega \cdot cm)^{-1}$	E' (ev)	Temp. Range (° K)
∥ to c axis	4.59×10^3	3.05	500° - 950°
⊥ to c axis	2.76×10^3	3.05	350° - 850°
∥ to c axis	8.38×10^4	3.67	950° - 1400°
⊥ to c axis	6.82×10^4	3.67	850° - 1400°

the excitation energy. A theoretical calculation by Cronemeyer for the ionization of the first electron from an oxygen vacancy gives 0.74 ev, which is in good agreement with the experimental results.

Further experimentation with slightly reduced rutile showed that the A.C. conductivity, measured at 100 cps between 250°C and 500°C, corresponds almost exactly with the D.C. data. Below approximately 900°C, the conductivity is sensitive to the applied field strength for magnitudes greater than 10 volts/meter.

Cronemeyer (1952) found that for low fields, the log σ vs. 1/T plot started off at room temperature with a slope determined by E' - 0.19 ev, leveled off at approximately 80° C, and, in the vicinity of 160°C, rose again with a steeper slope. The cooling curve followed an entirely different curve with greater activation energy and less conductivity. On reruns, suggested peaks or troughs in the curves almost disappeared and the conductivity became nearly reproducibile in subsequent heating and cooling cycles. In the case of a high field strength, it was observed that the cooling curve was essentially a straight line which resulted in a greater overall conductivity. After being cooled in such a field, the slightly reduced crystals sometimes exhibited a blue color concentration at the cathode. Cronemeyer believes that this may possibly be due to the migration of solor centers (oxygen defects) toward the negative electrode.

Strongly reduced rutile resulted in an opaque material which had properties closer to those of a metallic conductor. This material was actually an n-type, blue-black semi-conductor with an activation energy of approximately 0.070 ev at room temperature and a corresponding conductivity in the $100\Omega^{-1}m^{-1}$ region.

Finally, it was observed that the initial, overall conductivities of a number of samples appeared to depend on the cross-sectional area. Cronemeyer suggests that this might indicate carrier injection with predominant recombination at sample surfaces.

Thus far, we have been concerned with the temperature dependence of the electrical conductivity. However, before these data may be applied efficiently to geophysical investigations of the interior of the earth, it is necessary to determine how pressure affects these measurements.

Pressure experiments have been carried on by Hughes (1955,1959), who determined the pressure effect on the electrical conductivity of peridot and corundum, Paul and Pearson (1955), who found the pressure dependence of the conductivity of silicon, Long (1956), who investigated the effects of pressure on the conductivities of several semi-conductors, and Balchan and Drickamer (1959), who studied the effect of pressure on the spectra of olivine and garnet.

The effect of pressure on the ionic conductivity of peridot was measured by Hughes (1955) and was discussed in

terms of its influence on the electrical conductivity and temperature of the earth's mantle. The specimen used was a small cylinder of peridot 0.35 cm long and 0.17 cm in diameter (similar in size to the samples used in the present investigation). Experimental difficulties were encountered due to chemical changes in the apparatus and subsequent alteration of the sample. However, the final specimen measured gave no indications of being altered. Three usable runs were made at temperatures of 1333 $^{\circ}$ K, 1429 $^{\circ}$ K, and 1513 $^{\circ}$ K. At each temperature, measurements were made at pressures of 1000, 2500, 4000, 5500, 7000, and 8500 kg/cm^2 in an ascending and descending pressure cycle. The two readings at each temperature were averaged, a straight line relationship assumed, and the pressure effect determined from the slope. The data obtained from these three runs gave the decrease of the conductivities with pressure as being (2.9 $\pm$ 0.9)%, (3.7 $\pm$ 0.3)%, and (2.3 $\pm$ 0.6)% per 1000 kg/cm^2 respectively. The conductivities extrapolated to zero pressure were 1.48, 6.9, and 21.3, all times $10^{-6}\ \Omega^{-1}\text{cm}^{-1}$. Hughes states that these values satisfy the ionic semi-conduction equation if $\sigma_o'' = 4 \times 10^5\ \Omega^{-1}\text{cm}^{-1}$ and $E'' = 2.7$ ev since tha magnitudes of these constants indicate conductivity of an ionic nature. Further, assuming that the change in the log σ_o'' with pressure is negligible as compared with the pressure effect on E", he suggests that the measurements indicate that the initial increase of E" with pressure is 4.8×10^{-6} ev/kg/cm^2.

Hughes (1959) carried on further work along these lines by measuring the electrical conductivity of corundum at pressures up to 10,000 bars and temperatures up to 1350°- 1550°K. He believes that electronic conduction is predominant in this case and that it decreases with pressure by about 2% per 1000 bars. This is about half the rate of the decrease obtained for peridot at relatively higher temperatures, an effect which Hughes attributes to the higher concentration of mobile metallic ions in peridot. Extrapolating these results to the temperatures and pressures in the earth, Hughes suggests further that the conductivity there is not electronic as commonly thought, but predominantly ionic.

Paul and Pearson (1955) studied the variation of the conductivity of high-purity, single crystals of Si as a function of the applied hydrostatic pressure in the intrinsic range and interpreted their results to give a decrease in the energy gap (i.e.-increase in conductivity) between the conduction and valence bands with pressure. They maintain that a uniform increase in conductivity with pressure in the intrinsic range would give $(\partial E'/\partial p)_T = -1.5 \times 10^{-12}$ ev/dyne/cm^2 (-1.5×10^{-6} ev/kg/cm^2) at 250°C and emphasize strongly that this is true only in the absence of any significant changes in mobility with pressure.

Further work, along pure solid-state physics lines, was carried on by Long (1956) when he investigated the effect of hydrostatic pressures between 1 and 2000 atmospheres on the

electrical properties of several different semi-conductors: germanium, indium antimonide, indium arsenide, gallium antimonide, tellurium, and magnesium stannide. For indium antimonide, it was found that the energy gap widened with increasing pressure at a rate of approximately 14 x 10^{-6} ev/atm (14.5 x 10^{-6} ev/kg/cm^2) and that the electron mobility was smaller by approximately 12% at 2000 atm. Keyes (1955) found similar results and also that the hole mobility was not changed by pressure. Long determined further that the electron mobility in InAs decreases by approximately 7% at 2000 atm and that there is no such mobility change in GaSb. For tellurium, the energy gap is smaller by 0.032 ev at 2000 atm than its value of 0.336 ev at 1 atm and both the electon and hole mobilities increase with pressure.

The effect of pressure on the spectra of olivine and garnet was studied by Balchan and Drickamer (1959). It was found that the absorption edge of olivine shifts to the red by about 9% of the gap in the pressure range 0 to 150,000 atm (i.e.-the excitation energy decreases by 9%). The Fe peak in alamandite garnet was observed to shift to higher energies by 700 cm^{-1} in 170,000 atm. The temperature coefficient of the absorption edge of olivine was also measured at atmospheric pressure at temperatures up to 327°C. It exhibited a linear red shift of 4.21 x 10^{-4} ev/°C over this range (3.37 cm^{-1}/°C). Balchan and Drickamer suggest that if pressure and temperature effects are additive, then the edge

will have moved into the visible portion of the spectrum a few hundred kilometers under the surface.

I.3 Purpose of the Present Investigation

Previous investigations by others have indicated that increasing the proportion of iron greatly increases the electrical conductivity [e.g.-the curves of log σ vs. 1/T of Coster (1948) show increasing conductivity for increasing iron content]. However, as pertains to minerals containing ferrous iron, these measurements have been imprecise due to the reduction or further oxidation of the iron content as the sample is heated to elevated temperatures. Theoretically, this difficulty may be avoided in most instances by controlling the partial pressure of the oxygen in the vapor phase in the vicinity of the sample with a suitable buffer mixture. The first objective here, then, was to develop such a buffer mixture by a consideration of the oxidation - reduction phenomena associated with gas-solid equilibria of the sample and its vapor and, secondly, to design apparatus applicable to the measurement of electrical conductivity in a controlled atmosphere at elevated temperatures.

Experimental difficulty has been encountered in the past due to the polarizing effect possibly arising from minor constituents or impurities in certain minerals. However, the high conductivity of iron-rich minerals should minimize this effect. Therefore, a large number of mineral specimens selected for the measurement of electrical conductivity as a function of temperature are iron-rich. With the aid of A.C.

and D.C. measurement techniques, polarization and thermoelectric effects were examined at each temperature where the electrical conductivity was measured.

By comparing the measured conductivities of silicates of increasing iron content with the very low conductivity observed in the upper part of the earth's mantle, an upper limit to the iron content there should be determinable. The possibility of such application of the data is examined.

Finally, the results of the conductivity measurements are discussed in terms of solid-state physics in order to gain insight into the probable conduction mechanism(s) in operation throughout the various temperature intervals.

The concluding discussion is devoted to the geophysical significance of the electrical conductivity data obtained.

II REDUCTION-OXIDATION CONSIDERATIONS

2.1 General

To investigate gas-solid equilibria, we require a relationship between the partial pressures of the constituents in the vapor phase and the oxidation states of the solid components. Data for numerous metal-oxide systems have been compiled by Darken, Gurry, Muan, Richardson, Jeffes, and others.

Of particular interest is Figure II-1 for the standard free energy of formation of many metal oxides as a function of temperature. Darken and Gurry (1953) have modified the figure from the work of Richardson and Jeffes (1948) and include scales for the ratios CO/CO_2, H_2/H_2O, and p_{o_2}, the partial pressure of the oxygen in the vapor phase. A straight line through C, H, or O in the left hand margin and the corresponding scale on the right will determine the relationship between a particular reaction, the temperature for this reaction, and the nature of the vapor phase. For example, at $p_{o_2} = 10^{-17}$ and T = 850°C, the stable form of iron is FeO since this point lies within the region bounded by the reactions:

(2.1-1) $$6\ FeO + O_2 \rightleftharpoons 2\ Fe_3O_4$$

(2.1-2) $$2\ Fe + O_2 \rightleftharpoons 2\ FeO$$

If the p_{o_2} is maintained at 10^{-17} and the temperature is

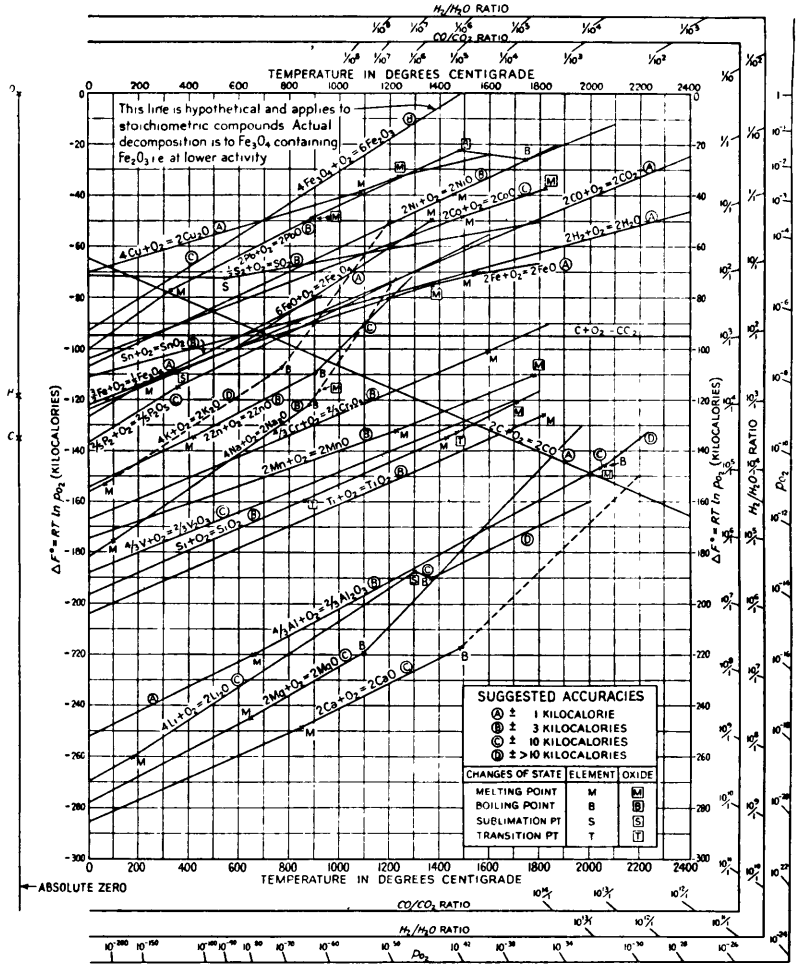

Fig. II-1. The standard free energy of formation of many metal oxides as a function of temperature. [after Richardson and Jeffes (1948) and modified by Darken and Gurry (1953)]

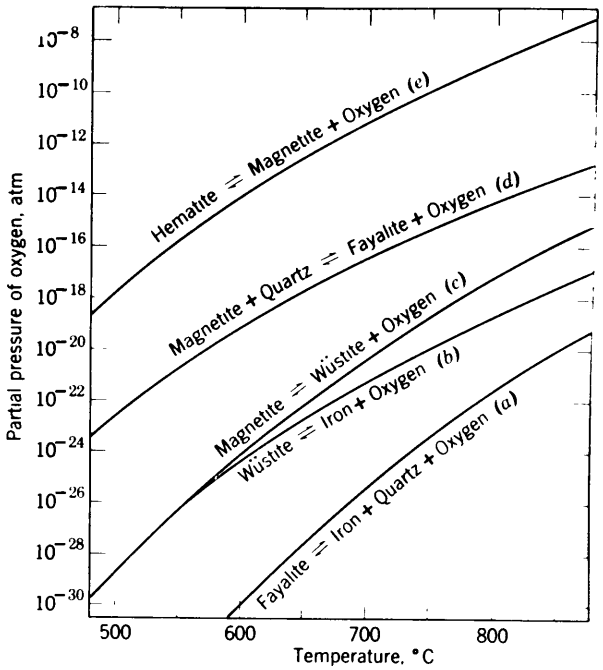

Fig.II-2. The stability diagram for fayalite at 1 atm pressure. (from Eugster, 1959)

lowered to 700°C, the first reaction will be favored in the forward direction to oxidize FeO to magnetite.

This may also be seen by inspection of the $\Delta F - RT \ln p_{O_2}$ scale, which results in a decrease in the free energy, ΔF, for this case. We recall the phase rule of Gibbs which defines the condition of equilibrium by the relation between the number of phases existing simultaneously and the number of components. This is represented by:

(2.1-3) $$F - C - P + 2$$

where, for the example under consideration:

C - 2 components (i.e. - Fe,O)

P - 3 phases (i.e. - FeO, O_2, Fe or Fe_3O_4)

and results in F - 1 degree of freedom. From thermodynamics we have that $\Delta F - RT \ln p_{O_2}$ for pressures on the order of a few atmospheres or less. If the temperature is the variable, then the p_{O_2} is determined by the temperature. Therefore, we may use changes in the free energy in the same manner as changes in the partial pressure of the oxygen for future discussions.

Geologically, the most important elements in the crust are O, Si, Al, Fe, Ca, Na, K, and Mg since these constitute approximately 99% of the total composition and, in the earth as a whole, Fe, O, Si, Mg, Ni, Ca, and Al (Mason, 1952). In the majority of minerals formed from these, all of the elements exist in their highest oxidation states except for iron, which

is either in the ferrous or ferric form, or both. Depending upon the partial pressure of oxygen but not otherwise upon the chemical composition (or total pressure, if small) of the vapor phase, when a representative mineral containing ferrous iron is heated over a wide temperature range, the iron may be oxidized or reduced unless its relationship to the vapor is such that chemical stability exists over the entire temperature interval.

Referring again to Fig. II-1, we see that if conditions are such that reactions (2.1-1) or (2.1-2) are in operation but never reach completion due to depletion of one of the reactants (i.e.-if FeO is always present), then all of the oxides below this portion of the figure cannot be reduced. Among these are SiO_2, Al_2O_3, MgO, CaO, K_2O, and Na_2O. Therefore, if the Fe^{++}/Fe^{+++} ratio can be held constant in the sample throughout an experiment involving large temperature variations, chemical stability should exist for all components of the common igneous or metamorphic rock-forming minerals except those containing Ni, Co, etc., in which case, oxides of these would be reduced.

Theoretically, the Fe^{++}/Fe^{+++} ratio can be controlled by buffering the system so as to give the proper p_{O_2} versus temperature relationship. Considerable work has been done on the action of buffers and the criteria for stability of a number of minerals by Eugster (1957, 1959) and others and these investigations will aid us in the problem of ferrous silicate alteration during high temperature studies.

2.2 The Stability of Fayalite Utilizing a Wustite Buffer

One of the products of Eugster's investigations is the stability diagram for fayalite at 1 atmosphere pressure as shown in Fig. II-2. Although the iron in wustite is in the same state of oxidation as that in fayalite, fayalite is stable also within the magnetite field and within the field for metallic iron. This is readily understood since the formation of fayalite from FeO and SiO_2 is an exothermic reaction and any dissociation consequent to oxidation or reduction of the iron is thus endothermic. Hence, if the p_{o_2} of the vapor phase is regulated so as to maintain the stability of wustite, the stability of any ferrous silicate is probable. In certain cases where sufficient data are available, this may be checked theoretically by a consideration of free energy changes.

The temperature-composition diagram for the system Fe - O, as determined by Darken and Gurry (1946), is illustrated in Fig. II-3. For a wustite buffer mixture composed of Fe and Fe_3O_4, the reactions to be considered are:

(2.2-1) $3/2\ Fe + O_2 \rightleftharpoons 1/2\ Fe_3O_4$

$\Delta F = -133{,}900 + 41.1\ T\ (298^\circ - 833^\circ K)$

$\log p_{o_2}\ (atm) = -(29{,}260/T) + 8.980$

(2.2-2) $2\ Fe + O_2 \rightleftharpoons 2\ FeO$

$\Delta F = -124{,}100 + 29.90\ T\ (298^\circ - 1642^\circ K)$

$\log p_{o_2}\ (atm) = -(27{,}120/T) + 6.534$

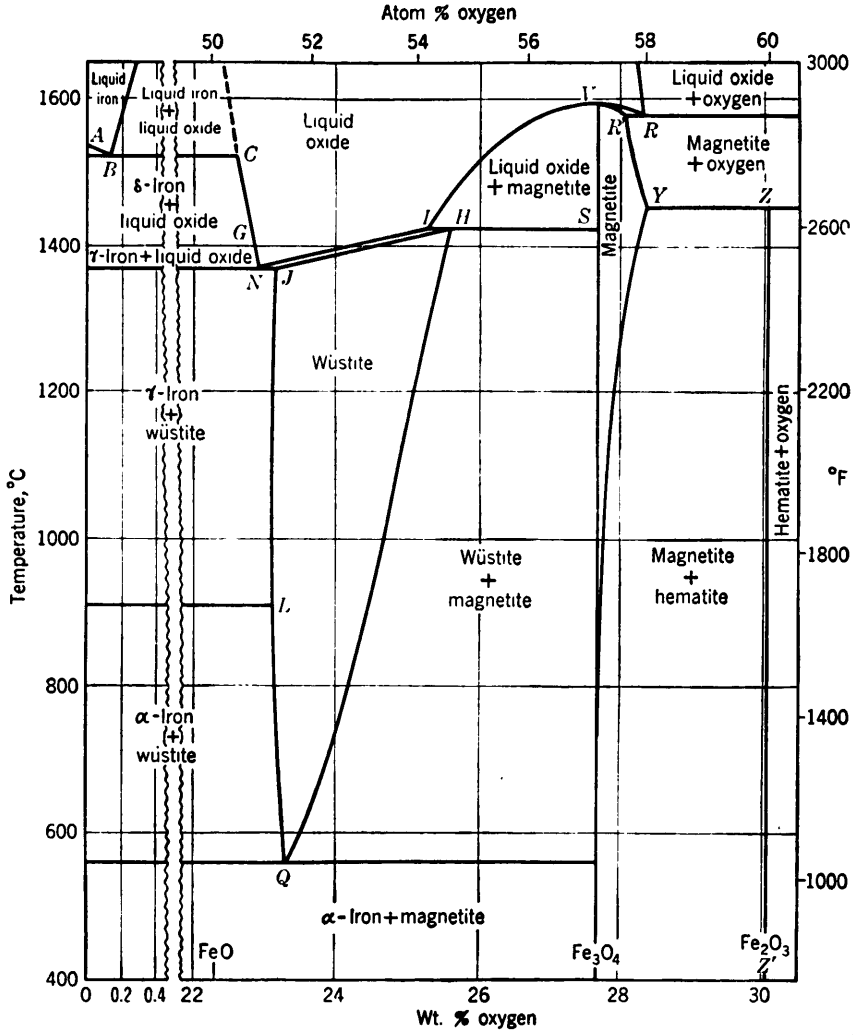

Point	°C	% O	p_{CO_2}/p_{CO}	Point	°C	% O	p_{CO_2}/p_{CO}	p_{O_2} (atm)
A.....	1539			*Q*.....	560	23.26	1.05	
B.....	1528	0.16	0.209	*R*.....	1583	28.30		1
C.....	1528	22.60	0.209	*R'*.....	1583	28.07		1
G.....	1400*	22.84	0.263	*S*.....	1424	27.64	16 2	
H.....	1424	25.60	16.2	*V*.....	1597	27.64		0.0575
I.....	1424	25.31	16.2	*Y*.....	1457	28 36		1
J.....	1371	23.16	0.282	*Z*.....	1457	30.04		1
L.....	911*	23.10	0.447	*Z'*.....		30.06		
N.....	1371	22.91	0.282					

* Values for pure iron.

Fig. II-3. The temperature-composition diagram for the system Fe - O. (from Darken and Gurry, 1946)

(2.2-3) $6\ FeO + O_2 \rightleftharpoons 2\ Fe_3O_4$

$\Delta F = -149{,}250 + 59.80\ T\ (298^\circ - 1642^\circ\ K)$

$\log p_{O_2}\ (atm) = -(32{,}616/T) + 13.068$

(2.2-4) $4\ Fe_3O_4 + O_2 \rightleftharpoons 6\ Fe_2O_3$

$\Delta F = -114{,}000 + 65.9\ T\ (298^\circ - 1730^\circ\ K)$

$\log p_{O_2}\ (atm) = -(24{,}912/T) + 14.400$

where ΔF and $\log p_{O_2}$ are linear approximations by Richardson and Jeffes (1948, 1949) and Norton (1955).

For T = 500° K:

(2.2-1')	$\Delta F = -113{,}350$ cal	
(2.2-2')	$\Delta F = -109{,}150$ "	for the reactions
(2.2-3')	$\Delta F = -119{,}350$ "	as shown
(2.2-4')	$\Delta F = -81{,}050$ "	

or:

(2.2-1")	$\Delta F = -226{,}700$	
(2.2-2")	$\Delta F = -54{,}575$	cal/gfw of product
(2.2-3")	$\Delta F = -59{,}675$	
(2.2-4")	$\Delta F = -13{,}508$	

A consideration of ΔF shows that reaction (2.2-1) is the most favorable one at T = 500° K for a buffer containing only Fe and Fe_3O_4 initially. In an atmosphere possessing a p_{O_2} in excess of the equilibrium value, the formation of magnetite proceeds until the Fe in the buffer has been depleted or the p_{O_2} has been regulated to its value at equilibrium. A deficiency in oxygen will drive the reaction in the reverse direction, thereby supplying the atmosphere with

oxygen from the magnetite and, at the same time, increasing the quantity of metallic iron.

A similar analysis for T = 1000° K results in the following; reaction (2.2-1) cannot occur; (2.2-2) will control any excess oxygen; (2.2-3) will correct any deficiency in oxygen; and (2.2-4) will not occur unless the buffer has been previously oxidized to magnetite.

From Eugster's work we have that wustite is stable within the stability field of fayalite and that the alteration of fayalite will occur as:

(2.2-5) $3\ Fe_2SiO_4 + O_2 \rightleftharpoons 2\ Fe_3O_4 + 3\ SiO_2$

or:

(2.2-6) $Fe_2SiO_4 \rightleftharpoons 2\ Fe + SiO_2 + O_2$

The free energy change for reaction (2.2-5), where ferrous iron is partially oxidized to ferric iron, is approximately - 80 kcal at a temperature of 1000° K. The corresponding buffer reaction (2.2-3) gives - 89 kcal. Similarly, for the case of reduction to metallic iron, reactions (2.2-6) and (2.2-2) result in approximately + 100 kcal and + 94 kcal respectively. Therefore, the buffer mixture will alter before the occurrence of oxidation or reduction in the sample and regulate the p_{o_2} so as to provide conditions necessary for the stability of the ferrous iron content of fayalite.

2.3 The Stability of Solid Solutions Containing Ferrous Silicates

Fayalite is the other end-member of the solid solution series beginning with forsterite (Mg_2SiO_4) and in which there is complete miscibility between these members. If stability is guaranteed for the iron-rich end-member (the magnesium-rich end-member is stable if the ferrous iron is unaltered), this necessarily holds true for all combinations of the end-members due to the relationship between the free energies of formation of these end-members and the change in free energy associated with mixing.

It is a well known fact that the properties of olivine, the intermediate member of the above solid solution series, approach those of an ideal solid solution. Assuming, then, that olivine belongs in an ideal solid solution, let us consider the mixing energy and its effect on the free energy of formation of the mixture.

For a binary solution, the free energy of 1 mole may be expressed by (after Darken and Gurry, 1953):

(2.3-1) $$F = N_1\bar{F}_1 + N_2\bar{F}_2$$

where: N_i - mole fraction

$\bar{F}_i$ - partial molal free energy

For an isothermal system:

(2.3-2) $$F = RT\,(N_1 \ln a_1 + N_2 \ln a_2) + N_1F_1^\circ + N_2F_2^\circ$$

where $N_1F_1^\circ$ and $N_2F_2^\circ$ are the free energies of the components in the standard states. Since the activity of a component in

an ideal solution is equal to its mole fraction, the free energy of formation of the solution (i.e.-the free energy change associated with the entropy of mixing) may be represented by:

(2.3-3) $\Delta F_m = RT\ (N_1 \ln N_1 + N_2 \ln N_2)$

For the case of $MgFeSiO_4$, this gives $\Delta F_m = -1.377$ kcal. Since, at a temperature of 1000 °K, $\Delta F_{f\ Fayalite} = -266.8$ kcal and $\Delta F_{f\ Forsterite} = -417.5$ kcal, the free energy of formation of olivine is -342.2 kcal/mole at this temperature if we disregard the mixing energy. Then the actual free energy of formation of this mineral from the end-members of an ideal solid solution is equal to -342.2 kcal plus -1.377 kcal or -343.6 kcal total.

Let us now consider the oxidation or reduction of olivine as given by:

(2.3-4) $6\ MgFe\ SiO_4 + O_2 \rightleftharpoons 2\ Fe_3O_4 + 3\ SiO_2 + 3\ Mg_2SiO_4$

or:

(2.3-5) $6\ MgFeSiO_4 + O_2 \rightleftharpoons 2\ Fe_3O_4 + 6\ MgSiO_3$

and:

(2.3-6) $2\ MgFeSiO_4 \rightleftharpoons 2\ Fe + SiO_2 + O_2 + Mg_2SiO_4$

or:

(2.3-7) $2\ MgFeSiO_4 \rightleftharpoons 2\ Fe + 2\ MgSiO_3 + O_2$

Then the related free energy changes for the reactions at 1000 °K are:

$\Delta F = -70$ kcal for (2.3-4)

$\Delta F = -75$ kcal for (2.3-5)

ΔF - 103 kcal for (2.3-6)

ΔF - 101 kcal for (2.3-7)

Therefore, upon comparing these values for the free energy changes with those obtained from equations (2.2-5) and (2.2-6), we see that olivine is even more resistant to alteration than is fayalite due to the effect of the entropy of mixing on the free energy relationships. From this it follows that, in any ideal solid solution containing an iron silicate end-member, if chemical stability is guaranteed for this member, then stability exists also for any intermediate member of this solid solution series.

In view of the preceding discussions, therefore, it appears that a buffer of wustite composition will prevent alteration of ferrous silicates by regulating the p_{O_2} so as to maintain a chemical potential of insufficient magnitude to drive the related silicate reaction. Furthermore, we are dealing with gas-solid equilibria, the reactions rates of which are dependent upon the surface area exposed to the vapor phases. Since the buffer mixture is a fine powder with tremendous surface area as compared to the limited surfaces of the cored samples, even if the sample reaction possessed a chemical potential somewhat greater than that for the corresponding buffer reaction, the sample could, in certain instances, remain unaltered for short periods of time (e.g.-the time required for conductivity measurements throughout a heating and cooling cycle).

Further discussion of the ability of the buffer to

extablish conditions of chemical stability in the minerals investigated is presented along with the section on garnets.

2.4 Buffer Composition

Since wustite does not exist below approximately 570° C, the buffer was prepared as a mixture of metallic iron and magnetite so as to produce an oxygen content equal to 23.26% by weight (point Q on the diagram in Fig. II-3). It should be memtioned here that stoichiometric FeO is thermodynamically unstable at all temperatures and that the maximum iron content corresponds to $Fe_{0.953}O$ (Darken and Gurry, 1946). Therefore, the composition determined by point Q should be the proper choice.

The question arises as to how much buffer mixture is required that there will be sufficient metallic iron to prevent alteration of the entire volume of buffer to magnetite at the lower temperatures. Calculations show that 0.2 gm of buffer mixture has a metallic iron content approximately 10 times that required when the gas in the furnace tube is composed of 100% oxygen. Since the tube is flushed with argon gas prior to each run, the iron is in excess by a factor of about 10^4. Therefore, between room temperature and 570° C, reaction (2.2-1) should regulate the p_{o_2} so as to produce equilibrium between the forward and reverse reaction rates, rather than go to completion and oxidize the entire buffer to magnetite. Above 570° C, equations (2.2-2) and (2.2-3) demonstrate that the buffer composition is not as critical.

III EXPERIMENTAL APPARATUS

3.1 General

Two experimental arrangements were employed in this investigation. Apparatus I provided only D.C. measurements while Apparatus II allowed both A.C. and D.C. measurements and minimized a few of the disadvantages and probable sources of error inherent in Apparatus I.

3.2 Apparatus I

3.21 General

The initial apparatus employed is shown in Figures III-1 and III-2 and the furnace may be examined in greater detail in Figures III-3 and III-4.

3.22 Furnace Construction

The furnace winding consists of 23 feet of 0.01 inch platinum wire would externally on a cylindrical high temperature ceramic core with inside and outside diameters of 1/2 and 3/4 inches respectively and a length of 3 inches. The heater core is enclosed by a concentric brass cylinder with a 2 inch outside diameter and the space between is filled with diatomaceous earth. The brass cylinder (1) is capped at both ends with pressed asbestos discs (2) and a screw (3) locks the furnace at any desired position along the vertical rods (4).

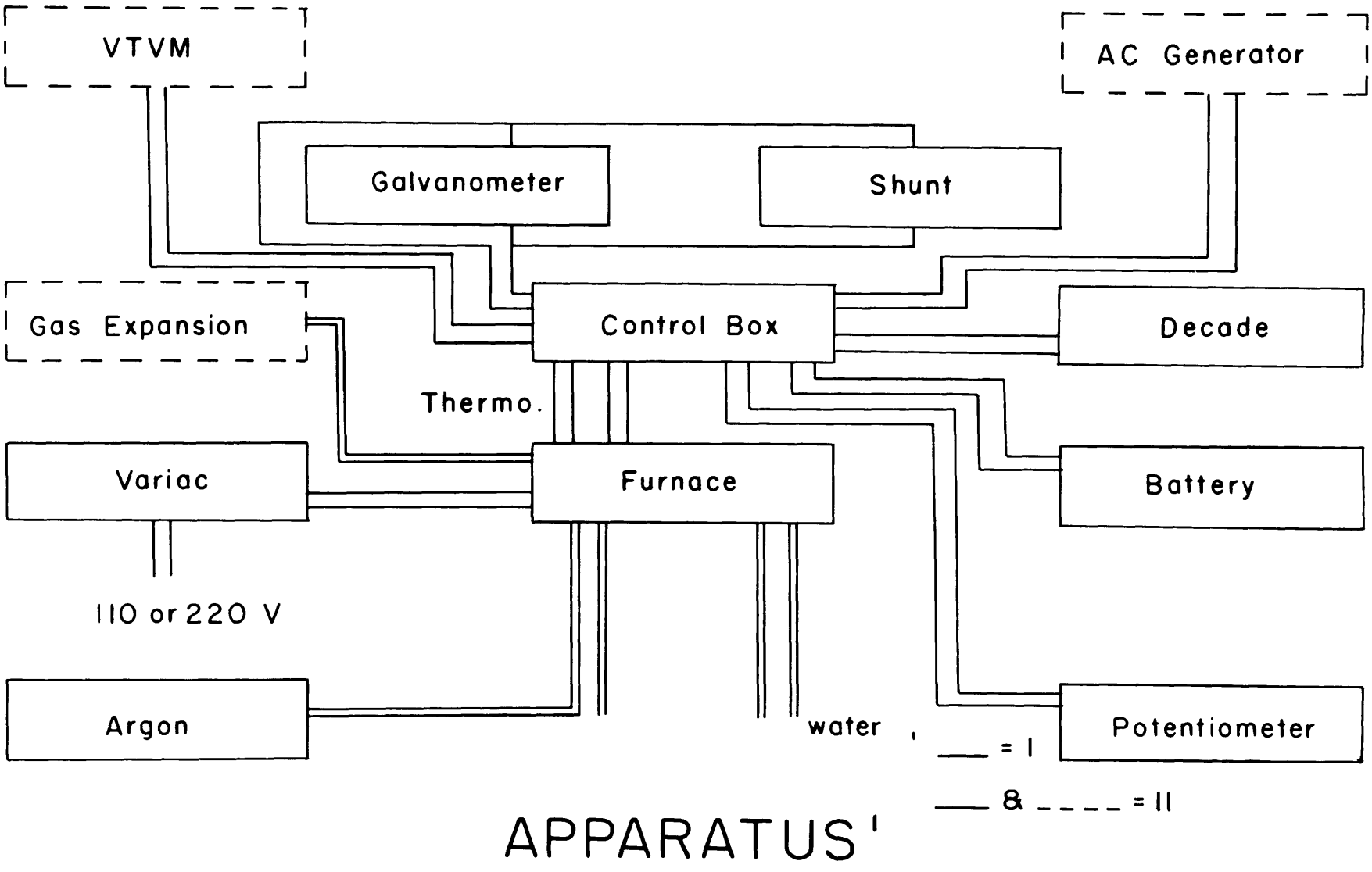

Fig. III-1. Experimental apparatus.

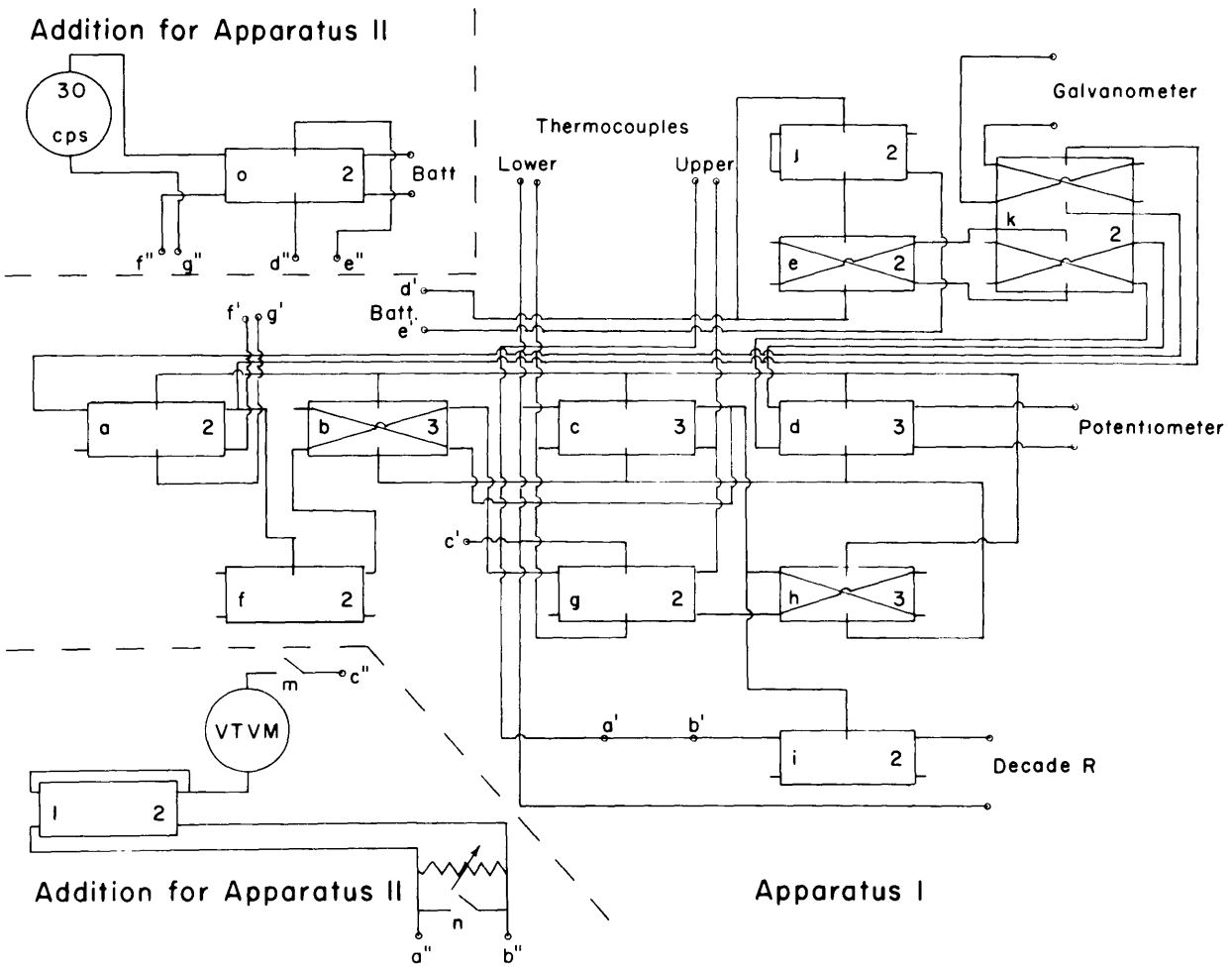

CONTROL BOX

Fig. III-2. Control Box.

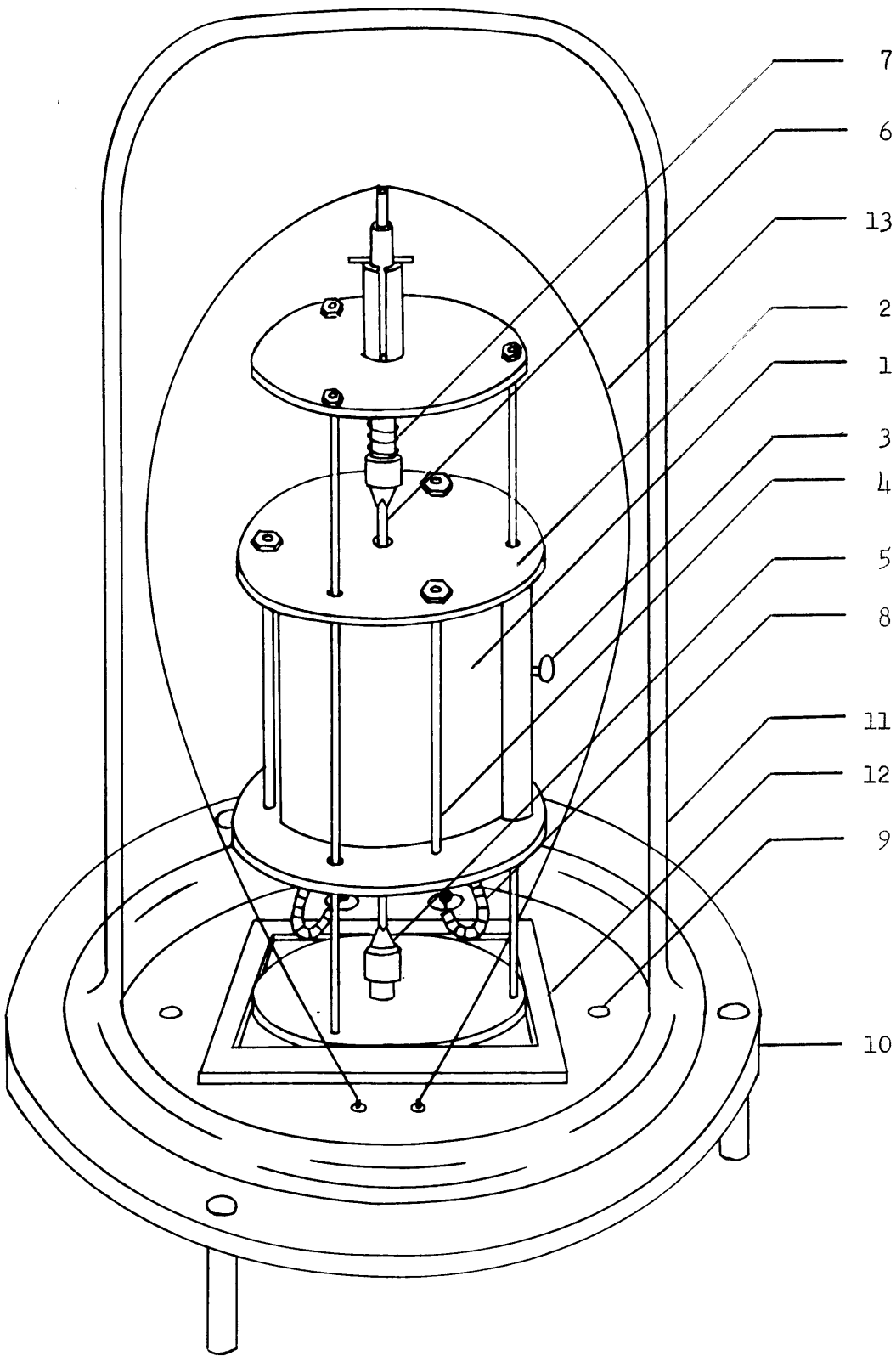

Fig. III-3. Furnace for Apparatus I.

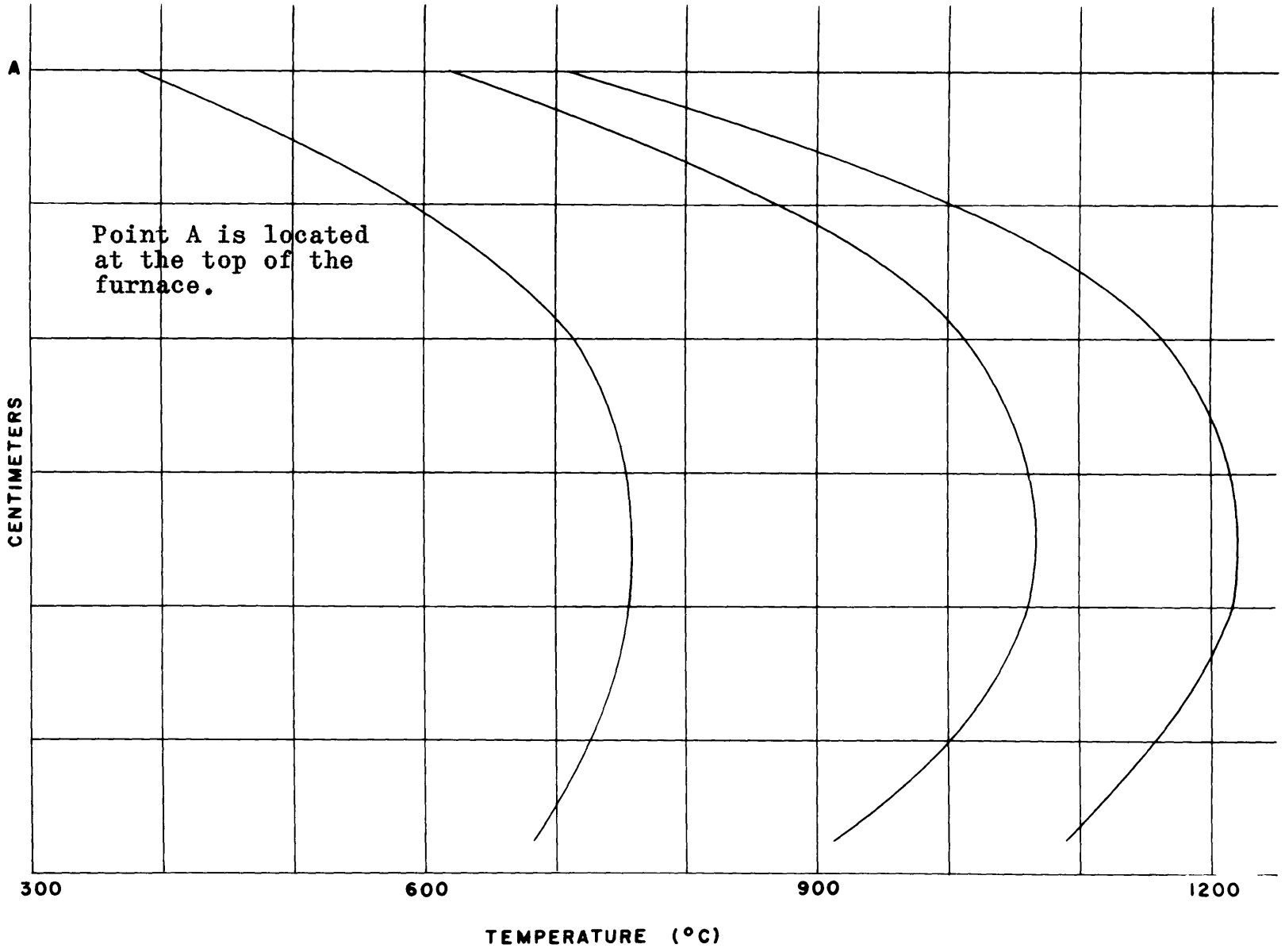

Fig. III-4. Temperature profile for the furnace of Apparatus I.

Miniature drill chucks or pin vises (5) hold ceramic thermocouple rods (6) which pass through small holes in the asbestos discs into the interior of the furnace. A spring (7) insures that the thermocouple rods are pressed against the sample throughout expansions and contractions of the apparatus. Current for heating the coil, controlled by the variac, flows through the leads at (8) and gas connections are located at (9). The furnace system is attached to a thick brass plate (10) and sealed inside a bell jar (11). Water flowing through the cooling duct (12) prevents the base from heating and makes it possible to rest the hand on the bell jar even when the furnace is over 1400° C. The thermocouple leads for the upper thermocouple (13) and those for the lower thermocouple (not shown) are connected to the control box of Figures III-1 and III-2.

3.23 Control Box

The circuit diagram for the control box is illustrated in Figure III-2 where the switch number 2 refers to 2 positions (on-off) and the number 3 refers to 3 positions (on-off-on). The purpose of each switch used for D.C. measurements is as follows:

(a) galvanometer - galvanometer short circuited
(b) voltage measurement across specimen reverse
(c) thermocouples: upper - lower
(d) potentiometer - battery

(e) battery polarity reverse

(f) voltage measurement across specimen(on-off)

(g) thermocouple sum

(h) thermocouple sum reverse

(i) thermocouples - decade

(j) polarization check on sample

(k) battery polarity reverse with same direction for galvanometer deflection

3.24 Other Components

The remaining components in the apparatus include a 1.5 volt dry cell battery, a variac, a decade resistor box and a decade booster, a shunt box, a potentiometer, and a galvanometer. The battery voltage is checked frequently for signs of drain. The shunt box regulates the current flow through the galvanometer and the decade resistor and booster are used in the calibration of the galvanometer. The potentiometer is used with platinum - platinum + 10% rhodium thermocouples in determining temperatures and for some of the measurements of voltages produced by the specimen.

3.3 Development of Apparatus II

D.C. measurements were made with the aid of apparatus I and, in the course of accumulating data, a number of questions arose pertaining to: 1) the presence of water vapor in the

system; 2) the adsorption properties of the diatomaceous earth insulation material; 3) the A.C. magnetic field produced by the heating coil; 4) the volume of gas to be controlled by the buffer; 5) convection currents in the gas; and 6) the advisability of obtaining A.C. measurements.

Water vapor was observed in Apparatus I in the first few sample determinations when it condensed on the cooling duct. A variety of techniques were attempted to remove this from the system but, in every case, condensation remained visible. Figure II-1 illustrates that the equilibrium curve for water lies slightly above that for the equilibrium of FeO and Fe (i.e.-the partial pressure of the oxygen is slightly higher). When the amount of water is large as compared with the sample volume and the amount of the buffer material, both the buffer and the sample should have their iron contents oxidized to hematite at temperatures of 700° C or less, providing the proper relationship between time at these temperatures and reaction rate is attained.

The diatomaceous earth insulation was probably the source of the water vapor since the flushing action of the argon gas would not be very efficient in such a medium. In addition, oxygen adsorbed by this material at low temperatures would be released gradually as the temperature climbs, thereby tending to increase the partial pressure of the oxygen which, in turn, would alter the sample if the capacity of the buffer were exceeded.

The approximate volume of the gas in the bell jar in Apparatus I was 4.9 liters. This volume was rather difficult to flush with argon due to the geometry of the system and required a fairly large amount of buffer material.

The geometry of the furnace was such that convection currents caused gas to rush past the sample, which was located immediately above the buffer, thereby creating a time lag between the sample's requirements on the partial pressure of the oxygen and the buffer's regulation of the same everywhere inside the bell jar.

The heating coil of the furnace was not non-inductively would and resulted in an alternating 60 c.p.s. magnetic field of approximately 18 oersteds. This could conceivably alter electrical processes and chemical kinetics.

Finally, the incorporation of A.C. measurements into Apparatus II should facilitate the interpretation of those samples which exhibit considerable polarization effects.

Therefore, Apparatus II was devised in such a manner as to eliminate or minimize the above effects; the heater coil was wound non-inductively; no insulation material was required inside the volume to be controlled by the buffer; convection is reduced to a minimum due to the horizontal position of the tube through the furnace; the volume to be controlled by the buffer has been greatly reduced; the flushing action of the argon gas is much more effective; and a few alterations in circuitry now permit A.C. measurements.

3.4 Apparatus II

3.41 General

The re-designed apparatus is illustrated in Figures III-1, III-2, III-5, and III-6.

3.42 Furnace Construction

The furnace winding consists of 23 feet of 0.01 inch platinum wire wound externally and non-inductively on a cylindrical alundum core with inside and outside diameters of 7/8 and 1 1/8 inches respectively and a length of 8 1/2 inches. The heater core is enclosed by a concentric alundum cylinder with inside and outside diameters of 1 3/8 and 1 3/4 inches respectively. Both tubes lie along the axis of a 6 inch diameter steel tube and the space between is filled with high temperature insulation material. The steel cylinder (1) (see Figure III-5) is capped at both ends with 3/8 inch thick "Transite" discs (2) and brass rods (3) hold these in position. The stand (9) for the furnace also supports 2 clamps (8) which stabilize a recrystallized alumina tube (4). This impervious, high-vacuum tube of interlocking corundum crystals passes through the center of the furnace and is sealed at both ends with universal compression seals (5). A combination of glass T's, rubber tubing, and clamps permit thermocouple entries (7) and gas flow (6).

The sample holder (Figure III-6) in the furnace tube

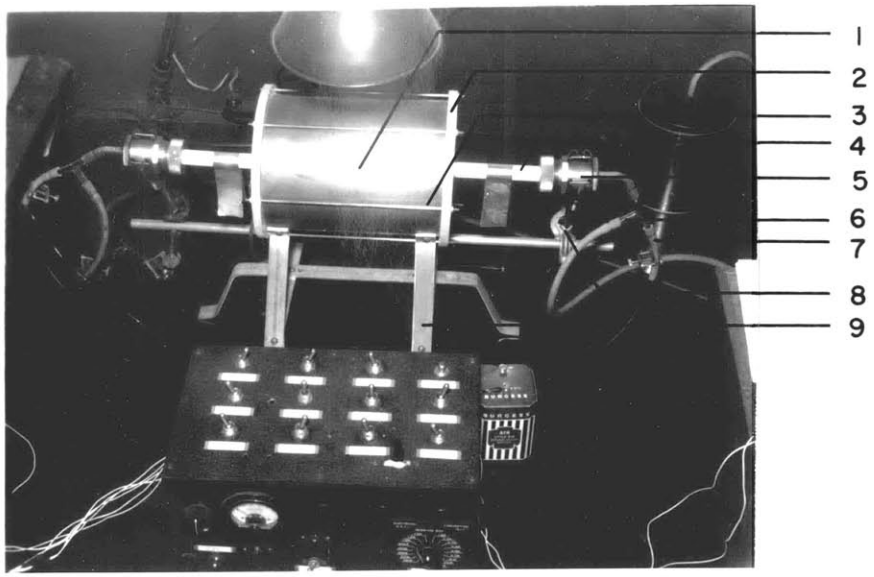

Fig. III-5. Furnace for Apparatus II.

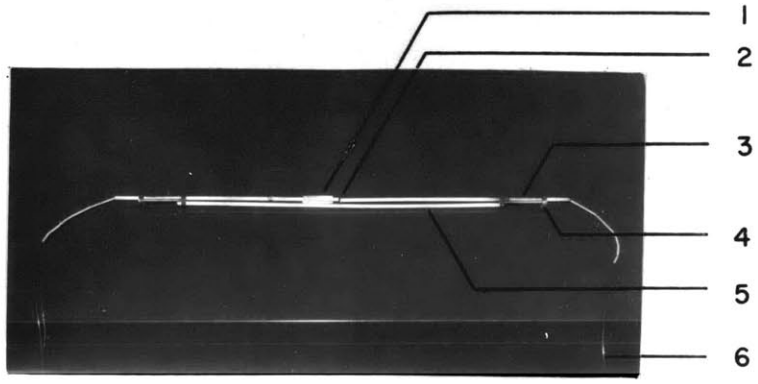

Fig. III-6. Sample holder in the furnace tube of Apparatus II.

is constructed of high temperature ceramic tubes (5) and tool steel stabilizers (4). Set screws in the steel stabilizers hold the ceramic rods in position. Thermocouple rods, pushed together by the spring (3), position the sample at (2) and allow for expansions and contractions of the sample during the heating cycle. Thermocouple leads are located at the ends of the ceramic tubes (6) and the platinum buffer container at (1).

3.43 Control Box

The control box is essentially the same as that in Apparatus I except for a few minor alterations. These are the addition of switches (l), (m), (n), and (o), and decade #1, and the wiring as illustrated in Figure III-2.

3.44 Other Components

The remaining components include those of Apparatus I, a vacuum-tube voltmeter, and an audio oscillator.

IV EXPERIMENTAL PROCEDURE

4.1 Sample Preparation

After numerous mineral specimens were collected, 2 or 3 cores were extracted from each with the aid of a diamond core drill. This core drill functions in a manner similar to those in the petroleum industry in that water is continually circulating the cuttings away from the drilling zone. The cores obtained had diameters on the order of 0.115 inch and varied in length. They were then placed into a special jig and the ends were squared with a diamond saw. After the diameters and lengths of the cores were measured, they were ready to be placed into the furnace.

Prior to being installed in the furnace, each sample was coated on the end faces with a platinum paste made by Johnson-Matthey & Company of London, England (#758). Considerable care was taken in the application of this paste to completely coat the ends of the sample and only these faces. At relatively low temperatures, the volatile component is driven off, leaving behind a thin film of platinum bonded to the surface of the sample and to the thermocouples, thereby insuring good electrical contacts.

4.2 Procedure With Apparatus I

Using Apparatus I, the usual procedure was first to load the buffer mixture and the sample into the furnace. For

conductivity measurements, the sample was located as near as possible to that position in the furnace which exhibited the least temperature gradient. (The temperature profile for the furnace is presented in Figure III-4.) The bell jar was then sealed to the base plate with stop cock grease and flushed with argon gas. After the battery voltage, the potentiometer zero, and the galvanometer were checked, the variac was put into operation to raise the temperature of the furnace. Measurements were recorded approximately every 5 minutes and the variac was adjusted upon completion of each series of measurements.

In the order of their determination, the quantities recorded were: 1) the voltages produced by the upper and lower thermocouples; 2) the galvanometer deflection produced at the end of 15 seconds by allowing the sample itself to drive the current; 3) the shunt position; 4) the galvanometer deflection at the end of the second 15 second interval produced by the battery driving the current through the sample; 5) the galvanometer deflection at the end of the third 15 second interval produced by the battery with its polarity reversed; 6) a repetition of 2); and 7) the room temperature.

In most cases, measurements were made during the heating and cooling of the sample and, in certain instances, one or more re-runs were made on the same sample.

4.3 Procedure With Apparatus II

The measurement technique with Apparatus II was essentially the same as that of Apparatus I. The quantities recorded were: 1) the sum of the thermocouple voltages; 2) the galvanometer deflection produced by allowing the sample to drive the current; 3) the shunt position; 4) the galvanometer deflection produced by the battery driving the current through the sample; 5) a repetition of 4) with the battery polarity reversed; 6) a repetition of 2); 7) the sum of the thermocouple voltages; 8) the room temperature; 9) the voltage reading of the V.T.V.M.; and 10) the sum of the thermocouple voltages. Occasionally, the voltages of the "upper" and "lower" thermocouples were recorded separately to be certain that too large a temperature gradient did not exist across the sample.

The voltage reading of the V.T.V.M. was approximately the total voltage across the sample and the decade #1. This instrument was calibrated in such a manner as to permit the determination of the sample resistance graphically providing the sample exhibited a voltage drop of 1.5 volts R.M.S. for 30 C.P.S. The voltmeter was calibrated on a 1.5 volt basis in order to maintain similar energy dissipation in the specimen in both A.C. and D.C. measurements.

V CHEMICAL ANALYSES

5.1 Spectrographic

Major element analyses of the minerals to be measured were attempted with the aid of the spectrographic facilities of the Cabot Laboratory. The technique followed was that of Jaycox (1947), which is essentially the dilution of the powdered sample with CuO to such an extent that, compared with the quantity of CuO, the elements comprising the sample exist in trace amounts in the final powder which is to be arced. This method has been demonstrated to be very satisfactory for the analyses of numerous ceramic materials. However, the author obtained erroneous results due to a matrix problem.

This type of difficulty follows from the matrix of the sample being different from those of the standards. For example, garnets were analyzed for Fe, Mg, Si, Ti, Al, Mn, and Ca. The usual procedure for iron determination in such a case is to obtain at least two garnets with different known iron concentrations and to prepare standards of different iron contents by combining various proportions of these. The iron contents of the spectrographic samples analyzed must be within these limits. The result of this procedure is that the silicate matrix (individual Si tetrahedra for garnets) will be the same in both the sample and the standards and, assuming no interference from the other elements present and maintaining that arcing conditions are constant, the

differences in the iron spectra will depend only upon the variations in iron content. If there exists a matrix difference, the samples and the standards may or may not arc in a similar manner (e.g.-the temperature of the arc is dependent upon the matrix).

However, properly analyzed garnets with sufficient ranges in iron content were not available and standards were prepared from oxides of the elements to give approximate garnet compositions, hence the matrix problem. Furthermore, this technique would not permit the determination of ferrous and ferric iron as separate entities. Therefore, wet chemical analyses were employed.

5.2 Wet Chemical

Chemical analyses of the minerals to be measured were accomplished following the procedure of Shapiro and Brannock (1956) for the "rapid analysis of silicate rocks". Using this technique, FeO, total iron as Fe_2O_3, MnO, and CaO plus MgO as equivalent MgO were determined for many of the samples and the results are recorded in Table V-1. The two silicates, G-1 and W-1 (see Fairbairn, 1951 and Table V-2) were run along with the samples as a check on the technique of the analyst and the accuracy of the results.

A solution of the samples, prepared by the digestion of the sample with HF and H_2SO_4 was used for the determination of total iron as Fe_2O_3 and MnO by spectrophotometric methods. Total iron was determined with orthophenanthroline and MnO as the permanganate. Additional aliquots of the solution were taken to determine CaO plus MgO as equivalent MgO with an automatic titrator using Versene (disodium ethylenediamine tetraacetate). FeO was determined by titration with $K_2Cr_2O_7$ after decomposition of a separate portion of the sample with HF and H_2SO_4. The latter technique is somewhat questionable as pertains to FeO percentage composition of the total sample but yields the relative values in which the author is interested.

Due to the similarity of compositions, enstatites #2 and #4 were eliminated from the group of samples to be measured. Such was the case with Dunites C and D.

The fayalite samples #1 and #2 exhibit considerably more Mn than would be expected and, therefore, a fair amount of alteration is suspected. On this basis, these samples were also eliminated.

For possible correlation with the results of the electrical conductivity measurements, the ratios Fe_2O_3/MnO, FeO/MnO, equivalent MgO/MnO, Fe_2O_3/FeO, and Fe_2O_3/equivalent MgO were determined and are recorded in Table V-3.

TABLE V-1. CHEMICAL ANALYSES: Rapid Silicate Analyses for Total Iron as Fe_2O_3, MnO, FeO, and CaO Plus MgO as Equivalent MgO in per cent by Weight

* ( ) Average

' One instead of two readings on spectrophotometer

Specimen	Total Fe as Fe_2O_3	MnO	FeO	Equiv. MgO
G - 1	1.78	0.025		1.34
	1.78	0.025		1.27
	(1.8)*	(0.03)		(1.3)
W - 1	11.02	0.204	8.36	14.13
	11.02	0.204	8.28	14.24
	(11.0)	(0.20)	8.42	(14.2)
			(8.4)	
Garnet #102	32.09	12.96	24.83	3.30
	32.13	12.55	26.07	3.21
	(32.1)	(12.8)	(25.4)	(3.3)
Garnet #103	37.38	0.846	30.94	5.51
	37.38'	0.824	31.95	5.46
	(37.4)	(0.84)	(31.4)	(5.5)
Garnet #104	37.76	0.866	31.60	5.45
	37.85	0.848	31.80	5.35
	(37.8)	(0.86)	(31.7)	(5.4)

TABLE V-1. (Continued)

Specimen	Total Fe as Fe_2O_3	MnO	FeO	Equiv. MgO
Garnet #105	34.95	0.920	30.18	7.04
	34.91	0.929	29.70	7.00
	(34.9)	(0.92)	(30.1)	(7.0)
Garnet #106	35.21	0.789	30.42	4.35
	35.27	0.814	30.64	4.22
	(35.2)	(0.80)	(30.6)	(4.30)
Garnet #106 Redox			31.20	
			31.99	
			(31.6)	
Garnet #107	37.97	0.668	30.46	4.96
	37.97	0.668	-	4.95
	(38.0)	(0.67)	(30.5)	(5.0)
Garnet #109	40.29	0.171	33.81	3.90
	40.29	0.177	34.02	3.90
	(40.3)	(0.17)	(33.9)	(3.9)
Garnet #112	8.97	0.204	1.99	24.28
	8.97	0.200	-	24.36
	(8.9)	(0.20)	(2.0)	(24.3)
Garnet #114	0.73	0.034	0.0	
	0.73	0.034	-	
	(0.73)	(0.03)	(0.0)	

TABLE V-I. (Continued)

Specimen	Total Fe as Fe_2O_3	MnO	FeO	Equiv. MgO
Garnet #115	3.72	0.232	1.41	25.01
	3.72	0.225	-	25.00
	(3.7)	(0.23)	(1.4)	(25.0)
Enstatite #1	10.60	0.068		
	10.60	0.049		
	(10.6)	(0.06)		
Enstatite #2	10.52	0.054		
	10.50	0.054		
	(10.5)	(0.05)		
Enstatite #4	9.81	0.200		
	9.75	0.197		
	(9.8)	(0.20)		
Hypersthene #1	19.59	0.344		
	19.59	0.393		
	(19.6)	(0.37)		
Dunite C	8.45			
	8.45			
	(8.5)			
Dunite D	8.30			
	8.36			
	(8.3)			

TABLE V-1. (Continued)

Specimen	Total Fe as Fe_2O_3	MnO	FeO	Equiv. MgO
Dunite G (Gf 1&2)	7.65	0.110		
	7.65	0.104		
	(7.7)	(0.11)		
Fayalite #1	50.38	2.26		
	50.75	2.27		
	(50.6)	(2.3)		
Fayalite #2	50.03	2.35		
	50.03	2.34		
	(50.0)	(2.3)		
Hornblende #1	29.56	1.09		
	29.56	1.09		
	(29.6)	(1.1)		

Table V-2. Results obtained by rapid and conventional analysis of two carefully studied rock samples. (from Shapiro and Brannock, 1956)

[Results shown for conventional method are averages of results obtained by five analysts in another laboratory of the Geological Survey. The samples used are described by Fairbairn and others (1951).]

	Granite (G-1)				Diabase (W-1)			
	Rapid			Conventional	Rapid			Conventional
	1	2	Av.		1	2	Av.	
SiO_2	72.4	72.5	72.4	72.5	52.7	52.7	52.7	52.6
Al_2O_3	14.7	14.3	14.5	14.3	15.3	14.9	15.1	15.2
FeO	.97	.94	.96	.95	8.8	8.8	8.8	8.7
Fe_2O_3	.84	.87	.86	.84	1.2	1.4	1.3	1.4
TiO_2	.23	.24	.24	.25	1.0	1.1	1.0	1.1
MnO	.02	.02	.02	.03	.18	.20	.19	.16
P_2O_5	.08	.07	.08	.09	.17	.16	.16	.15
CaO	1.3	1.4	1.4	1.3	10.8	10.6	10.7	10.9
MgO	.34	.28	.31	.36	6.5	6.7	6.6	6.6
Na_2O	3.3	3.3	3.3	3.3	2.2	2.1	2.2	2.1
K_2O	5.4	5.4	5.4	5.5	.66	.62	.64	.66
H_2O	.30	.32	.31	.34	.52	.56	.54	.59
CO_2	.10	.12	.11	.07	.07	.05	.06	.05
Sum	------	------	99.9	------	------	------	100.0	------
Total Fe as Fe_2O_3	1.8	1.8	1.8	------	10.8	11.0	10.9	------

TABLE V-3. Ratios of the Oxides from Rapid Silicate Analyses

Specimen	$\frac{\text{"}Fe_2O_3\text{"}*}{MnO}$	$\frac{FeO}{MnO}$	$\frac{\text{"}Fe_2O_3\text{"}}{FeO}$	$\frac{\text{"}MgO\text{"}}{MnO}$	$\frac{\text{"}Fe_2O_3\text{"}}{\text{"}MgO\text{"}}$
Garnet #102	2.51	1.98	1.26	0.258	9.74
Garnet #103	44.5	37.4	1.19	6.55	6.80
Garnet #104	44.0	36.9	1.19	6.28	7.00
Garnet #105	38.0	32.8	1.16	7.61	4.98
Garnet #106	44.0	38.2	1.15	5.38	8.19
Garnet #107	56.7	45.5	1.25	7.46	7.60
Garnet #109	237.0	199.0	1.19	23.0	10.3
Garnet #112	45.0	10.0	4.50	122.	0.370
Garnet #114	24.4	0.0	-	-	-
Garnet #115	16.1	6.09	2.64	109.	0.148
Hypersthene #1	53.0				
Dunite G	70.0				
Hornblende #1	26.9				

* "Fe_2O_3" - Total Fe as Fe_2O_3 ; "MgO"plus CaO as Equivalent MgO

VI GARNET SEQUENCE

6.1 General

Since one of the goals of this investigation is to obtain data applicable to the study of the earth's interior, the choice of garnets for study is evident. These, with pyroxenes in eclogite, may well be the principal constituent of the upper mantle and, furthermore, extremely little has been published on their electrical behavior and nothing on their geophysical consequences.

The eclogite facies, omphacite-garnet, is developed in gabbroic rocks, and certain types of these rocks are believed by some to be fairly representative of the mineralogical constitution of the earth at depths. Turner and Verhoogen (1951) demonstrate the chemical equivalence of olivine gabbro and bimineralic eclogite with the aid of the equation:

(6.1-1)
$$\underbrace{3\ CaAl_2Si_2O_8 + 2\ NaAlSi_3O_8}_{\text{Labradorite}} + \underbrace{3\ Mg_2SiO_4}_{\text{Olivine}}$$
$$\underbrace{n\ CaMg(SiO_3)_2}_{\text{Diopside}} = \underbrace{2\ NaAl(SiO_3)_2 + n\ CaMg(SiO_3)_2}_{\text{Omphacite}}$$
$$+ \underbrace{3\ CaMg_2Al_2(SiO_4)_3}_{\text{Garnet}} + \underbrace{2\ SiO_2}_{\text{Quartz}}$$

Certain properties and occurrences of eclogite suggest intrusive or tectonic transport from depths (Turner and Verhoogen, 1951). The high density of eclogite (2.9 - 3.1) and the high specific gravities of accessory minerals such as

rutile, kyanite, and diamond suggest initial conditions of high pressure. There is a constant presence of pyroxene, but the lack of silicates with an OH group. Finally, eclogites show a high susceptibility to retrograde metamorphism as compared with other mineral assemblages. Therefore, Turner and Verhoogen believe that eclogites may possibly originate in the outer part of the mantle, where only basic or ultrabasic material is present.

Lovering (1958), in his investigations into the nature of the Mohorovicic Discontinuity, made studies of eucritic achondrites. He demonstrates that an eclogitic composition, similar to that obtained by Turner and Verhoogen, may be derived from meteoric constituents.

Therefore, garnets and omphacites require conductivity investigations as they may produce a clue to the nature of the internal constitution of the earth.

6.2 Mineralogy

The garnet group (see Dana, 1951 and Kraus, Hunt, and Ramsdell, 1951) includes those minerals in the isometric crystal system with the general formula $R_3^{++}R_2^{+++}(SiO_4)_3$ where R^{++} - Ca, Mg, Fe^{++}, or Mn and R^{+++} - Al, Fe^{+++}, Cr, or Ti^{+++}. Ti may also replace Si in part.

X-ray studies show that garnets are composed of individual silicate tetrahedra, coupled in such a manner as to produce dodecahedral and trapezohedral crystal faces. The SiO_4 tetrahedra are independent of each other ; the R^{+++} atoms lie in the center of a group of six oxygen atoms and the R^{++} atoms in the center of a group of eight oxygen atoms (Dana, 1951).

The different garnet varieties have slight to considerable miscibility with each other and are:

Grossularite	$Ca_3Al_2(SiO_4)_3$
Pyrope	$Mg_3Al_2(SiO_4)_3$
Spessartite	$Mn_3Al_2(SiO_4)_3$
Almandite	$Fe_3Al_2(SiO_4)_3$
Uvarovite	$Ca_3Cr_2(SiO_4)_3$
Andradite	$Ca_3Fe_2(SiO_4)_3$

Their hardnesses range from 6.5 to 7.5, their specific gravities from 3.4 to 4.3, and their colors are red, brown, yellow, green, black, and sometimes white or colorless.

6.3 Experimentation

6.31 General

Garnets were chosen on the basis of color and specific gravity to give a fairly wide range of values for the iron contents. The specimens were then examined macroscopically for twinning, fractures, homogeneity, and massiveness or crystallinity. These are listed in detail in Table VI-1. Samples were cored from these specimens and prepared for conductivity measurements as in the section describing sample preparation, the remainder of the specimens being retained for wet chemical analyses. Quantitative analyses were then made by the "rapid silicate method" (Shapiro and Brannock, 1956) and the results are recorded in Table V-1.

Conductivity measurements were made on the specimens at temperatures up to their melting points and under various conditions. Some of the measurements were performed using Apparatus I, which employed a furnace heating coil that was not non-inductively wound, while those made with the aid of Apparatus II were carried out under non-inductive conditions. Different buffer mixtures were used and, in certain instances, the measurements were made in air for comparison purposes. The pertinent data for the conditions under which these measurements were obtained may be examined in Table VI-2.

The conductivity data for the garnet sequence is illustrated by plots of log σ vs. 1/T in Figures A-1 through

TABLE VI-1. Macroscopic Properties of the Garnet Sequence

Garnet	Properties
#102	Penetration twinning; homogeneous; no alteration.
#103	Single crystal; well developed crystal faces; homogeneous; no alteration.
#104	Same as #103
#105	Single crystal; well developed crystal faces; fairly homogeneous; weathered surface.
#106	Same as #103
#107	Same as #103
#109	Repeated twinning striations; possible internal fractures; fairly homogeneous; no alteration?
#112	Massive; fairly homogeneous; no alteration?
#114	Massive; probably not too homogeneous; no alteration?
#115	Massive and crystalline; multiple twinning striations; fairly homogeneous.

TABLE VI-2. Experimental Conditions Existing During Conductivity Measurements of the Garnet Sequence

Specimen	Run or Rerun	D.C. and/or A.C.	T_{max}(°C)	Apparatus I or II	Buffer	Remarks
Garnet #1	Run 1	D.C.	1100	I	Fe_3O_4	$CaCl_2$ at base of bell jar; did not open furnace between runs; preheated empty furnace while argon flowing; slight melting at T_{max} in run 1→glossy black surface on completion.
	Rerun 1	D.C.	655	I	"	
Garnet #1-Air	Run 1	D.C.	878	I	None	Run in air.
	Rerun 1	D.C.	912	I	"	
Garnet #3	Run 1	D.C.	910	I	0.241 gm Fe per gm Fe_3O_4	Flushed with argon between runs; same buffer throughout runs.
	Rerun 1	D.C.	937	I		
	Rerun 2	D.C.	1104	I		
Garnet #102	Run 1	D.C. and A.C.	910	II	Wustite	Thermocouple failed at T_{max}.

TABLE VI-2. (Continued)

Specimen	Run or Rerun	D.C. and/or A.C.	T_{max}(°C)	Apparatus I or II	Buffer	Remarks
Garnet #103	Run 1	D.C. and A.C.	1011	II	Wustite	No apparent alteration.
Garnet #104	Run 1	D.C. and A.C.	894	II	"	Tube remained sealed between runs buffer → hematite and magnetite; no apparent alteration
	Rerun 1	D.C.	798	II	"	
Garnet #104 Air	Run 1	D.C.	877	II	None	Run in air.
Garnet #105	Run 1	D.C. and A.C.	1030	II	Wustite	
Garnet #106	Run 1	D.C. and A.C.	1042	II	Wustite	
Garnet #106	Run 1	D.C.	901	II	Wustite	Buffer saturated with H_2O and 2 ml at ends of tube; furnace coil failed at T_{max}.
Garnet #106	Run 1	D.C.	980	II	Wustite	H_2O as in Aqueous 1

TABLE VI-2. (Continued)

Specimen	Run or Rerun	D.C. and/or A.C.	T_{max}(°C)	Apparatus I or II	Buffer	Remarks
Garnet #107	Run 1	D.C. and A.C.	1028	II	Wustite	No apparent alteration.
Garnet #109	Run 1	D.C. and A.C.	973	II	Wustite	
Garnet #112	Run 1	D.C. and A.C.	1001	II	Wustite	
Garnet #114	Run 1	D.C. and A.C.	924	II	Wustite	Ends of sample uneven.
Garnet #115	Run 1	D.C. and A.C.	1067	II	Wustite	Ends of sample uneven.

A-31 in the Appendix. Inspection of these graphs and the corresponding compositions of the various garnets shows that similar compositions result in similar conductivity plots, providing measurements were carried out under the same conditions. All garnets measured in an atmosphere controlled by the wustite buffer in Apparatus II exhibit a discontinuity at approximately 570° C and a conductivity peak or a suggestion of a peak at approximately 800° C. The values of the conductivities decrease for a short range of temperatures after the peak temperature, then increase, apparently asymptotic to a line determined by extremely large values for σ_o and E. The cooling curves in each case tend to be straight lines as well as the heating curves in the region below 570° C. Upon reheating, both the heating and cooling curves correspond rather closely to the initial cooling curve providing the maximum temperature in the initial run is not exceeded.

In view of the discontinuity at 570° C in all of the above conductivity plots, let us assume that there may be irreversible processes (chemical, electrical, and/or structural) in operation in the higher temperature region. Then, since the excitation energy E and the constant σ_o probably change with these effects, several straight line segments have been fitted to the plots of log σ vs. 1/T. The vertical line in these plots is located at 570° C.

Since conductivity peaks of the magnitude observed in this investigation were not encountered in earlier studies by others, a discussion of this phenomenon is in order. At

first, it may seem unlikely that such curvature may be readily explained other than to attribute it to some peculiarity of the apparatus or property of the garnets. However, if we consider the possibility that, in certain regions of the data plot, the excitation energy changes rather rapidly with the temperature, a curve could result in the plot especially in the case where measurements have been made at fairly large temperature intervals as compared with the temperature interval required for an observable change in E. On the other hand, if we maintain that the excitation energy remains constant, we may still encounter curvature in regions of the plot where there is an increase in the number of charge carriers, possibly in the region of a structural or chemical change. In particular, if the heating rate were such that dynamic rather than equilibrium conditions prevailed throughout a run, a phase transition (a bond-breaking process) could conceivably begin at a given temperature and yet not complete the process until the system had attained a temperature far beyond that for the transition under conditions close to those for equilibrium. In such a case, the process of rearrangement of ions would greatly increase the potential number of charge carriers throughout this temperature region. Therefore, the possibility of conductivity peaks, as well as straight line segments, should not be ruled out. This discussion will be continued later after the introduction of additional data.

As parameters of possible value in the interpretation of the data, the following quantities have been extracted from the graphs: 1) the excitation energy E and the constant σ_o as determined from the slopes and intercepts of the straight line segments; 2) the peak conductivities of certain curved portions and the associated temperatures; and 3) the differences in conductivity values as determined by passing current through the sample in the forward and reverse directions (see Table VI-3).

6.32 Comparison of Results from Apparatus I and Apparatus II

At this point, it might be well to consider Figures A-5 through A-7 and A-11 through A-13 for garnets #3 and # 104. Both garnets were obtained from the same specimen, but #3 was measured with Apparatus I and #104 with Apparatus II. Garnet #3 exhibits remarkable correspondence between heating and cooling curves on the initiial run and subsequent runs, expecially in the high temperature region, while #104 produces a plot similar in characteristics to others measure with Apparatus II. Since the main differences between the two systems are that water condensed in Apparatus I, while Apparatus II was essentially free from water and had a non-inductively wound furnace coil, are the differences between the conductivity plots due to: 1) the effect of water on the chemical nature of the sample or on rate processes; 2) magnetic effects associated with the coil windings; 3) chemical alteration

TABLE VI-3. Parameters Extracted from the Plots of Log σ vs. 1/T for the Garnet Sequence

E - electron volts [as in $\sigma = \sigma_o \exp(-E/kt)$]

σ_o - $(\text{ohm-centimeters})^{-1}$

[d] - difference in σ between forward and reverse measurements

Specimen	Run or Rerun	D.C. or A.C.	E	Line	σ_o	Peak	Remarks
Garnet #1	Run 1	D.C.	1.52	1	5.58×10^{3}		[d]Very little
			0.649	2	1.41×10^{-1}		
			1.33	3	1.18×10^{2}		
			10.45	4	2.62×10^{37}		
			0.535	5	3.50×10^{0}		
Garnet #1	Rerun 1	D.C.	0.377	1	1.17×10^{-1}		[d]Very little
			0.471	2	1.08×10^{0}		
			0.549	3	3.68×10^{0}		
			0.462	4	1.25×10^{0}		
Garnet #1 Air	Run 1	D.C.	1.72	1	1.30×10^{5}		[d]Very little
			0.613	2	5.58×10^{-2}		
Garnet #1 Air	Rerun 1		0.549	1	1.79×10^{-2}		[d]Very little
Garnet #3	Run 1		1.18	1	2.74×10^{1}	None	[d]Very little
			1.36	2	9.29×10^{1}		
			0.889	3	1.06×10^{0}		

TABLE VI-3. (Continued)

Specimen	Run or Rerun	D.C. or A.C.	E	Line	σ_o	Peak	Remarks
Garnet #3	Rerun 1	D.C.	1.39	1	1.60×10^{2}	None	[d]Very little
Garnet #3	Rerun 2	D.C.	1.37 2.78	1 2	1.26×10^{2} 5.97×10^{7}	None	[d]Very little except below 570°C.
Garnet #102	Run 1	D.C.				6.5×10^{-4} @0.926 & suggest. 2.6×10^{-4} @1.098	[d]Little
Garnet #102	Run 1	A.C.				6.3×10^{-4} @0.965 & suggest. 2.8×10^{-4} @1.100	
Garnet #103	Run 1	D.C.	1.41 3.61 1.41 1.23	1 2 3 4	4.38×10^{2} 4.14×10^{10} 9.31×10^{1} 1.31×10^{1}	1.2×10^{-4} @0.913	[d]Very little
Garnet #103	Run 1	A.C.	**		**	1.1×10^{-4} @0.930	A.C. values lower than D.C. on high T side of peak.

TABLE VI-3. (Continued)

Specimen	Run or Rerun	D.C. or A.C.	E	Line	σ_o	Peak	Remarks
Garnet #104	Run 1	D.C.	1.55 1.32 1.56	1 2 3	5.87×10^{3} 7.94×10^{1} 4.94×10^{3}	8.0×10^{-5} @0.955	[d]Very little
Garnet #104	Rerun 1	A.C.	**		**		A.C.peak approx. same as D.C.
Garnet #104	Run 1	D.C.	1.02 0.875 1.12	1 3 2	2.82×10^{0} 5.28×10^{0} 9.89×10^{-1}	None	[d]Very little
Garnet #104 Air	Run 1	D.C.	1.69 0.571 0.450	1 2 3	1.29×10^{5} 2.15×10^{-1} 4.20×10^{-2}	8.8×10^{-4} @0.900 & suggest. @ lower T	[d]Very little
Garnet #104 Air	Run 1	A.C.	**		**		A.C. values sli. higher than D.C. before peak; coincide thru cooling
Garnet #105	Run 1	D.C.	1.19 2.27 1.72 1.41	1 2 3 4	2.01×10^{1} 8.32×10^{4} 6.04×10^{2} 1.90×10^{1}	2.1×10^{-5} @0.963	[d]Very little

TABLE VI-3. (Continued)

Specimen	Run or Rerun	D.C or A.C.	E	Line	σ_o	Peak	Remarks
Garnet #105	Run, 1	A.C.	**		**		Lines thru A. C. points give same slopes but sli. higher σ_o.
Garnet #106	Run 1	D.C.	1.20 9.31 0.749	1 2 3	1.07×10^{1} 1.95×10^{32} 4.42×10^{-1}	6.9×10^{-6} @0.898	[d]fair in high T region.
Garnet #106	Run 1	A.C.	**		**		A.C.peak coincides with D.C. peak.
Garnet #106 Aqueous 1	Run 1	D.C.	1.09 1.31	1 2	2.24×10^{0} 4.90×10^{0}	suggestion of peak	[d]Very little
Garnet #106 Aqueous 2	Run 1	D.C.	1.02 1.58 1.22 1.08	1 2 3 4	8.09×10^{-1} 6.43×10^{1} 1.59×10^{0} 3.07×10^{-1}	suggestion 8.3×10^{-6} @0.919	[d]Very little
Garnet #107	Run 1	D.C.	5.67 1.23 0.901	1 2 3	3.94×10^{18} 2.37×10^{1} 6.25×10^{-1}	3.9×10^{-5} @0.960	

TABLE VI-3. (Continued)

Specimen	Run or Rerun	D.C. or A.C.	E	Line	σ_o	Peak	Remarks
Garnet #107	Run 1	A.C.	5.30 1.25 0.903	1 2 3	1.85×10^{17} 3.32×10^{1} 7.33×10^{-1}	5.5×10^{-5} @0.960	A.C. values sli. higher than D.C.; peak not well defined.
Garnet #109	Run 1	D.C.	1.45 1.37 0.959 0.806	1 2 3 4	7.16×10^{3} 1.30×10^{2} 1.34×10^{0} 1.71×10^{-1}	6.6×10^{-3} @0.925	[d]Very little
Garnet #109	Run 1	A.C.	**		**		A.C. peak approx. same as D.C. peak.
Garnet #112	Run 1	D.C.	0.707 1.48 0.487	1 2 3	7.40×10^{-2} 4.85×10^{1} 5.89×10^{-3}	3.7×10^{-5} @0.950	[d]Very little
Garnet #112	Run 1	A.C.	**		**		A.C. peak coincides with D.C. peak.
Garnet #114	Run 1	D.C.					Rapid, extreme drift of galv. deflection at high T.

TABLE VI-3. (Continued)

Specimen	Run or Rerun	D.C. or A.C.	E	Line	σ_o	Peak	Remarks
Garnet #114	Run 1	A.C.					A.C. values lower than D.C. by factor of 3 at worst.
Garnet #115	Run 1	D.C.	1.79 1.27 0.600	1 2 3	2.53×10^{4} 3.21×10^{-1} 3.47×10^{-4}	2.8×10^{-5} @0.955	[d]little in high T region.
Garnet #115	Run 1	A.C.	**				A.C. peak coincides with D.C. peak.

through oxidation or reduction of cations; or 4) other effects? The ideal procedure would have been to continue using the same specimen, but sufficient material was not available. Therefore, further investigations were carried out with garnet #106.

6.33 Changes in Conductivity Due to the Presence of an Aqueous Vapor Phase

In order to investigate the effect of water vapor in the system on the values obtained for the electrical conductivities, a sample from garnet #106 was prepared and placed in the furnace as in previous measurements but, in this case, the buffer was saturated with water and approximately 2 ml of water was introduced into the ends of the gas-tight tube. The tube was partially sealed, flushed with argon gas for 10 minutes, and then completely sealed for conductivity measurements. Due to failure of the furnace coil at the maximum temperatures in this run, a second sample was measured in order to determine the nature of the cooling curve. The results of these runs are plotted in Figures A-20 and A-21. It is to be noted that the aqueous runs give almost identical curves and that the conductivity in the peak area is less by approximately one order of magnitude than that of the normal run in Figure A-18. Aqueous run #2 agrees well with the normal run in the temperature region above the peak area but does not show the same separation of points at a given temperature.

Therefore, water vapor reduces the conductivity in the conductivity peak region and prevents the separation of points (from measurements in the forward and reverse directions) in the high temperature region. Furthermore, there is little difference between the initial slopes of the dry and aqueous runs in the region below 570° C, illustrating that an aqueous vapor has little effect in this region.

6.34 Efficiency of the Buffer in Preventing Sample Alteration

A large sample from garnet #106 and approximately 0.2 gm of buffer mixture were placed in the furnace, which was then flushed with argon gas for 15 minutes. The furnace tube was sealed and heated to 800° C in 1.3 hours. The temperature was maintained between 800° and 826° C for 5 hours, whereupon, it was gradually decreased, the entire heating and cooling process requiring about 8 hours. Sebsequent wet-chemical analyses demonstrated the ferrous iron content to be very close to those values for #106 in Table V-1, thereby confirming the fact that the buffer is efficient in preventing significant oxidation or reduction of the ferrous iron content in this garnet for periods of time of at least 8 hours (the approximate length of time required for a run) at elevated temperatures.

6.35 Changes in Conductivity due to Sample Oxidation

An initial run and a rerun, under conditions of a buffered atmosphere, were made on garnet #104 (Figures A-11 through A-13). Following these, a third run was made with air passing through the furnace tube at a rate of approximately 100 cc per minute (Figures A-14 and A-15). The most striking difference between these curves is the increase in conductivity upon cooling for the oxidized sample. Furthermore, the conductivity as a whole for both heating and cooling curves is greater when the specimen is run in air. Garnet #1 (Figures A-1 through A-4), which was also run in air, shows a similar increase in conductivity between the heating and cooling curves. The subsequent rerun of garnet #1 in air demonstrates further that the major part of the alteration occurred during the initial run. The similarity of the heating curves for this specimen run in air and the curve for the same specimen run in a buffered atmosphere demonstrates that Fe_3O_4 had no buffering effect and that both runs indicate oxidation of the sample.

The effects of oxidation might have been anticipated if one were familiar with the work of Engelhard (1933, as in Mott and Gurney, 1953) and others on Cu_2O. Experiments performed by Engelhard (1933) and Juse and Kurtschatow (1933, as in Mott and Gurney, 1953) show that the conductivity of Cu_2O increases with increasing oxygen content. Engelhard

carried out further measurements for the Hall effect and found that the current was being carried by positive holes, thereby making the material a defect conductor.

Therefore, we see that a buffered atmosphere is an absolute necessity in measuring conductivities of the rock-forming minerals containing ferrous iron and that any conductivity measurements obtained in air may tend toward values that are excessively large.

6.36 Dependence of the Electrical Conductivity upon Chemical Composition

The conductivity plots of the garnet specimens (see Figures A-8 through A-31) were compared and Tables V-1, V-3, and VI-3 were examined in order to determine the dependence of the electrical conductivity on chemical composition.

For all the garnet specimens as a group which were run in an atmosphere buffered with wustite in Apparatus II, the slopes of the initial heating curves in the region below 570° C do not appear to depend upon the abundance of any particular element in Table V-1 (e.g.-there are no trends in the magnitudes of the excitation energies (E) or the constants (σ_0) with the percent by weight of ferrous iron oxide). However, with the exception of garnet #112, the magnitudes of the tabulated excitation energies suggest that "Fe_2O_3"/FeO may be important since these increase with this ratio. In this case, the comparison of the garnet specimens should probably be

made only on the basis of garnets #103 through #107 since we do not know the effects of twinning, the degree of crystallinity, and other differences listed in Table VI-1. Using these specimens only, E and σ_o increase with increasing FeO and Fe_2O_3 (actual) contents respectively. Other chemical oxides or ratios show no trends.

Between 570° C and the maximum temperatures, each conductivity plot exhibits a peak and then a decrease in the conductivity before a final rise beginning in the temperature region 1040° - 1210° K (i.e.- 1/T - 0.96 to 0.83). There is no apparent correlation of the magnitudes of the conductivity peaks or the temperatures at which there peaks occur with the tabulated chemical data except for a possible dependence of the temperature at which the peak occurs in specimens #103 through #107 on the ratios "MgO"/MnO.

Upon cooling, the curves become well-defined straight line segments. When the first straight line segment of each garnet cooling curve is compared with the chemical data, it becomes evident that, on the basis of garnets #103 through #107, there is a correlation of E and σ_o with the "MgO" content (i.e.-E and σ_o increase as the concentration of MgO and CaO as equivalent MgO increases). The ratio "Fe_2O_3"/"MgO" shows the opposite trend but the nature of this is probably due to "MgO"

Further cooling produces new straight line segments in certain instances. For those lines passing completely

through the conductivity peak region or beginning in this region and extending to lower temperatures, there is a possible dependence of E on the "MgO" content.

Therefore, it appears that the lower temperature conductivities depend upon the concentrations of FeO and Fe_2O_3 (actual), the highest temperature conductivities upon "MgO" content, and the intermediate temperature conductivities possibly upon "MgO" and/or "MgO"/MnO.

VII ENSTATITE-HYPERSTHENE SERIES

7.1 General

Since enstatite ($MgSiO_3$) and hypersthene ($FeSiO_3$) may be representative of the earth's mantle, the electrical conductivities of these minerals were measured. That enstatite and hypersthene may predominate in certain portions of the earth is a plausible hypothesis. It is generally accepted that the molten core of the earth is iron or a mixture of iron and nickel and Gutenberg (1951) suggests that the sialic portion of the crust is approximated rather well by a granodioritic composition. Therefore, for a layered earth formed by the differentiation of the chemical components, the siliceous constituents of the crust grade downward (except for chemical discontinuities) into silica-deficient, iron-rich material in the vicinity of the core-mantle boundary. On this basis, then, a mineral such as hypersthene should be more important in the upper regions of the earth, whereas fayalite (Fe_2SiO_4) should become more predominant with depth as the ratio Fe/Si increases.

7.2 Mineralogy

Enstatite and hypersthene are members of the pyroxene group and crystallize in the orthorhombic system. These minerals have structures containing chains of linked SiO_4 tetrahedra and generally contain no Ca and little or no Al (Kraus, et al., 1951). Enstatite and hypersthene are part of a continuous isomorphous series, which has the general formula: $(Mg,Fe)_2(SiO_3)_2$; those specimens containing less than 15% FeO are termed enstatite and those with a greater concentration, hypersthene, with the specific gravity increasing from 3.1 to 3.5 with the iron content (Dana, 1951). The enstatite specimen used in this investigation was cored from a lamellar, homogeneous mass and the hypersthene specimen, from a homogeneous, cleavable aggregate. Finally, it should be pointed out here that both enstatite and hypersthene undergo a phase transformation to monoclinic forms in the vicinity of 1100° C.

7.3 Experimentation

Samples were cored from the specimens and prepared for conductivity measurements as in the section describing sample preparation, the remainder of the specimens being retained for wet-chemical analysis. Quantitative analyses were then made by the "rapid silicate method" (Shapiro and Brannock, 1956) and the results are recorded in Table V-1. The pertinent data for the conditions under which the conductivity measurements were obtained may be examined in Table VII-1 and, the parameters extracted from Figures A-39 and A-40 for log σ vs 1/T, in Table VII-2.

The curve for enstatite in Figure A-39 demonstrates a shape similar to the majority of minerals measured in this investigation. Polarization is considerable to extreme in the temperature region above 570° C and "corrections" made for this effect result in the solid black points as being comparable with the A.C. conductivity. The vertical line at the left side of Figure A-39 is located at 1140° C, the temperature for the transition of enstatite to clino-enstatite. On the basis of the magnitudes of the parameters in Table VII-2, it appears that it is in this temperature region that the conductivity changes from intrinsic semi-conduction to predominantly ionic conduction. The small circles represent points of the cooling curve and demonstrate that the heating and cooling curves do not coincide.

The plot of log σ vs 1/T for hypersthene in Figure A-40 possesses the same general shape as that for enstatite and yields comparable values for the excitation energies, but this is where the similarity ends. The most striking difference is the absence of polarization in the hypersthene measurements. Although not as obvious, another important factor is the overall increase in conductivity by approximately one order of magnitude. Therefore, the enstatite-hypersthene measurements demonstrate the validity of the initial assumption: The high conductivity of iron-rich minerals should minimize the effect of polarization.

TABLE VII-1. Experimental Conditions Existing During Conductivity Measurements of Enstatite, Hypersthene, Quartz, and Hornblende

Specimen	Run or Rerun	D.C. and/or A.C.	T_{max}(°C)	Apparatus I or II	Buffer	Remarks
Enstatite 1	Run 1	D.C.	1308	II	Wustite	A.C. oscillator failed.
Hypersthene 1	Run 1	D.C.	1306	II	Wustite	
Quartz 1	Run 1	D.C.	1276	II	Wustite	Thermocouple failed.
Hornblende 1	Run 1	A.C.	1103	II	Wustite	Furnace coil failed @T_{max}; sample showed signs of melting

TABLE VII-2. Parameters Extracted from the Plots of log σ vs. 1/T for the Enstatite, Hypersthene, Quartz, and Hornblende Specimens

E - electron volts [as in $\sigma = \sigma_o \exp(-E/kT)$]

σ_o - $(\text{ohm-centimeters})^{-1}$

[d] - difference in σ between forward and reverse measurements

Specimen	Run or Rerun	D.C. or A.C.	E (ev)	Line	σ_o ($\Omega^{-1}cm^{-1}$)	Peak	Remarks
Enstatite #1	Run 1	D.C.	0.860	1	3.29×10^{-2}	9.8×10^{-4} @ 0.978	[d]extreme above 570° C.
			1.18	2	3.90×10^{-1}		
			1.94	3	1.59×10^{2}		
Hypersthene #1	Run 1	D.C.	1.15	1	1.50×10^{1}	1.0×10^{-3} @ 0.925	[d]very little; equipment difficulties in high T region as approx. values.
			2.51	2	1.69×10^{9}		
			1.04	3	1.12×10^{1}		
			2.67	4	2.74×10^{6}		
			0.919	5	5.20×10^{-1}		
			1.25	6	6.67×10^{1}		
Quartz #1	Run 1	D.C.	0.430	1	4.99×10^{-5}		[d]extreme in high T region.
			4.62	2	2.40×10^{10}		
Hornblende #1	Run 1	A.C.	0.662		4.87×10^{1}		Essentially single straight line to melting point.

VIII HORNBLENDE

8.1 General

When it became evident that water vapor in the furnace system affects the values of the conductivities in the intermediate temperature region, it was decided that hornblende conductivity measurements might help to determine more facts concerning this effect. This assumption was made not only due to the fact that hornblende usually contains on $(OH)^-$ radical, but also due to the possibility of excess water having been trapped in the interstices of the crystal at the time of formation.

8.2 Mineralogy

Hornblende, a member of the amphibole group, crystallizes in the monoclinic system and differs structurally from the pyroxenes, enstatite and hornblende, in that it is composed of double silicate chains. The specific gravity may range from 2.9 to 3.3, depending upon the chemical composition, which may be considered as being composed, in varying proportions, of $Ca_2(Mg,Fe)_4Al(OH)_2(AlSi_7O_{22})$ and $Ca_2Na(Mg,Fe)_4$-$Al(OH)_2(Al_2Si_6O_{22})$. In addition to the $(OH)^-$ radical, a small amount of water is usually present (Kraus, et al., 1951). The sample used in the present investigation was a black, homogeneous, single crystal and showed no evidence of alteration.

8.3 Experimentation

A sample was cored from the hornblende specimen and prepared for conductivity measurements as in the section describing sample preparation, the remainder of the specimen being retained for wet-chemical analyses (see Table V-1). The pertinent data for the conditions under which the conductivity measurements were obtained may be examined in Table VII-1 and, the parameters extracted from Figure A-42 for log σ vs 1/T, in Table VII-2.

Since the D.C. equipment was not designed to handle such large conductivities, only A.C. measurements are illustrated. However, in the lower temperature regions where D.C. measurements were possible, polarization was not evident. This specimen exhibits a curve for log σ vs 1/T unlike the majority of specimens in that a straight line may be passed through all of the low temperature points on the graph on into the temperature region of the conductivity peak illustrated by other curves. It is difficult to state with certainty whether or not a conductivity peak occurs here since the conductivity decreases with extreme rapidity on the high temperature side of this region. Upon completion of the run, it was observed that the sample had decreased in length and bulged slightly at the sides, thereby indicating that partial melting had taken place. A change in the sample's dimensions in this direction should result in an increase in the apparent electrical conductivity since well-bonded electrode contacts

were maintained throughout the run. Then, the observed decrease in the conductivity suggests that the predominant conduction mechanism in operation at the lower temperatures ceased suddenly as the melting point was reached and that no new mechanism of any significant magnitude came into play.

It was demonstrated in the previous section (7.3) that the overall magnitude of the conductivity is dependent upon the iron content. According to the chemical data in Table V-1, hornblende contains 29.6% Fe as Fe_2O_3, an intermediate value as compared with the majority of specimens, but has an electrical conductivity that is greater by several orders of magnitude. It may be possible that this is due not only to the constituent cations, but also the $(OH)^-$ radical.

IX OLIVINE SERIES

The possibility that olivine [$(Fe,Mg)_2SiO_4$] may be a major constituent of the earth's mantle is generally agreed upon by most geophysicists and it is because of this that a number of investigations into the electrical properties of members of the olivine series have been carried on in the past. Hughes (1953,1955) has measured temperature and pressure effects on the conductivity of olivine, both individually and simultaneously. Balchan and Drickamer (1959) examined the variation of the absorption edge of olivine as a function of temperature and pressure, as did Runcorn and Tozer (1955). However, in many of these measurements sequences, there existed the possibility of alteration of the ferrous iron content in the specimen. Therefore, it seemed worthwhile to determine whether or not the data obtained previously would correspond to measurements performed in a buffered atmosphere.

9.2 Experimentation

A number of samples of dunite (in this case, polycrystalline aggregates containing approximately 90% olivine) were cored, analyzed, and measured as in the previous sections. The chemical data may be found in Table V-1, the conditions under which the measurements were performed in Table IX-1, and, the parameters extracted from the plots of log σ vs 1/T (Figures A-32 through A-38), in Table IX-2.

It is to be noted that these specimens were measured with the aid of Apparatus I and, as mentioned earlier, it is not known how efficiently the buffer prevented alteration of the sample since some water vapor was present in the sealed system and the buffer was not wustite in every case. However, all the dunite curves exhibit peaks similar to other minerals measured in this investigation.

Dunite #H-5 (Figure A-32) illustrates a shift of the conductivity peak to higher temperatures on the rerun and some polarization in the lower and intermediate temperature regions. Dunite #H-6 (Figures A-33 to A-35) demonstrates a conductivity peak in the same temperature region as the initial run for #H-5 and similar values for the conductivities at higher temperatures, but with considerable more polarization. The reruns on #H-6 are interesting in that a "hysteresis" effect is illustrated by the heating and cooling curves for the first rerun and, although the polarization is extreme in the vicinity of the conductivity peak, both reruns demonstrate excellent reproducibility in the high temperature region and little polarization.

Dunites #Gf1 (Figures A-36 and A-37) and #Gf2 (Figure A-38) were two specimens from the same sample. The initial heating curve for dunite #Gf1 exhibits high temperature conductivities almost identical with #H-6, a conductivity peak, and a suggestion of a second conductivity peak. The rerun reproduces the high temperature results well with little

polarization, but the separation of points is extreme at lower temperatures. The maximum temperature attained for dunite #Gf2 was obtained in a series of steps. The specimen was heated to approximately 300° C, cooled to room temperature, reheated to about 700° C, cooled again to room temperature, heated to the vicinity of 1000° C, and then cooled. The conductivity data for #Gf1 is, perhaps, most indicative of the conduction properties of dunites here for comparisons with the other minerals investigated since this is the only dunite specimen that was measured in the same manner.

TABLE IX-1. Experimental Conditions Existing During Conductivity Measurements of the Olivine Sequence

Specimen	Run or Rerun	D.C. and/or A.C.	T_{max}(°C)	Apparatus I or II	Buffer	Remarks
Dunite #H-5	Run 1	D.C.	1337	I	Fe	$CaCl_2$ at base of bell jar; did not open furnace between runs; buffer container close to sample.
	Rerun 1	D.C.	1250	I	"	
Dunite #H-6	Run 1	D.C.	1328	I	1/2 Fe & 1/2 magnetite by vol.	$CaCl_2$ at base of bell jar; flushed with argon between runs; buffer container at bottom of furnace.
	Rerun 1	D.C.	1350	I		
	Rerun 2	D.C.	1338	I		
Dunite #Gf1	Run 1	D.C.	1345	I	Fe & magnetite	Flushed with argon between runs.
	Rerun 1	D.C.	1333	I		
Dunite #Gf2	Run 1	D.C.	350	I	Fe & magnetite	Flushed with argon during Run 1; water condensed during Reruns 1 and 2.
	Rerun 1	D.C.	746	I		
	Rerun 2	D.C.	1001	I		

TABLE IX-2. Parameters Extracted from the Plots of log σ vs. 1/T for the Olivine Sequence

E - electron volts [as in $\sigma = \sigma_o \exp(-E/kT)$]

σ_o - $(\text{ohm-centimeters})^{-1}$

[d] - difference in σ between forward and reverse measurements

Specimen	Run or Rerun	D.C. or A.C.	E (ev)	Line	σ_o ($\Omega^{-1}cm^{-1}$)	Peak	Remarks
Dunite #H-5	Run 1	D.C.	1.03 2.02	1 2	1.35×10 8.65×10^{1}	6.7×10^{-6} @ 0.894	[d]fair; considerable in peak region.
Dunite #H-5	Rerun 1	D.C.				4.8×10^{-5} @ 0.795	
Dunite #H-6	Run 1	D.C.				1.2×10^{-4} @ 0.954	[d]considerable to extreme in high T region.
Dunite #H-6	Rerun 1	D.C.					[d]extreme except in high T region; hysteresis between heating & cooling in peak region.
Dunite #H-6	Rerun 2	D.C.					[d]extreme except in high T region.

TABLE IX-2. (continued)

Specimen	Run or Rerun	D.C. or A.C.	E (ev)	Line	σ. ($\Omega^{-1}cm^{-1}$)	Peak	Remarks
Dunite #Gf1	Run 1	D.C.				4.0×10^{-7} @ 1.185 & 8.4×10^{-8} @ 0.994	[d]extreme in peak area upon cooling.
Dunite #Gf1	Rerun 1	D.C.	2.58	1	1.09×10^{3}		[d]extreme except in high T region.
Dunite #Gf2	Rerun 1 & 2	D.C.				2.2×10^{-6} @ 0.945	[d]extreme in high T region.

X SiO_2

10.1 General

Since SiO_2 is a constituent of many eclogites, the electrical conductivity of a specimen cored from a single crystal of quartz was measured in a controlled atmosphere. The conditions under which the measurements were obtained are recorded in Table VII-1 and, the parameters extracted from the plot of log σ vs 1/T (Figure A-41), in Table VII-2.

10.2 Experimentation

The specimen was prepared in the same manner as the other specimens in this investigation, but no chemical analyses were performed. The α and β quartz regions [regions (a) and (b) in Figure A-41] demonstrate that polarization is all but absent and that the conductivity peak is as predominant as in many of the garnet curves. The tridymite region (c) is characterized by extreme polarization and a change in the conduction mechanism. On the basis of the "corrected" points, it appears that the highest temperature measurements may be located in another conductivity peak area. The cooling curve exhibits even greater polarization and the "corrected" values correspond rather well to the heating curve values in region (c). Upon termination of the run, it was observed that the specimen had not changed its

appearance whatsoever (including the transparency and the formation of fractures).

XI DISCUSSION

11.1 Reproducibility of Measurements

In every specimen measured, there existed a distinct difference between the initial heating curve and the subsequent cooling curve, this difference being rather pronounced in the majority of runs. However, the two samples from garnet specimen #106, which were measured in aqueous vapors (Figures A-20 and A-21), demonstrate that, although the cooling curve differs from the initial heating curve for a particular sample, both of these curves may be reproduced by measuring another sample from the same specimen under similar conditions. The excitation energy E and the value of σ_o for each of the straight line segments of the plot for Garnet #106 - D.C., aqueous 1 were determined as:

Line	E (ev)	σ_o ($\Omega^{-1}cm^{-1}$)
1	1.09	2.24×10^0
2	1.31	4.90×10^0

and those for Garnet #106 - D.C., aqueous 2 corresponding to aqueous 1:

Line	E (ev)	σ_o ($\Omega^{-1}cm^{-1}$)
1	1.02	8.09×10^{-1}
3	1.22	1.59×10^0

The values of the excitation energies for the two cases are observed to be in good agreement. Furthermore, considerable extrapolation is necessary in order to determine the

values of σ_o , a slight variation in the slope of the line resulting in a significant effect on the magnitude of σ_o . Therefore, it appears that the reproducibility of the measurement technique employed in this investigation is very satisfactory.

11.2 Differences Between Initial Heating and Cooling Curves

For the minerals investigated, correspondence between the initial heating and cooling curves for a given sample should not be expected for at least two reasons: 1) the "freezing-in" of defects at elevated temperatures during cooling and 2) the separation of grain boundaries upon cooling during an experimental run.

Solid state theory suggests that conductivity in such crystals is due to the presence of lattice defects (i.e.- atomic displacements or irregularities involving an increase in free energy because of the increased entropy). The equilibrium number of defects, and thus the conductivity, increases rapidly with temperature as $\exp(-E/kT)$. Between the displaced atom and its regular position there will be an energy barrier, of magnitude U say, and if the temperature is reduced rapidly enough, the defect may be "frozen in". Quantitatively, this occurs when:

$$\nu \exp(-U/kT) << 1/t$$

where: ν is the frequency of atomic vibration

$\exp(-U/kT)$ represents the probability of the atom having sufficient energy to overcome the energy barrier

t is the time scale of the experiment

The rate of cooling in the experiment being many orders of magnitude higher than in nature, many more "frozen-in" defects

may be present upon cooling than in the initial heating and the associated conductivity may be correspondingly higher.

The freezing-in of defects, like any other change in the conductivity mechanism, should be revealed by a kink in the log σ vs. 1/T curve. At low temperatures the conductivity is proportional to:

$$n_o \exp(-E'/kT)$$

where n_o is the number of defects (fixed by the freezing-in in excess of the equilibrium number and independent of the temperature at low temperatures) and E' is some excitation energy. At high temperatures, the conductivity is dependent upon:

$$n \exp(-E'/kT) - N \exp(-E/kT)\exp(-E'/kT)$$
$$- N \exp(-[E + E']/kT)$$

where:

$n = N \exp(-E/kT)$ - the equilibrium number of defects

N - the number of atoms capable of displacement

$\exp(-E/kT)$ - the probability of a displacement

In addition to the freezing-in of defects, we must also consider the effect of grain boundary separation. Separation of grain boundaries during heating and cooling, should, at first sight, reduce the conductivity by severing conduction paths. However, new surfaces may be created (e.g.-by the spreading apart of internal fractures) and this may lead to an

an increasing conductivity from surface defects or along surface paths.

Therefore, in view of the above discussion, it is not to be expected that the heating and cooling curves will coincide.

11.3 Polarization and Thermo-electric Effects

The reasons for the measurement procedure followed in Section IV will now become apparent. It was assumed that iron-rich minerals would minimize the effects of polarization and that maintaining a constant temperature with no temperature gradient across the sample would eliminate thermo-electric voltages. In order to check for possible polarization, Coster (1948), employing D.C. techniques, measured the current, first in one direction, then in the reverse direction. He found that, in most cases, the measurements coincided, demonstrating that polarization was negligible. This process was followed in the present investigation and, in addition, thermo-electric effects were sought by allowing the sample itself to drive current through a galvanometer possessing high sensitivity. Furthermore, A.C. measurements were made at 30 c.p.s. and it was observed that A.C. and D.C. measurements coincided in those temperature regions where the D.C. measurements indicated no polarization.

In certain instances, the D.C. points for a given temperature were so different that, in order to use the data, some form of polarization and/or thermo-electric correction had to be made. It was noted that, in most instances, the voltage produced by the sample itself was different before the measurement was performed than after and that it was fairly constant with time. This value was subtracted or added to the for the sample, depending upon the direction of the current

through the sample and whether this "correction" value was obtained before or after the measurement sequence. The "corrected" values coincided fairly well with each other and with the A.C. measurements. Therefore, the "corrected" values represent the A.C. conductivity, the separation of the D.C. points indicating the degree of polarization and thermo-electric effect. Then the A.C. and D.C. conductivity is represented by the same curve when all points coincide and, in the temperature regions where this is not true, there are three values for the conductivity: 1) the D.C. conductivity in the forward direction; 2) the D.C. conductivity in the reverse direction; and 3) the A.C. conductivity. The A.C. conductivity exhibited little frequency effect (i.e.-there was no significant difference in the values for 30, 300, or 3000 c.p.s.). As was expected, the higher temperature regions demonstrated the greatest separation of D.C. values. Although, for the earth, with its sinusoidal electrical variations, it is the A.C. conductivity that should be considered as representative of the actual electrical conductivity, D.C. values are applicable in many instances (i.e.-those temperature regions where A.C. and D.C. values coincide).

11.4 Sources of Error and Accuracy of Results

There are many sources of error inherent in this type of investigation and may be attributed to displacement currents or frequency effects, polarization, electrode phenomena and the associated voltage distribution across the specimen, sensitivity limits of the meters utilized in the actual measurement circuit as well as those used to determine the values of circuit components, the accuracy of the measurements of the dimensions of the specimens, contact and lead resistances, accuracy of the graphical calibration curves for the A.C. measurements, etc.

Calculations demonstrate negligible displacement current for 30 c.p.s. A.C. measurements and no frequency dependence was observed as the frequency was varied from 30 to 300 to 3000 c.p.s. Polarization effects may be essentially "corrected" according to the procedure in Section 11.3. The error introduced by the sensitivity limits of the meters, measurements of sample dimensions, etc. may be determined by the differential approach to error analysis. However, electrode phenomena and the associated voltage distribution across the sample may introduce greater uncertainty into the results than all other sources of error combined.

The voltage distribution across the sample was not considered in this investigation, but Cronemeyer (1952) made measurements of this for single crystals of rutile by placing probes at appropriate intervals across the specimen. He found

that the field is markedly distorted near the electrodes so that the net field in the central portion of the crystal is appreciably smaller than the applied field strength. He shows, further, that the true conductivity may then be considerable different from the overall conductivity (by as much as 1 order of magnitude). This is in accordance with the theory concerning metal-semi-conductor contacts as in Spenke (1958).

Therefore, without data pertaining to this phenomenon in the present investigation, the values obtained for the electrical conductivity data are estimated to be within approximately 10% of the actual values.

11.5 Comparison with Other Investigations

The majority of curves for log σ vs 1/T are quite different from those obtained by other investigators, however, Hughes (1953), Coster (1948), Cronemeyer (1952), and others observed a distinct difference between the heating and cooling curves, a phenomenon noted in this investigation and discussed in Section 11.2. Aside from this, Cronemeyer (1952) is the only one to illustrate a suggestion of a conductivity peak; all others found that the electrical conductivity σ could be represented rather well by $\sigma = \sigma_1 \exp(-E_1/kT) + \sigma_2 \exp(-E_2/kT)$ for any particular temperature. The conductivity peak is the most striking difference between the present and previous investigations and, without a predominant peak, all the curves are quite similar in shape. The present research differs from the others in that the sample was not in contact with the laboratory atmosphere but utilized a buffer in a sealed system to control the partial pressure of the oxygen. Previous calculations demonstrated that the buffer was efficient in controlling the p_{O_2} so as to prevent alteration of the sample and wet-chemical analysis reinforced this argument. Cronemeyer (1952) made measurements of very slightly to extremely reduced single crystals of rutile. Cronemeyer's curves must be somewhat similar to those of the present investigation then due to the absence of oxygen in the system. However, water is produced by $2\ TiO_2 + H_2 \rightleftharpoons Ti_2O_3 + H_2O$ for the slightly reduced case. Garnet #106, measured in an equeous

vapor, was almost without a peak and demonstrated a curve very similar in shape to Cronemeyer's curve for slightly reduced TiO_2, while garnet #106, measured in a dry buffered atmosphere, exhibited a predominant conductivity peak. This suggests that Cronemeyer, if he had eliminated the water vapor from the system prior to measuring the sample and yet prevented oxidation, would have observed a significant conductivity peak.

Therefore, it appears that water vapor tends to prohibit the possibility of a conductivity peak and it may be that the water content of the air in the laboratory is sufficient to eliminate this peak. Garnets #104 and #1, which were run in air, illustrate no conductivity peak and possess curves which approximate those of Hughes (1953) and Coster (1948) more closely than they do the other curves of the present investigation.

The facts are: 1) a dry silicate [i.e.-one containing no H_2O or $(OH)^-$] run in air produces no conductivity peak; 2) a dry silicate run in a dry buffered atmosphere yields a conductivity peak; and 3) a dry silicate run in an aqueous buffered atmosphere gives no conductivity peak. Therefore, one might expect that a mineral containing H_2O or $(OH)^-$ run in a dry buffered atmosphere would produce no conductivity peak, that the same mineral run in air would demonstrate a conductivity peak, and that the same mineral run in an aqueous buffered atmosphere would give a peak. It was pointed out

in Section 9.3 that the curve for hornblende, measured in a dry buffered atmosphere, was a straight line with apparently, not even a suggestion of a conductivity peak and that the maximum temperature attained exceeded that of the melting point of the specimen. Time did not permit the investigation of the other two possibilities by further measurements on hornblende.

It appears, then, that the presence of water vapor in the mineral or the atmosphere surrounding it will greatly influence the shape of the log σ vs 1/T curve and that dry silicates will not exhibit a conductivity peak if water vapor is present.

11.6 Geophysical Implications

11.61 The Possibility of a Phase Transformation at the Mohorovicic Discontinutiy

In order to discuss the electrical conductivity of the earth in anything but general terms, some estimate of the chemical nature of the region of investigation must be at hand. Numerous speculations and hypotheses have been presented, but the ever-increasing compilation of geophysical data is limiting these possibilities rather rapidly. Peridotites, dunites, oxides, sulfides, eclogites, etc. have been suggested as the major constituents of the mantle, but it appears that eclogites conform most thoroughly to the imposed geophysical restrictions on the materials comprising the earth.

The possibility of eclogite at depth has been considered by a number of investigators: Lovering (1957, 1958); Turner and Verhoogen (1951); Verhoogen (1956); Lyubimova (1959); Robertson, Birch, and MacDonald (1957); Birch (1952); and others. Brief mention was made of the works of Turner and Verhoogen (1951) and Lovering (1958) in the section pertaining to the garnet measurements, but, here, we should expand somewhat on the arguments concerning a major eclogitic constituent for the earth.

The chemical composition in the vicinity of the Moho discontinuity has been a subject of considerable controversy. Speculations as to the chemical nature of the earth range

from an earth consisting largely of hydrogen (Kuhn and Rittman, 1941) to one composed primarily of iron, magnesium, oxygen, and silicon. The latter is the most widely accepted view due to the close correspondence of the meteoric and solar abundances of the elements. It is also generally accepted that the material comprising the earth's mantle may be inferred by the chemical composition of stony meteorites, which are supposedly representative of the silicate mantle of the parent meteoric body of planetary dimensions. Lovering (1958) points out that previous models for the composition of the mantle of the parent meteoric body and the earth have been confused by data from a variety of meteoric types and that only achondrites can be legitimately considered as primary sources of the differentiated silicate mantle of the parent meteoric body. On the basis of the abundances of achondrites of a given range in composition, Lovering (1957) arrives at a model in which the outer zone (approximately 60%) of the mantle is composed of basaltic or euchritic achondrites, with compositions very similar to terrestrial basalts and norites.

This hypothesis is not in discord with any concrete facts pertaining to the earth's internal constitution. Many geophysicists visualize a definite chemical change at the Moho, say from basaltic to dunitic material, due in part, perhaps, to Birch's (1952) computations utilizing a number of the properties of dunite. However, Birch (1952) states that "the notion that the mantle consists exclusively of olivine or dunite

finds no support in the chemistry or mineralogy of meteorites". Furthermore, dunites tend to strain the seismic data for the velocities of wave propagation in the upper portion of the mantle and, since the garnets and pyroxene minerals, jadeite and spodumene, show higher velocities (i.e.-an assemblage of olivine, pyroxene such as jadeite and its potassium equivalent, and garnets can have the required velocities), Birch (1952) believes that the eclogite hypothesis should be considered.

Lyubimova (1959) objects to an eclogite concentration in the upper portion of the mantle since, below the oceans, it follows that one should expect a low velocity layer for seismic waves at depths of 40 km. and this has not been observed. However, until it has been demonstrated that this layer is definitely absent, the eclogite hypothesis should not be challenged on these grounds.

There are many more arguments in favor of rather than against the eclogite hypothesis. Turner and Verhoogen (1951) (see section 6.1), on both petrological and geochemical grounds, suggest that basalt, if it undergoes a phase transformation at the Moho, should become a high pressure modification best approximated by eclogite and they illustrate the chemical equivalence of olivine basalts and eclogites (see equation 6.1-1). Similarly, Lovering (1958) refers to the work of Hess and Henderson (1949) which results in the chemical equivalence of euchritic achondrites and eclogites:

(11.61-1) $$\underbrace{4\ CaAl_2Si_2O_8 + NaAlSi_3O_8}_{\text{bytownite}} +$$

$$\underbrace{8\ MgSiO_3 + n\ CaMg(SiO_3)_2}_{\text{pigeonite}} \rightleftharpoons \underbrace{5\ SiO_2}_{\text{quartz}} +$$

$$\underbrace{NaAl(SiO_3)_2 + n\ CaMg(SiO_3)_2}_{\text{omphacite}}$$

$$\underbrace{4\ CaMg_2Al_2(SiO_4)_3}_{\text{garnet}}$$

Finally, Robertson and others (1957), as a result of their investigation of jadeite stability relations to 25,000 bars, conclude that the pressures required to form omphacite in an eclogite are lower, perhaps much lower, than those for the reaction: albite + nepheline = 2 jadeite and that the omphacites in quartz-bearing eclogites would require pressures no greater than those for the reaction: albite = jadeite + quartz. Their equilibrium curves vs. depth illustrate the estimates of continental and oceanic conditions and suggest an eclogite hypothesis.

It appears, then, that the Moho discontinuity may represent a phase change from an eclogitic mantle component to basaltic crustal material. The existence of such a phenomenon could then explain the following (Lovering, 1958): 1) the relationship between the occurrence of diamonds in eclogitic material and the fact that the pressures required to form diamonds are on the order of those in the mantle at 130 - 190 km; 2) there would be no difficulty in determining the parent magma for the variety of differentiated intrusive

and extrusive crustal materials; 3) an eclogite layer of sufficient thickness could produce the equality in the observed heat flows over the continents and oceans; and 4) the existence of a phase change at the Moho provides the mechanism for mountain formation.

Therefore, the presence of eclogite in the upper regions of the mantle is not unreasonable or remote.

11.62 The Electrical Conductivity of the Earth's Crust and Upper Mantle

The electrical conductivity of the upper portion of the earth's mantle may be estimated by analysis of transient variations in the geomagnetic field. Lahiri and Price(1939) employed this approach to obtain the electrical conductivity as a function of depth and suggest probable values for depths as great as 800 km. Some uncertainty in the shielding effect of the oceans results in a corresponding uncertainty in the actual conductivity versus depth distribution. Furthermore, although several distributions are compatible with the observed geomagnetic variations, each curve demonstrates that the conductivity increases rapidly in the upper portion of the earth. Lahiri and Price conclude, then, that their interpretation has greater validity at depth than in the near surface region and, as Rikitake (1951), that the electrical conductivity rises sharply in the upper few kilometers of the earth.

More detailed information pertaining to the near surface region has been acquired by Cantwell (1960). Magnetotelluric sounding techniques were utilized to determine the electrical conductivity at depths on the order of 70 km. Cantwell states that, due to the measurement technique and the method of interpretation, this value may be stretched to 100 km. A discontinuity at these depths demonstrates an abrupt shift in conductivity from $1.25 \times 10^{-6}\ \Omega^{-1}\ cm^{-1}$ to greater

than $1.25 \times 10^{-4}\ \Omega^{-1}\ cm^{-1}$ (the equipment will not permit a distinction between the latter value and infinite conductivity), a shift of at least 2 orders of magnitude. Cantwell proposes an explanation for the conductivity discontinuity: "Above roughly 70 km, the conductivity is determined by pore fluids, with probably some ionic conductivity beginning as the pore fluid conductivity is "squeezed out". At about this critical depth, the temperature effects begin to take over, and from there on the ionic conductivity dominates."

The possibility that the conductivity discontinuity is due to a fairly rapid change in the dominant conductivity mechanism is a plausible argument, however to attribute this to an abrupt change in the water content seems rather unlikely in the absence of a phase change. However, if the presence of a phase change is inferred, then it is conceivable that water could be excluded in the second phase, thus a sudden change in water content.

For the earth, let us assume that this phase change represents a transition from eclogitic to basaltic material at the Moho discontinuity. Since garnets comprise approximately 1/3 of the composition of eclogites, there may be a correlation of the electrical conductivity data in this investigation with the "Ohmo" discontinuity. Furthermore, it may be possible that the Moho and the Ohmo do not necessarily coincide. Therefore, we should look for an abrupt change in electrical conductivity of at least 2 orders of magnitude due to a phase change

from basaltic material and its associated water content to essentially dry eclogite.

In order to make such considerations, we require the variation of the temperature with depth. Numerous estimates have been made by many investigators [MacDonald (1959), Lubimova (1958), Adams (1924), Jeffreys (1929), Gutenberg (1939), Rikitake (1952), Urey (1952), but these require a variety of assumptions, the validity of which would be difficult to test. However, regardless of the approach to this problem, it appears that the temperatures in the vicinity of the Moho discontinuity should fall within the temperature range of 300° to 700° C. MacDonald (1959) states that a temperature much in excess of 600° to 700° C appears unreasonable and illustrates various temperature profiles, depending upon the models employed for a 30 km crust.

However, in the case under consideration, we require different models. Therefore, several temperature distributions have been derived in Appendix II and result in:

(11.62-1) For a single layer (i.e.-no sialic crust):

$$T_2 - \frac{(H - 1/2\,\rho_2 A_2 x)x}{K_2}$$

(11.62-2) For a crust with a total thickness greater than 70 km and a 10 km sialic component:

$$T_2 - \frac{(2H - \rho_1 A_1 x_1)x_1}{2K_1} +$$

$$\frac{(H - \rho_1 A_1 x_1)(x - x_1)}{K_2} - \frac{\rho_2 A_2 (x - x_1)^2}{2K_2}$$

(11.62-3) For a crust with a total thickness of 35 km and a 10 km sialic component floating on a high density mantle:

$$T_3 = \frac{(2H - \rho_1 A_1 x_1) x_1}{2K_1} +$$

$$\frac{(H - \rho_1 A_1 x_1)(x_2 - x_1) - 1/2\, \rho_2 A_2 (x_2 - x_1)^2}{K_2} +$$

$$\frac{[H - (A_1 \rho_1 - A_2 \rho_2) x_1 - A_2 \rho_2 x_2](x - x_2)}{K_3} -$$

$$\frac{1/2\, \rho_3 A_3 (x - x_2)^2}{K_3}$$

(11.62-4) For a crust with a total thickness greater than 70 km and a 20 km sialic component:

Same as equation (11.62-2)

where:

the subscript indicates the specific layer

K_i - thermal conductivity

ρ_i - density

H - heat flux at the surface

A_i - rate of radioactive heat production per unit mass

x_i - thickness of the layer

Fig. XI-1. Temperature vs. Depth for:

A - 10 km granodiorite overlying olivine basalt
B - 20 km granodiorite overlying olivine basalt
C - Olivine basalt
D - 10 km granodiorite and 25 km olivine basalt overlying eclogite

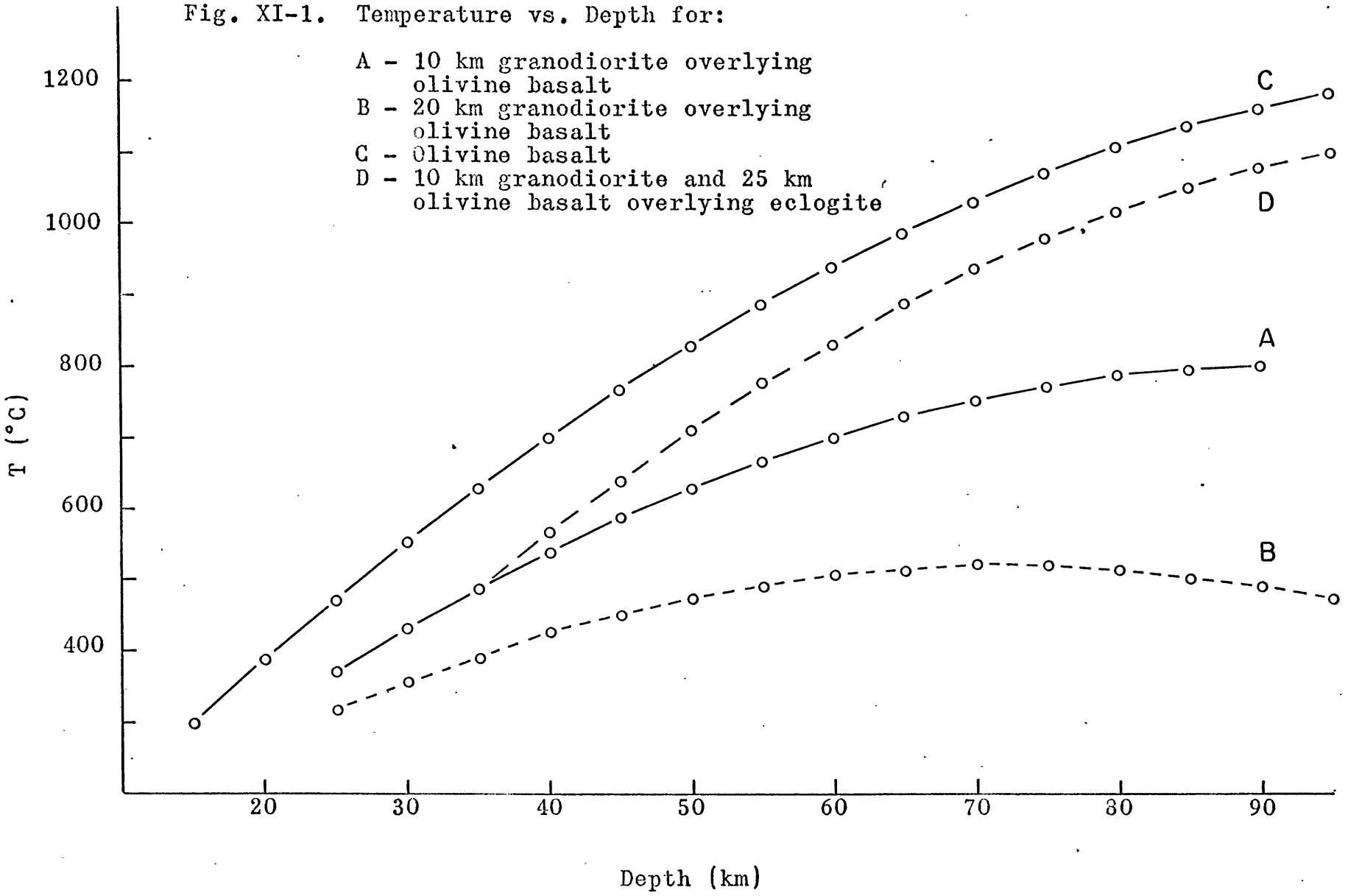

TABLE XI-1. Temperature vs Depth for Models A, B, C, and D as Calculated from Equations (11.62-1) to (11.62-4)*

Depth (km)	Temperature (°C)			
	Curve A	Curve B	Curve C	Curve D
15			295	
20			385	
25	369	313	469	369
30	428	353	550	428
35	484	389	625	484
40	535	421	696	564
45	582	448	763	637
50	624	470	825	707
55	661	487	882	771
60	695	501	935	829
65	723	509	983	883
70	747	517	1027	931
75	766	513	1066	974
80	781	508	1101	1011
85	789	498	1131	1045
90	797	484	1156	1071
95		465	1177	1093

* The values substituted into the equations were:

$H = 1.2 \times 10^{-6}$ cal/cm^2 sec (Bullard, et al., 1956)

$A_1 = 1.2 \times 10^{-13}$ cal/gm sec (Jacobs, 1956)

TABLE XI-1. (Continued)

K_1 - 0.0065 cal/cm sec deg (mean of values in Birch, et al., 1942)

ρ_1 - 2.76 gm/cm^3 (Poldervaart, 1955)

A_2 - 3.5 x 10^{-14} cal/gm sec (Jacobs, 1956)

K_2 - 0.0057 cal/cm sec deg (mean of values in Birch, et al., 1942)

ρ_2 - 2.97 gm/cm^3 (Poldervaart, 1955)

A_3 - A_2

K_3 - K_2

ρ_3 - 3.4 gm/cm^3 (Lovering, 1958 and Birch, et al., 1942)

A temperature distribution has been obtained for each of the preceding cases, subject to certain assumptions: 1) A_i, ρ_i, and K_i are constant throughout a given layer; 2) the portion of the earth that is being considered is small enough as compared with the overall dimensions that plane slabs may be considered rather than the volumes of spherical shells and that the initial temperature conditions in the depths of the earth have little effect on a region so close to the surface; 3) the thermal conductivities of basalt and eclogite are approximately the same; and 4) all phase boundaries are stationary (i.e.-there is no heat production due to phase changes). No measurements have been made of the radioactive heat production in eclogite, but if eclogite may be regarded as a high pressure phase of basalt with the same chemical composition, then both must possess the same radioactive heat production per unit mass (providing one phase does not exhibit a greater affinity for radioactive elements than the other), resulting in a consideration of only the effect of the increased density on the heat flow. Several curves are plotted in Figure XI-1 and the numerical data is tabulated in Table XI-1.

The average thickness of the continental crust is generally accepted as being 35 km, but mountainous regions with "roots" sometimes extend this value to 60 or 70 km. Furthermore, the granodioritic layer in the average continental crust is of the order of 10 km (Gutenberg, 1951). If this layer increases proportionally with the overall thickness,

then a 70 km crust may possess a granodioritic layer as great as 20 km in thickness.

Due to the geographical location of Cantwell's (1960) investigation, some "root" effect should be present. Therefore, the sialic layer should probably range from 10 to 20 km in thickness and the base of the crust should be found at depths greater than 35 km, possible 70 km (the approximate depth of the conductivity discontinuity). Then, possible temperatures at depth for Cantwell's area of investigation should lie between those determined by curves B and D in Figure XI-1.

The question arises as to whether or not the Moho could occur at shallower depths and the conductivity discontinuity still occur at approximately 70 km. Coster (1948) has made conductivity measurements of basalt, gabbro, eclogite, etc., but not under conditions of a controlled atmosphere. We have seen that measurements in a dry buffered atmosphere result in conductivity peaks in most instances while those where water vapor is present yield no peaks or, at least, no peaks of any significant magnitude. Therefore, the effect of a basalt-eclogite phase change on the electrical conductivity may be represented by Coster's curves down to the phase change region and then by the garnet curves from this investigation at greater depths. This assumes that the effects of oxidation are not extreme in Coster's work and that water vapor in the air is the important factor. Since oxidation tends to increase the conductivity in dry silicates,

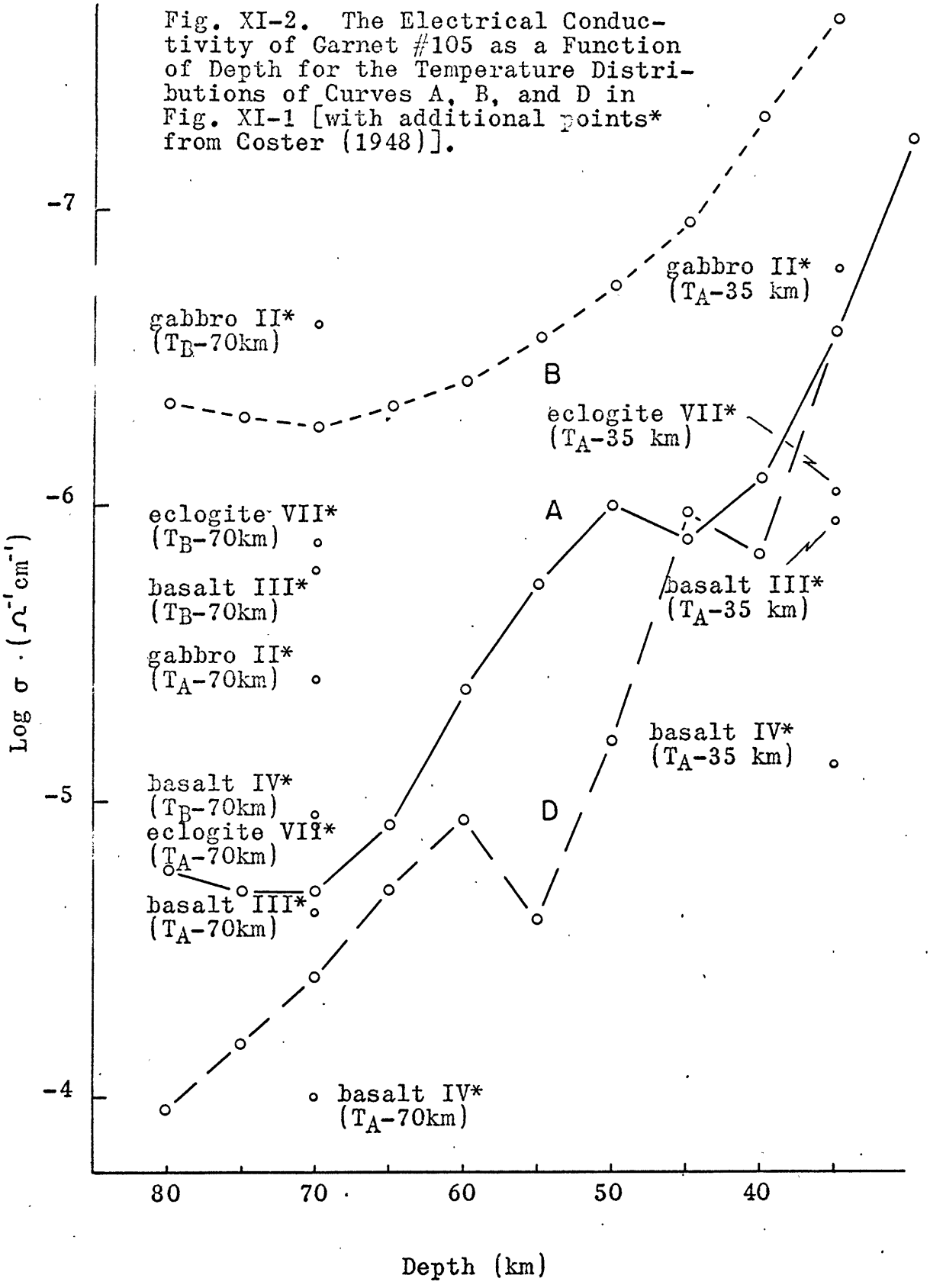

Fig. XI-2. The Electrical Conductivity of Garnet #105 as a Function of Depth for the Temperature Distributions of Curves A, B, and D in Fig. XI-1 [with additional points* from Coster (1948)].

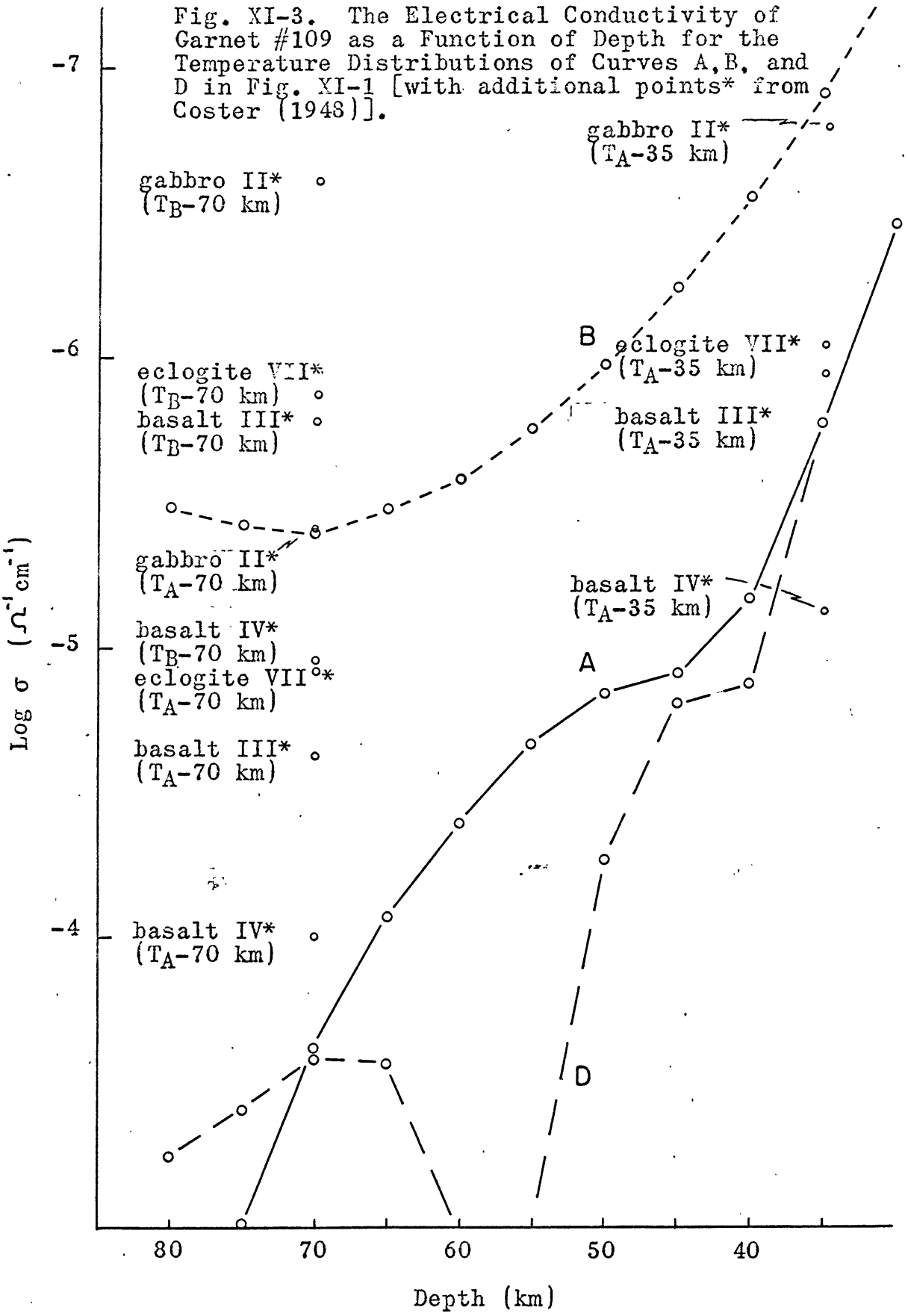

Fig. XI-3. The Electrical Conductivity of Garnet #109 as a Function of Depth for the Temperature Distributions of Curves A, B, and D in Fig. XI-1 [with additional points* from Coster (1948)].

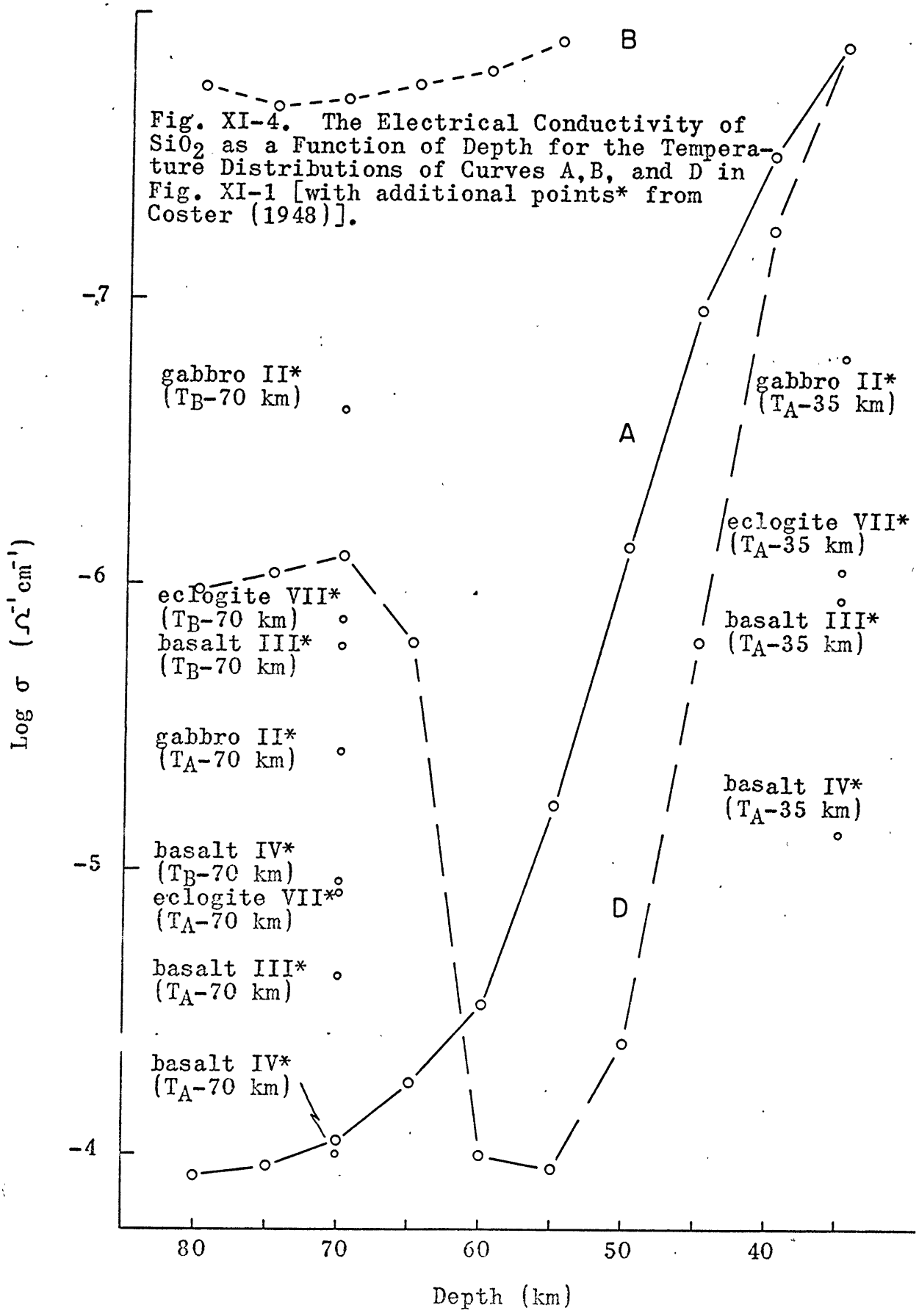

Fig. XI-4. The Electrical Conductivity of SiO_2 as a Function of Depth for the Temperature Distributions of Curves A, B, and D in Fig. XI-1 [with additional points* from Coster (1948)].

his curves should be represented by smaller conductivities if oxidation is significant. Furthermore, such a comparison requires that the electrical conductivity of garnet is essentially the same as for eclogite as a whole and that the pressure effects on Coster's specimens are of the same order of magnitude as on the garnet specimens.

Assuming no pressure effect on the electrical conductivity, the temperature data for curves A, B, and D in Figure XI-1 were used to plot the conductivities of garnets #109 and #105 and SiO_2 as a function of depth (see Figures XI-2 through XI-4). Values of the conductivities for gabbro, basalt, and eclogite have been calculated from Coster's (1948) data for temperatures determined by curves A and B at 70 km and by curve A at 35 km and are also plotted on these Figures. (The values were obtained by substitution of his tabulated ρ_i and A_i into: $\sigma = A_1 \exp[-\epsilon_1/kT] + A_2 \exp[-\epsilon_2/kT]$.)

It is immediately obvious that the curves here are quite different from those obtained by assuming that a single conductivity mechanism is predominant [e.g.-see Cantwell (1960)]. In particular, the plot of log σ vs depth for garnet #109, associated with the temperature distribution of curve A, demonstrates a rapid increase in the electrical conductivity at depths on the order of 60 km. The temperature in this region corresponds to the temperatures required to observe the conductivity peak in garnet #109 and, due to the flatness of the temperature distribution curve, the peak represents a

considerable vertical spread (i.e.-a fairly thick zone with high conductivity). Although it is not shown here, the curve should demonstrate a decrease in conductivity at greater depths prior to the final increase associated with the predominance of ionic conductivity.

Coster's curves should represent the lower part of the crust down to the Moho discontinuity, at which point, the curves from the present investigation should be utilized (in this case, garnet #109). The basal portion of the crust is generally accepted as being of basaltic composition, but not necessarily basalt. For the same composition, we may have gabbro, basalt, basalt glass, or eclogite, but density considerations and thermodynamics suggest gabbro or basalt, most likely gabbro. If the Moho occurs at 70 km and the temperature is determined by curve A, then a phase change from gabbro to eclogite would result in an abrupt shift in the conductivity from $3.9 \times 10^{-6}\ \Omega^{-1}cm^{-1}$ to $2.4 \times 10^{-4}\ \Omega^{-1}cm^{-1}$ [approximately 2 orders of magnitude in the same conductivity region as Cantwell's(1960) measurements]. A basalt-eclogite phase change produces a discontinuity of less than 1 order of magnitude and, basalt glass-eclogite, much less. Therefore, within the limitations imposed by the previous assumptions, a gabbro-eclogite phase transition at 70 km conforms conductivity-wise to the magneto-telluric data remarkably well.

The plot of log σ vs depth for garnet #109, associated with the temperature distribution of curve B, is a smooth curve since the maximum temperature attained is below that of

the conductivity peak region. The gabbro-eclogite phase change in this case gives rise to an increase in conductivity of approximately 1 order of magnitude, basalt-eclogite an increase of less than 1 order of magnitude, and basalt glass-eclogite a decrease in conductivity. This case does not appear to fit the magneto-telluric data.

The third temperature distribution for garnet #109, based on a 10 kmsialic layer, 25 km of basaltic material, and eclogite below this, results in a log σ vs depth curve which is contracted laterally as compared with the previous example and demonstrates higher conductivities at shallower depths. For this model, a peak occurs in the conductivity between 55 and 60 km. The range of depths covered by this peak is much less than that for the preceding peak. However, the peak area may be shifted to greater depths and somewhat greater vertical extent by adjustment of the parameters influencing the shape of the temperature vs depth curve. It appears, then, that a rapid change in conductivity could occur at a depth of 60 to 70 km, demonstrating a change of at least 2 orders of magnitude in a depth interval of 10 km. Possible, this may also correspond to the magneto-telluric data, the important point being that, for this case, the Moho occurred at 35 km and, in the other case, the top of the mantle was taken at 70 km. However, for a gabbroic basal crustal layer, magneto-tellurio measurements should indicate a jump in conductivity of approximately 1 order of magnitude in the vicinity of 35 km as well as several orders of magnitude increase in the 60-70 km

region.

Similar curves have been plotted for SiO_2 and garnet #105 and may be analyzed in an analogous manner. Garnet #105 exhibits the same type of curve as garnet #109, but with a depressed peak for the case of the 3-layer problem and conductivities, in general, on the order of a factor of 10 less. The curve for SiO_2 is also similar, but demonstrates a wider range of magnitudes and rates of change for the conductivity.

It was assumed previously that A_i, ρ_i, and K_i are constant for a given layer. A_i and ρ_i approximate this requirement, but K_i requires further consideration. Birch and Clark (1940) measured the thermal conductivity of a number of rocks in order to determine the dependence upon temperature and chemical composition. The highest temperatures attained were 300° C, except for a diabase and gabbro sample, which were carried to 400° C. The crystalline diabase and gabbro samples exhibit little variation of K with temperature and, for two samples, K remained essentially constant. However, diabase glass, Rockport granite, and Westerly granite demonstrated a change in K between 100° and 200° C of approximately 10.0%, 11.7% and 5.6% respectively. This change is, no doubt, due to the effect of radiative heat transfer. Clark (1957) shows that the contribution of radiation to thermal conductivity is approximated by:

(11.62-5) $$C_r = \frac{16\, n^2 s\, T^3}{3\epsilon} \approx \frac{22 \times 10^{-12} T^3}{\epsilon} \quad \text{cal/cm sec °C}$$

where: s - Stefan - Boltzmann constant

n - index of refraction (~ 1.7 for ferromagnesian silicates)

and, futhermore, that ϵ is probably of the form:

(11.62-6) $$\epsilon = \frac{\epsilon_o + 120\pi\sigma_o \exp(-E/2kT)}{n}$$

where: ϵ_o - the opacity at low temperatures (~ 10 cm^{-1})

$\sigma_o \exp(-E/2kT)$ - the electrical conductivity

resulting in: $$K = C + C_r$$

$$= C + \frac{16\, n^3\, s\, T^3}{n\epsilon_o + 120\pi\sigma_o \exp(-E/2kT)}$$

where: C - the thermal conductivity at low temperatures

Since the granodioritic layer of the crust does not experience very high temperatures, the variation of thermal conductivity with temperature will not be great. The basaltic or gabbroic layer can have, essentially, a constant thermal conductivity (see Birch and Clark, 1940), but eclogite, if the garnet content is the prime factor, should exhibit considerable radiative effects. Therefore, C_r for garnet #109 was plotted as a function of the temperature in Figure XI-5 as if electronic conduction predominated throughout the run. We see, then, that the thermal conductivity K for garnet #109 is approximately 1 1/2 times that of gabbro (~ 24 watts/cm deg at low temperature) at temperatures on the order of

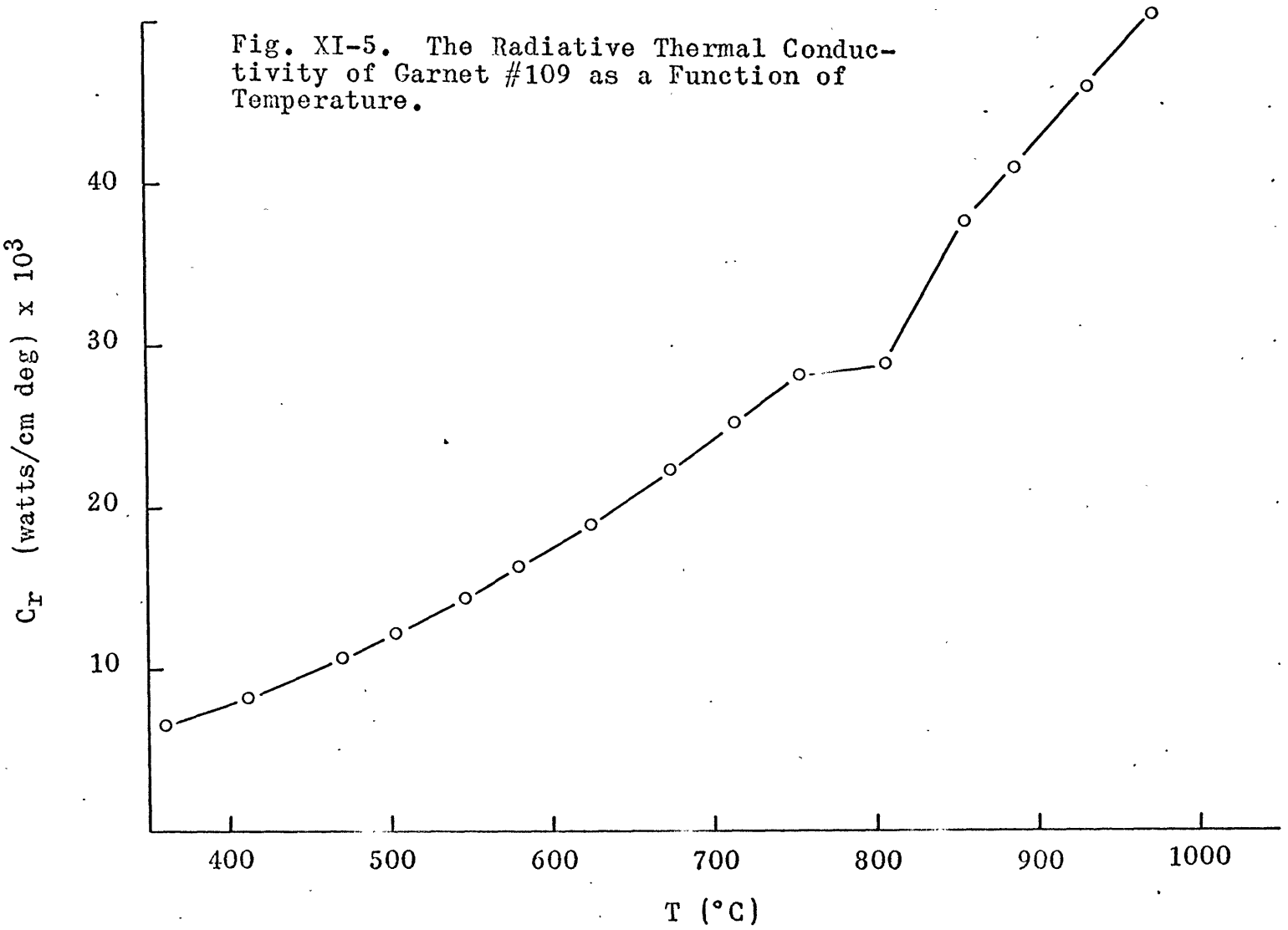

Fig. XI-5. The Radiative Thermal Conductivity of Garnet #109 as a Function of Temperature.

500° C, twice that for 750°- 800° C (the conductivity peak region), and about 3 times that at 1000° C. This should not change curves A and B in Figure XI-1, but will affect curve D through reduction of the values for the temperature in the eclogite material. Taking twice the low temperature thermal conductivity as a reasonable "average" for garnet #109 in the temperature region between 500° and 800° C, calculations show that temperatures at depth are lower than those of curve D and that the conductivity peak region associated with the temperature distribution of curve D is shifted toward lower temperatures and possesses greater vertical extent. In the earth, a small change in the same direction may possibly be due to the increased thermal conductivity associated with the pressure effect on the electrical conductivity.

It is difficult to state with certainty whether or not Cantwell (1960) was actually measuring a conductivity discontinuity at the Moho discontinuity. If, upon further magnetotelluric investigations in the Boston area, it is determined that the conductivity discontinuity at 70 km is the only significant one down to that depth, then the Ohmo corresponds to the Moho and, for a gabbro-eclogite phase change, represents a shift from the conductivity vs depth curve for gabbro to that of eclogite (garnet) at 70 km. The crust, in this case, is composed of 10 - 20 km of granodioritic material and approximately 60 - 70 km of gabbro. However, if an electrical discontinuity occurs at about 35 km (~ 1 order of magnitude) and another at 60 - 70 km (~ 2 orders of magnitude), the Ohmo

(70 km discontinuity) does not correspond to the Moho and, for a gabbro-eclogite phase change, represents a shift from the conductivity vs depth curve for gabbro to that for eclogite (garnet) at 35 km. The 70 km discontinuity, in this case, corresponds to the rapid increase in conductivity in the peak area of the conductivity curve.

A possible electrical conductivity vs depth distribution may now be proposed for the upper portion of the earth. The electrical conductivity of the basic layer of the crust corresponds to that of gabbro, measured in a buffered atmosphere in the presence of an aqueous vapor. For the Moho at 35 km, a jump in the conductivity of apporximately 1 order of magnitude will occur at this depth as the shift is made to the conductivity vs depth curve for eclogite, obtained in a dry buffered atmosphere. The conductivity will peak at still greater depths, decrease, and then, as ionic conductivity predominates ($\sim$70 km) increase again. For the Moho at 60 - 70 km, a similar phenomenon will be observed, but the conductivity vs depth curve will be expanded, thus prolonging the onset of predominantly ionic conductivity until greater depths ($\sim$ 150 - 200 km).

11.63 A Maximum for the Iron Content in the Upper Portion of the Mantle

Proceeding along the lines of an eclogite-gabbro phase change at the Moho discontinuity, it is not difficult to arrive at an upper limit for the iron concentration in the top part of the earth's mantle. Lovering (1958) has tabulated the mean compositions of eclogites, olivine basalts, norites, and euchritic achondrites in order to demonstrate their chemical similarity. These data were obtained by several investigators, who analyzed numerous samples so that a mean value for each is well defined. For FeO, the mean percentage compositions for eclogite, olivine basalt, norite, and euchritic achondrites were 12.6%, 11.96%, 9.37%, and 16.73% respectively. A gabbro-eclogite phase change, then, suggests that 12.6% or 11.96% is the proper value for the FeO content at the base of the crust.

However, this is not the maximum FeO content that is possible. It may be that the eclogites observed at the surface have been differentiated from a parent eclogitic body of higher iron content. Equation (6.1-1) illustrates the chemical equivalence of olivine basalt and eclogite, while equation (11.61-1) shows the relationship between euchritic achondrites and eclogites. Neither of these have iron as a constituent element, however, Dana (1951) states that, for silicates, variations in composition may involve the substitution of Si by Al, of Al, Mg, and Fe by each other, Na by

Ca, etc. The plagioclase minerals, labradorite and bytownite, exhibit negligible Fe substitution, but olivine may range from forsterite [Mg_2SiO_4] to fayalite [Fe_2SiO_4]. Diopside [$CaMg(SiO_3)_2$] has hedenbergite [$CaFe(SiO_3)_2$] as an iron-rich variety. As pertains to the pigeonite [$(Fe,Mg)SiO_3$ + n $CaMg(SiO_3)_2$], a mixture of clino-enstatite and diopside, a similar compound may occur in the series between clino-enstatite and hedenbergite [i.e.- $(Mg,Fe)SiO_3$ + n $CaFe(SiO_3)_2$] (Dana, 1951). Therefore, the iron-rich equivalent of equation (11.61-1) is:

(11.63-1)
$$\underbrace{4\ CaAl_2Si_2O_8 + NaAlSi_3O_8}_{\text{bytownite}} +$$
$$\underbrace{8\ FeSiO_3 + n\ CaFe(SiO_3)_2}_{\text{"pigeonite"}} \rightleftharpoons$$
$$\underbrace{4\ CaFe_2Al_2(SiO_4)_3}_{\text{garnet}} +$$
$$\underbrace{NaAl(SiO_3)_2 + n\ CaFe(SiO_3)_2}_{\text{"omphacite"}} + \underbrace{5\ SiO_2}_{\text{quartz}}$$

Due to the "n" molecules of hedenbergite in the products above, an extreme case is that where "n" is so large that the other products are insignificant. The specific gravity and elastic properties will still be similar to those of eclogite since the substitution of Fe and Mg in diopside has little effect on these parameters (zero pressure density of eclogite - 3.35 - 3.6 gm/cm^3; hedenbergite - 3.58 gm/cm^3). For this case, then, the maximum Fe and FeO

contents are 22.6% and 29.0% respectively. The garnet alone gives Fe - 23.2% and FeO - 29.8% and corresponds to a mineral composed of 1 part grossularite garnet and 2 parts almandite garnet on a molecular basis. For the eclogite in equation (11.63-1), with no hedenbergite, but only garnet, jadeite [$NaAl(SiO_3)_2$], and quartz, Fe - 18.4% and FeO - 23.7%. Almandite, the iron-rich garnet [$Fe_3Al_2(SiO_4)_3$] exhibits Fe and FeO contents of 33.7% and 36.9% respectively, but contains no Ca, a requirement imposed by the basicity of the plagioclase.

Therefore, the preceding percentages of iron and their relationships to a particular transformation suggest that, for a phase change at the Moho analogous to equation(11.61-1), the maximum possible Fe content in the upper portion of the mantle is on the order of 23% and, for the FeO content, 29%. It is interesting to note that almost identical values are obtained for the case where hedengergite is considered as being the major constituent of the eclogitic material and for the case where garnet is the major component. Furthermore, the garnets measured in this investigation approximate the garnet in equation (11.63-1) rather well since this garnet has not only an FeO content of 29.8% but also a CaO content of 8.36% when calculated as equivalent MgO (compare with Table V-1).

11.64 Conductivity Mechanisms in the Upper Portion of the Mantle

At present, there exists a fair amount of disagreement as to the exact mechanisms of electrical conduction in the interior of the earth. Hughes (1959) attributes the conductivity of the mantle to ionic processes while Runcorn (1955), Tozer (1955), and Clark (1957) suggests that intrinsic semi-conduction is the predominant mechanism. Coster (1948) found that the electrical conductivity of most rocks could be represented by two sets of parameters, one with an activation energy of about 0.7 ev, and the other, appearing at higher temperatures, with an activation energy on the order of 2 ev, where the associated constants in the conduction equation were 10^{-1} to 10^{-4} and approximately 10^{5} respectively. He suggests that the first set of parameters may be indicative of impurity electronic semi-conduction. Hughes (1933) arrived at the parameters in Table I-1 and has associated σ_o - 10^{-4} - 10^{-6}(Ω-cm)$^{-1}$ and E - 0.5 - 1.0 ev with impurity semi-conduction, σ_o - 5 x 10^{1} (Ω-cm)$^{-1}$ and E - 2.0 - 3.0 ev with intrinsic semi-conduction, and σ_o - 10^{4} - 10^{10}(Ω-cm)$^{-1}$ and E - 2.8 - 4.0 with ionic conduction. In his work with crystals of TiO_2, Cronemeyer (1952) obtained the values σ_o - 2.76 x 10^{3} - 8.38 x 10^{4} (Ω-cm)$^{-1}$ and E - 3.05 - 3.67 ev and places these under the heading of electronic semi-conduction since passing current through the sample for appreciable lengths of time had no apparent destructive effect on the electrical properties of

the crystal.

The magnitudes of the parameters calculated for the garnets measured in this investigation suggest that electronic semi-conduction predominates up to temperatures just below the melting point. Therefore, for an eclogitic upper mantle, ionic conductivity will not become important as the major conduction mechanism until the temperatures at depth approach those of the melting point curve. We have seen previously that this will not occur at depths less than 70 km and, more likely, will be on the order of 150 - 200 km.

This was suggested on the basis of the shapes of the conductivity curves for gabbro and garnet and with the assumption that pressure effects were negligible. However, Hughes (1959) determined an increase in the excitation energy of olivine of approximately 4.8×10^{-6} ev/kg/cm^2 and an overall decrease in the electrical conductivity of about 20% in the pressure range of 1 atmosphere to 8500 kg/cm^2. This does not necessarily mean that the effect of pressure is to increase the electrical conductivity in all minerals. Paul and Pearson (1955) find a decrease in the energy gap of single crystals of Si of approximately $- 1.5 \times 10^{-6}$ ev/kg/cm^2 at 250° C and emphasize strongly that this is true only in the absence of any significant changes in mobility with pressure. Other investigations (see Section 1.2) demonstrate that the excitation energy may increase or decrease and that carrier mobility is also a function of the pressure. Therefore, whether the conductivity increases or decreases with the pressure

depends upon the particular mineral in question and the nature of the conductivity mechanism.

For eclogitic material composed of garnet, omphacite, and quartz, we have the following data: 1) the excitation energy of almandite garnet increases with pressure; 2) the conductivity of garnet at 1 atmosphere pressure as a function of temperature is as in Figures A-1 through A-31: 3) the electrical conductivity of quartz as a function of tmeperature at 1 atmosphere pressure is an in Figure A-41; and 4) the predominant mode of conduction in garnet is electronic. However, the data that are necessary for a detailed discussion but are lacking are: 1) the exact conductivity mechanisms for quartz, omphacite, and garnet; 2) the electrical conductivity of omphacite as a function of temperature and pressure; 3) the effect of pressure on the individual constituents of omphacite and quartz; and 4) the effect of pressure on the mobilities of the carriers in quartz, omphacite, and garnet. This demonstrates the value of simultaneous high temperature and high pressure measurements, since all these measurements would not be required. However, as a first approximation to the actual case, the curves discussed in Section 11.62 may be taken as representative of the electrical conductivity vs depth distribution since, as compared with the entire earth, it is a thin shell at the surface that is being considered in this investigation rather than a position at depth under extreme pressures.

On the basis of the σ_o's and the E's for the cooling

curves, it seems likely that the main conduction process in garnets is of an intrinsic type. The slopes of the curves in the conductivity peak region indicate that, upon initial heating, ionic conduction is also in operation for a small temperature range and that the true ionic conductivity region at higher temperatures demonstrates a rearrangement of ionic or polar molecules in such a manner that the conductivity does not peak upon cooling due to the absence of this component.

The question arises at this point, should the heating or cooling curves be taken as representative of the electrical conductivity in the earth? Section 11.2 discusses the possible reasons for differences in the heating and cooling curves in terms of "freezing in" of defects. If a phase change is in operation at the Moho, then one might expect that "freezing in" of defects might play an important part in the overall conductivity, depending upon whether the phase boundary is rising or falling. However, since this process occurs on a geological time scale, such considerations should be of little concern and the heating curves should be taken as representative of the actual electrical conductivity.

Therefore, for the outer portion of the earth, the following processes probably determine the electrical conductivity: 1) in the near surface region of the crust - ionic conductivity determined by abundant pore fluids; 2) in the lower portion of the crust - impurity and intrinsic semi-conduction; 3) in the basal portion of the crust or upper mantle

- intrinsic semi-conduction and ionic conduction together (peak conductivity region); and 4) in the deeper mantle - intrinsic semi-conduction giving way to ionic conductivity with depth.

XII CONCLUSIONS

The design of Apparatus II is applicable to the measurement of A.C. and D.C. conductivities in a controlled atmosphere at elevated temperatures and, as was demonstrated on both a theoretical and chemical analysis basis, the atmosphere may be efficiently controlled by a wustite buffer mixture.

Although the majority of specimens measured exhibited an electrical conductivity peak or a suggestion of a peak, garnets were the only specimens investigated in detail. Experimentation with garnets indicates that conductivity curves obtained from heating and cooling measurements do not coincide, but a given set of curves may be reproduced exactly providing another sample from the same specimen is measured under identical conditions. The presence of an aqueous vapor phase tends to eliminate the electrical conductivity peak and suggests that the water vapor in the laboratory air may be responsible for the absence of the conductivity peak associated with a sample run in air. Oxidation of the sample appears to increase the overall conductivity. Therefore, a buffered atmosphere is an absolute necessity in measuring rock-forming minerals containing ferrous iron.

For those garnets run in a dry buffered atmosphere, a possible dependence of the electrical conductivity upon chemical composition is demonstrated. It appears that the lower temperature conductivities depend upon the concentrations of

FeO and Fe_2O_3, the highest temperature conductivities upon "MgO" (CaO plus MgO as equivalent MgO), and the intermediate temperature conductivities possibly upon "MgO" and/or "MgO"/MnO.

Polarization and/or thermo-electric effects become predominant in the higher temperature regions for many of the minerals investigated, especially quartz and enstatite. However, as the iron contents of the minerals increase, these effects become suppressed to the point of being unobservable. Corrections were attempted where polarization and thermo-electric effects occurred and the accuracies of all the measurements are estimated to be within 10% of the actual values.

The majority of the curves obtained for log σ vs 1/T are quite different from those obtained by other investigaters and this may be due to the following: 1) a dry silicate run in air produces no conductivity peak; 2) a dry silicate run in a dry buffered atmosphere yields a conductivity peak; and 3) a dry silicate run in an aqueous buffered atmosphere gives no conductivity peak.

The possibility of a phase transformation from eclogite to gabbro at the Mohorovicic discontinuity is not unreasonable or remote. For this case, the electrical conductivity data of Coster's (1948) measurements and the data from this investigation may be combined to fit the electrical discontinuity at approximately 70 km observed by Cantwell (1960), who utilized magneto-telluric sounding techniques.

Proceeding along the lines of an eclogite-gabbro phase change at the Moho discontinuity, it is not difficult to arrive an upper limit for the iron concentration in the top part of the mantle. Data suggest that the actual FeO content is 11.96 - 12.6% at the base of the crust or in the upper mantle and calculations demonstrate that 29% is an upper limit.

Finally, on the basis of the magnitudes of the electrical parameters and the suggested conductivity vs depth distributions, the following processes probably determine the electrical conductivity in the outer portion of the earth: 1) in the near surface region of the crust - ionic conductivity determined by abundant pore fluids; 2) in the lower portion of the crust - impurity and intrinsic semi-conduction; 3) in the basal portion of the crust or upper mantle - intrinsic semi-conduction and ionic conduction together (peak conductivity region); and 4) in the deeper mantle - intrinsic semi-conduction giving way to ionic conductivity with depth.

FUTURE INVESTIGATIONS

There is still considerable work to be done along the lines of the present investigation. The most desirable materials to measure are synthetic crystals of approximately the same chemical composition as the natural minerals of interest. In such a case, various elements could be added to or withdrawn from the initial mixture in order to ascertain the effect of the variability of a given element concentration upon the electrical conductivity. If natural mineral specimens are employed, complete chemical analyses, both wet-chemical and spectrochemical (including trace element analysis), should be undertaken.

Auxiliary experimentation should be performed concurrently with the conductivity measurements in order to determine the number, character, and mobility of the conducting particles. Part of this could be determined by observing the Hall effect. Thermo-electric and polarization studies would also be helpful in the case of iron deficient minerals.

Microscopic work on thin-sections would be advantageous in "before" and "after" comparisons for determining the magnitude of the effect of grain boundary separation on the conductivity. In a similar manner, X-ray techniques might be employed to investigate the effect of the formation of internal fractures.

Further investigations of buffers would also be desirable. This would result from the calculation and compilation

of additional free energy data.

Simutaneous high temperature and high pressure conductivity measurements would demonstrate a "short cut" to possible conductivities existing at depths in the earth. This would eliminate the necessity of determining the conductivity under a number of experimental conditions and then combining the results to produce the final answer.

Finally, since the metal - semi-conductor contacts may be the source of considerable error, it may be possible to develop an inductive or dielectric method for measuring the electrical conductivity under high temperatures and pressures, thereby eliminating the need of metal contacts.

APPENDIX A

PLOTS OF LOG σ VS. 1/T FOR THE SPECIMENS MEASURED IN THIS INVESTIGATION

(See Table A-1 for pertinent symbols)

TABLE A-1. Symbols for Figures A-1 through A-42

σ ..... Electrical conductivity in $\Omega^{-1}cm^{-1}$

T ..... Temperature in °K

For Figures A-1 through A-7 and A-32 through A-38:

Heating Curves:

○ ..... Conductivity determined by passing current through the sample in the forward direction

◐ ..... Conductivity determined by passing current through the sample in the reverse direction

◑ ..... Conductivity determined by passing current through the sample in either direction gives the same point

Cooling Curves:

○ ..... Conductivity determined by passing current through the sample in the forward direction

○ ..... Conductivity determined by passing current through the sample in the reverse direction

○ ..... Conductivity determined by passing current through the sample in either direction gives the same point

For Figures A-8 through A-31 and A-39 through A-42:

Heating Curves:

◔ ..... Conductivity determined by passing current through the sample in the forward direction

◐ ..... Conductivity determined by passing current through the sample in the reverse direction

◔ ..... Conductivity determined by passing current through the sample in either direction gives the same point

TABLE A-1. (Continued)

Cooling Curves:

⊖ ..... Conductivity determined by passing current through the sample in the forward direction

⊖ ..... Conductivity determined by passing current through the sample in the reverse direction

⊖ ..... Conductivity determined by passing current through the sample in either direction gives the same point

⊙ ..... Approximate location of point

. ..... Point determined by "correcting" for [d]

For all A.C. Curves:

○ ..... Heating curve points

⊖ ..... Cooling curve points

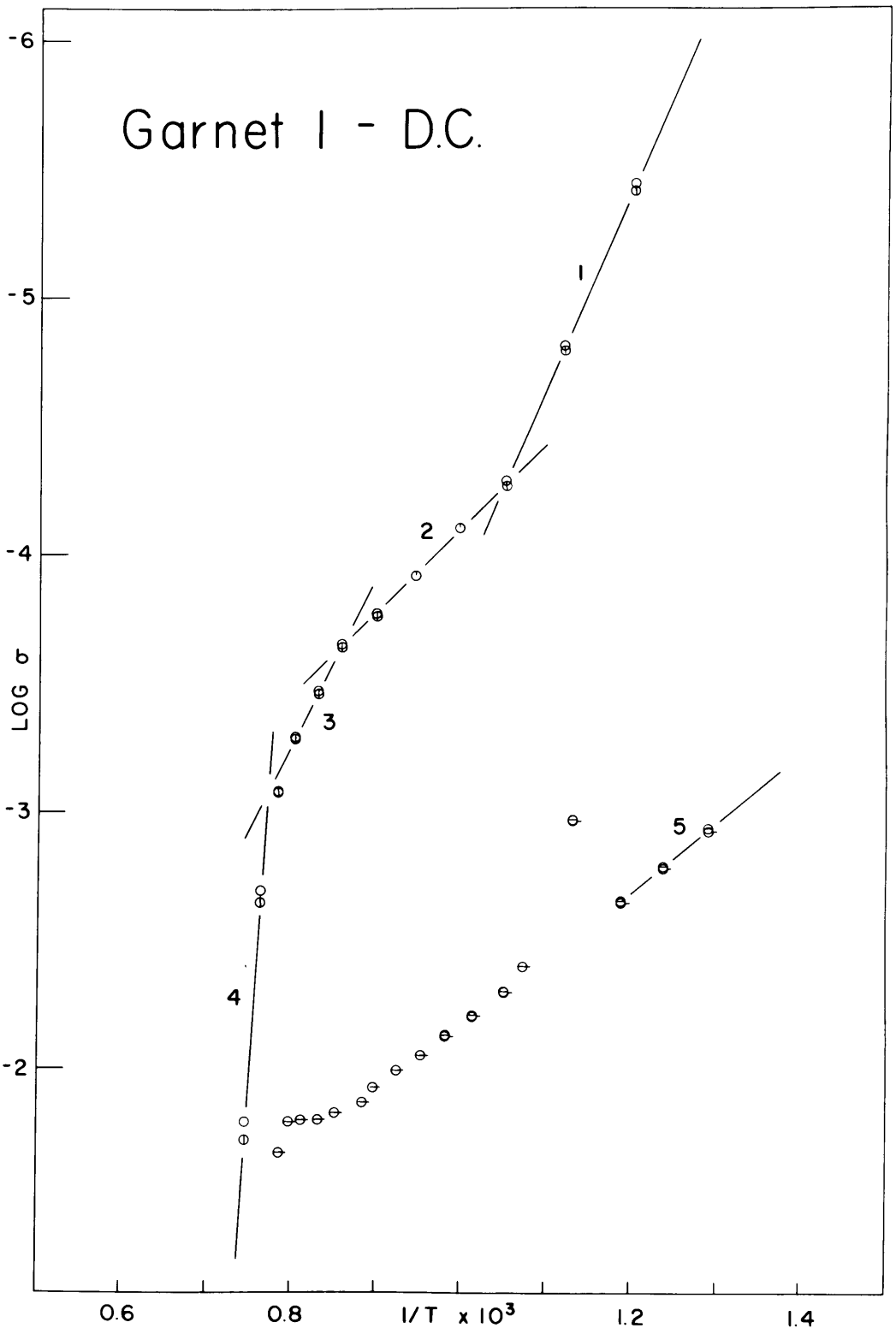

Fig. A-1

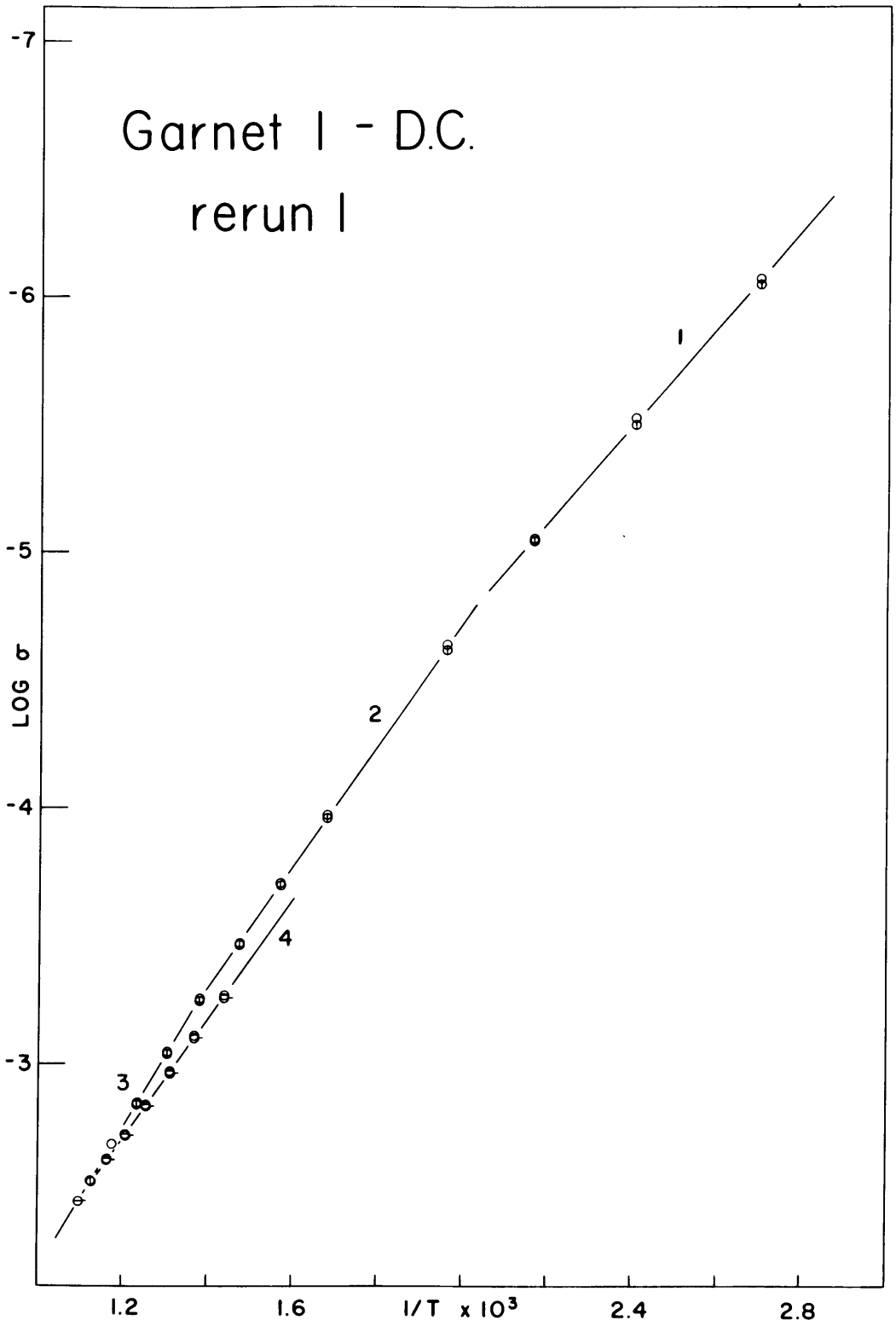

Fig. A-2

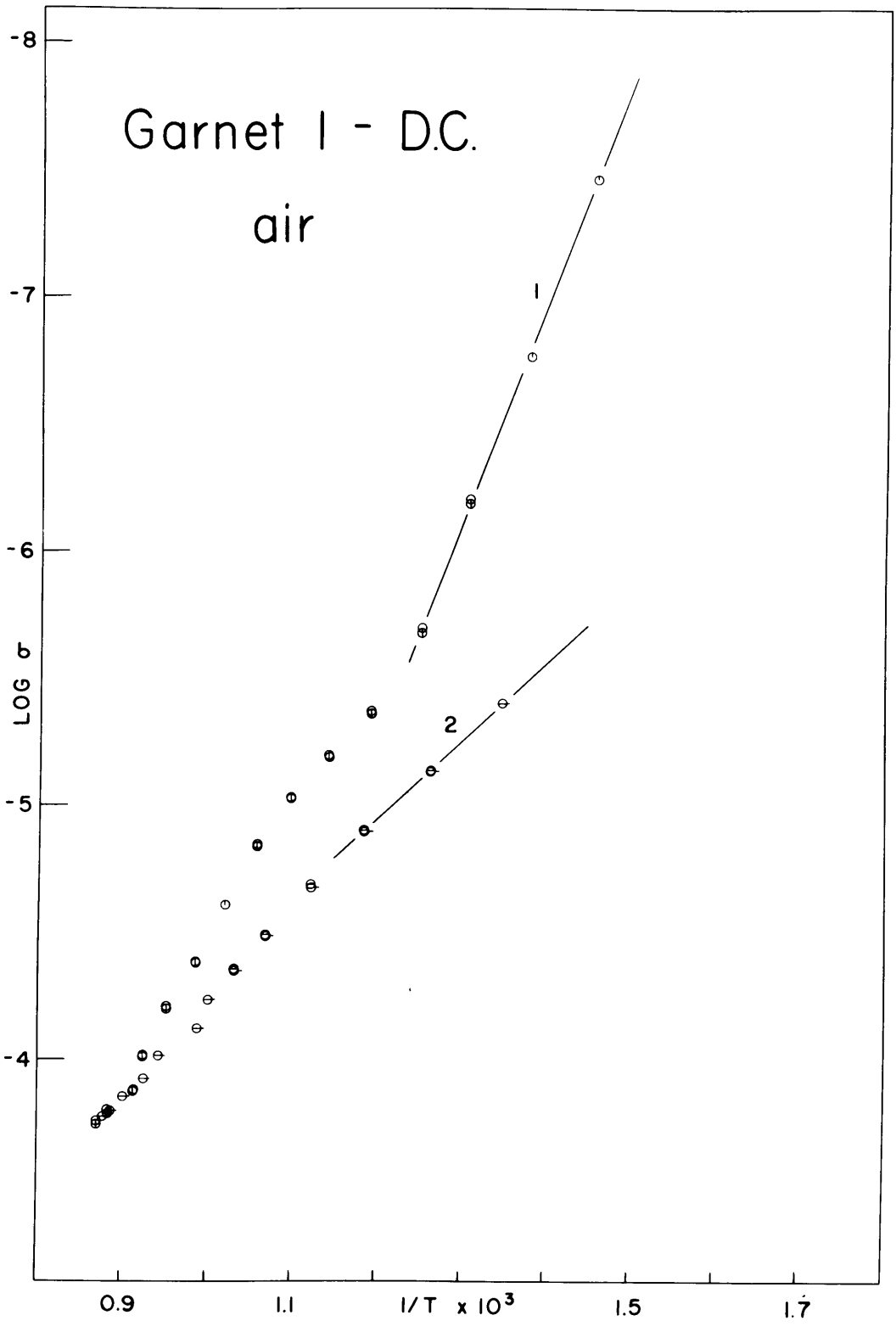

Fig. A-3

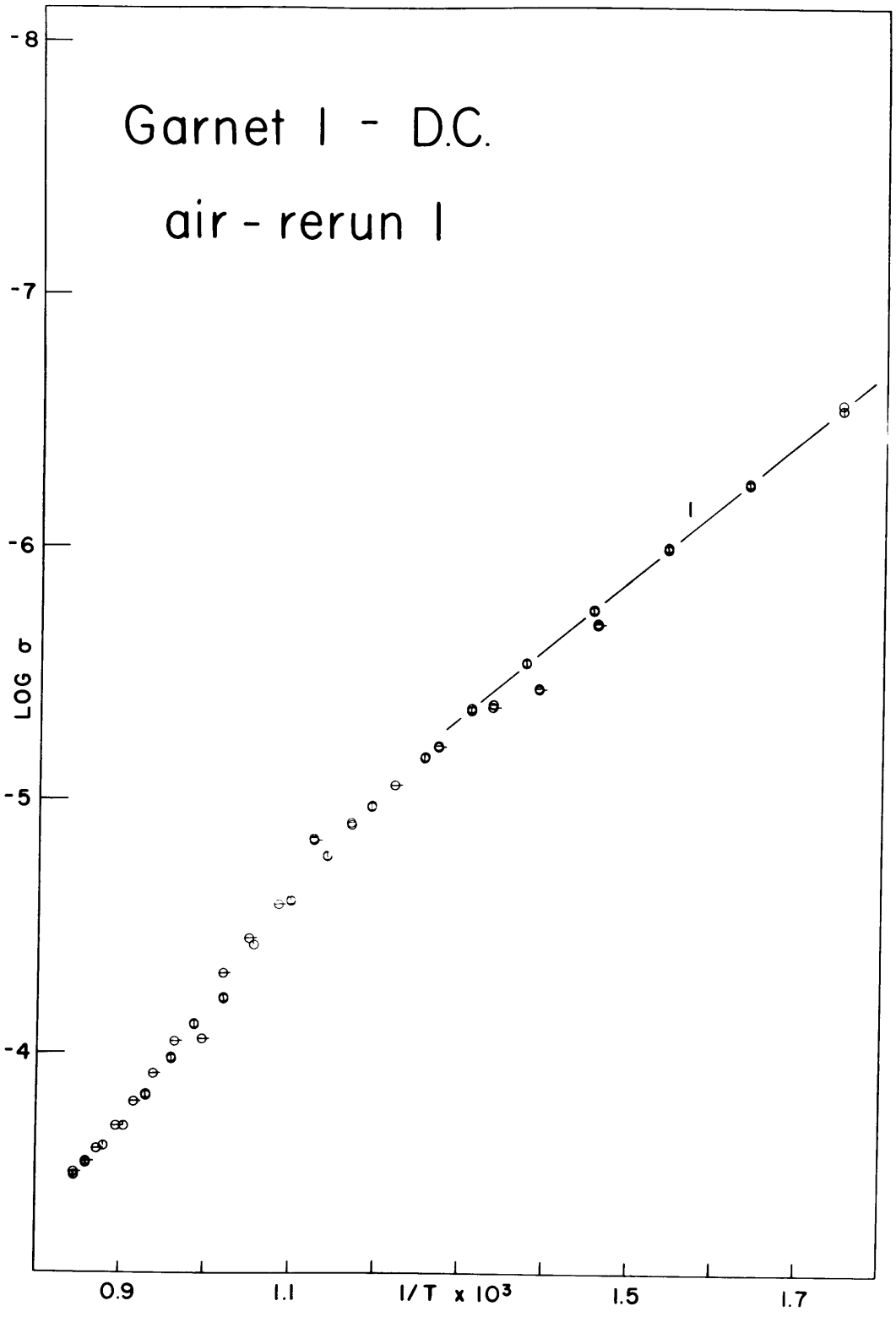

Fig. A-4

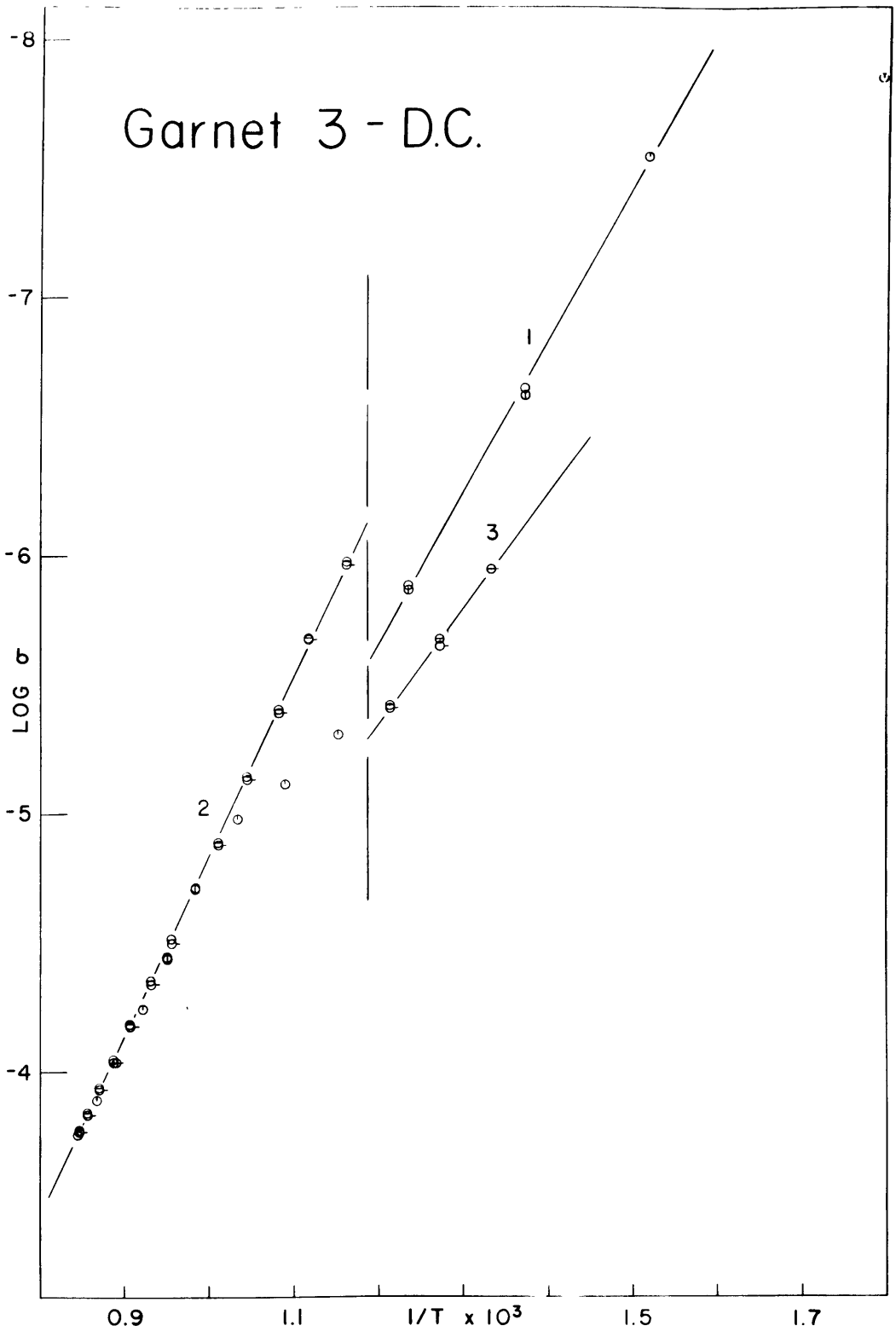

Fig. A-5

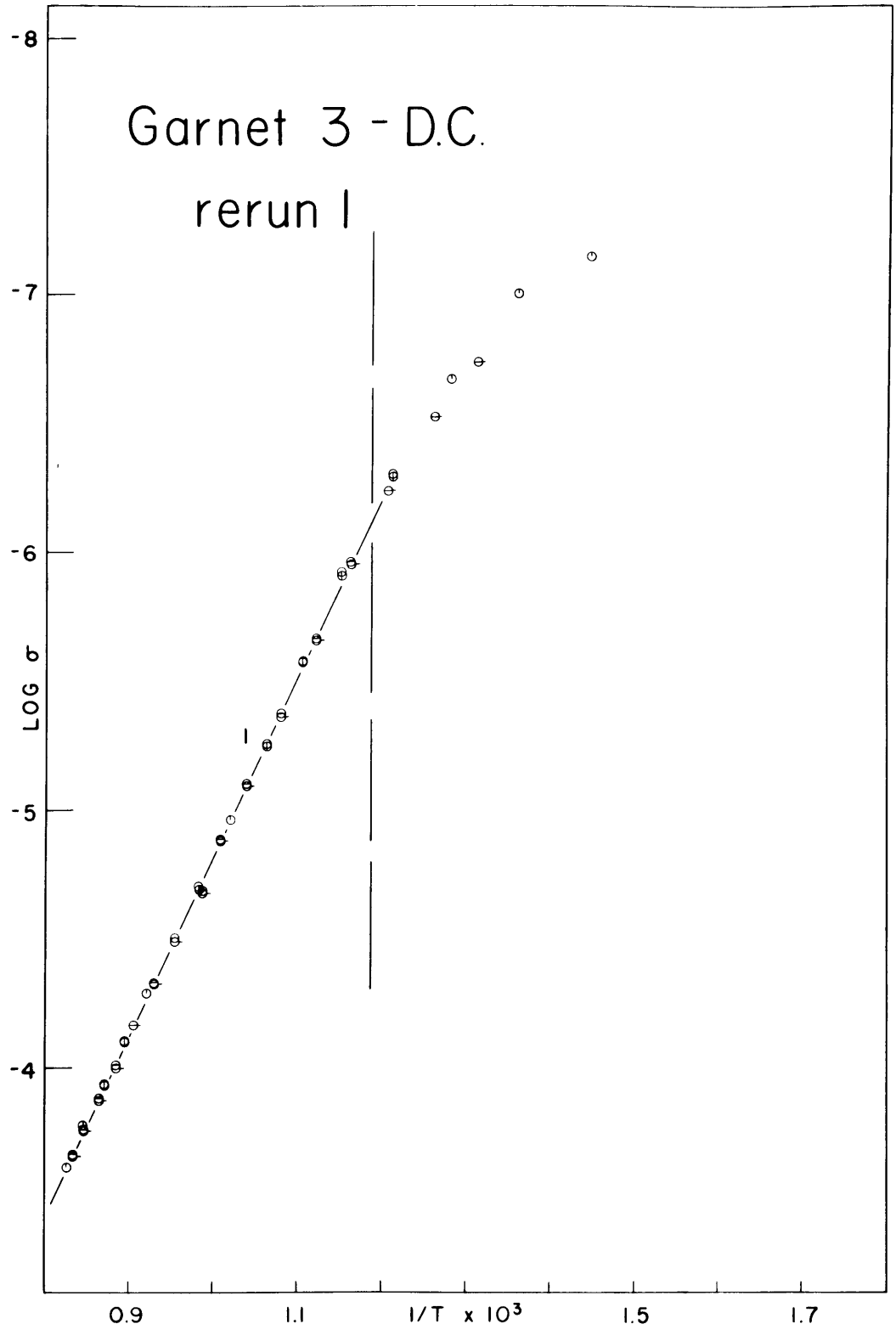

Fig. A-6

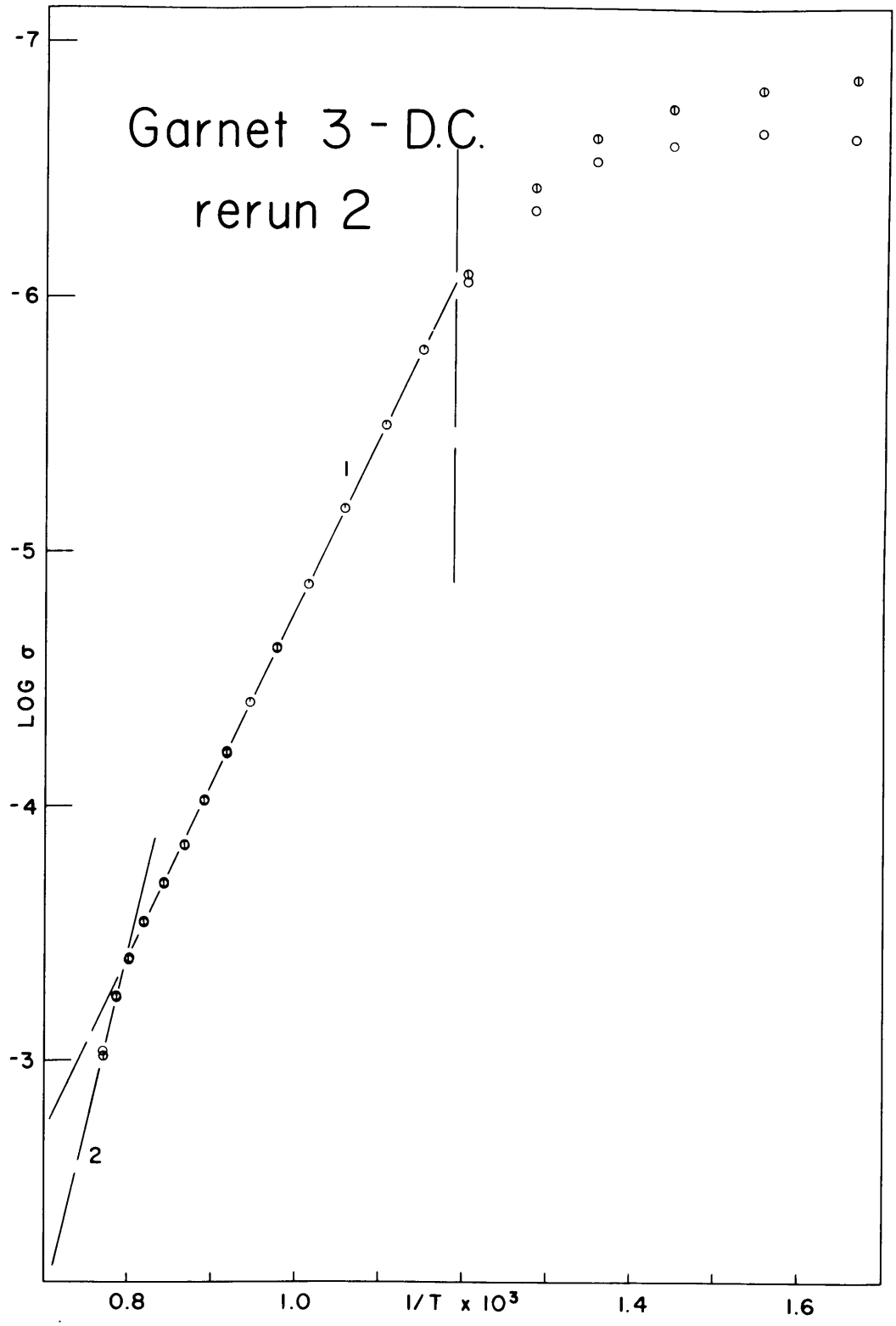

Fig. A-7

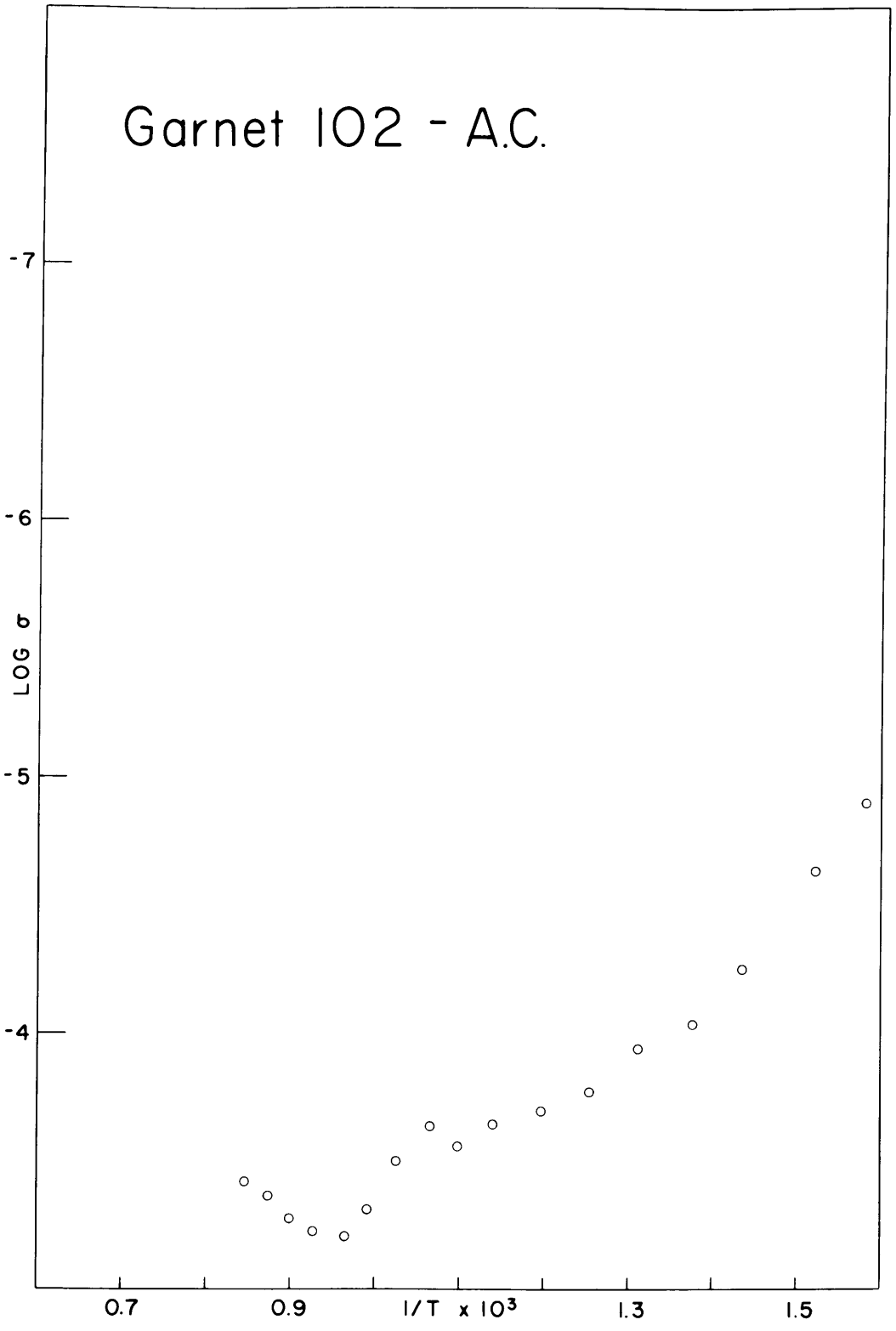

Fig. A-8

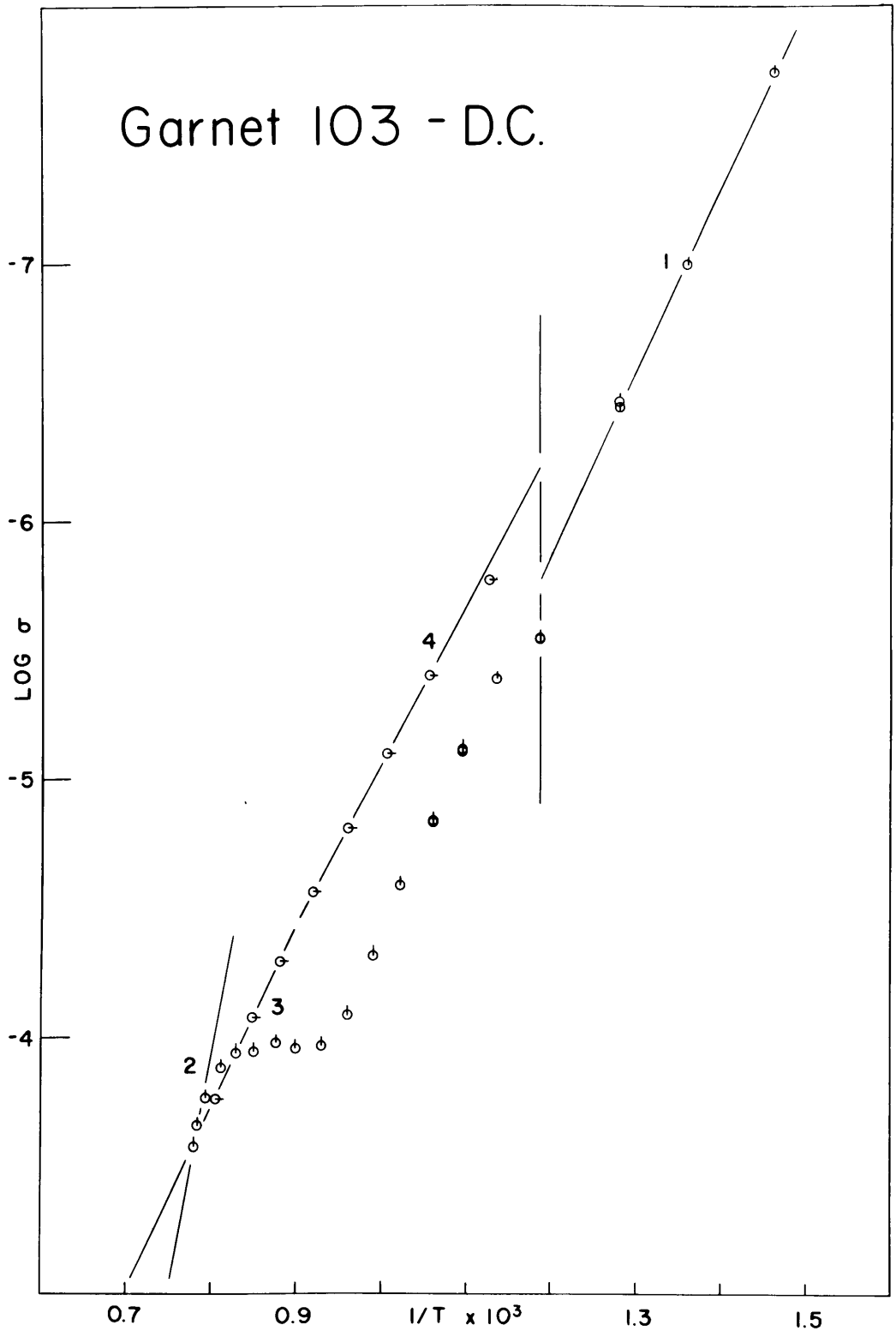

Fig. A-9

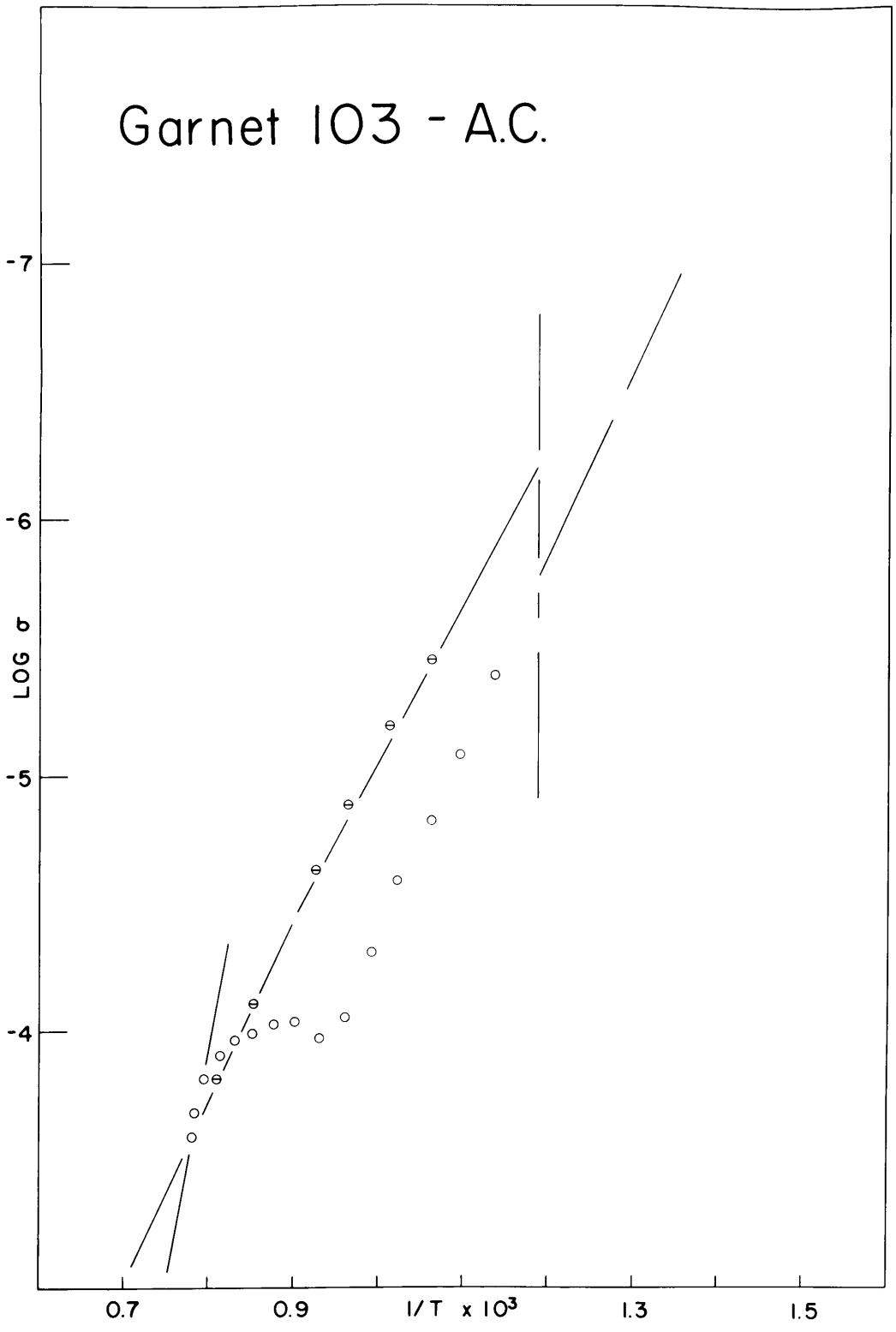

Fig. A-10

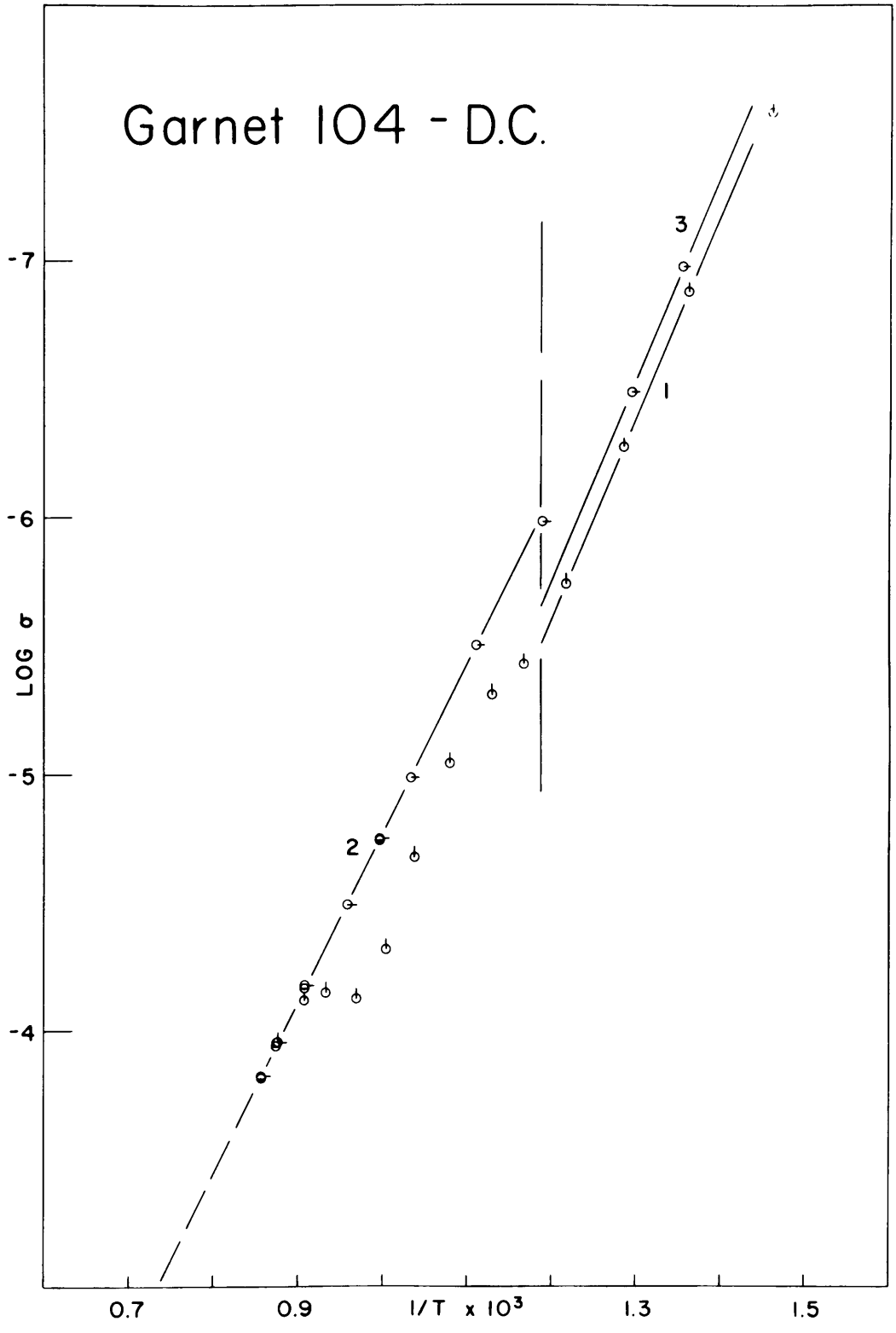

Fig. A-11

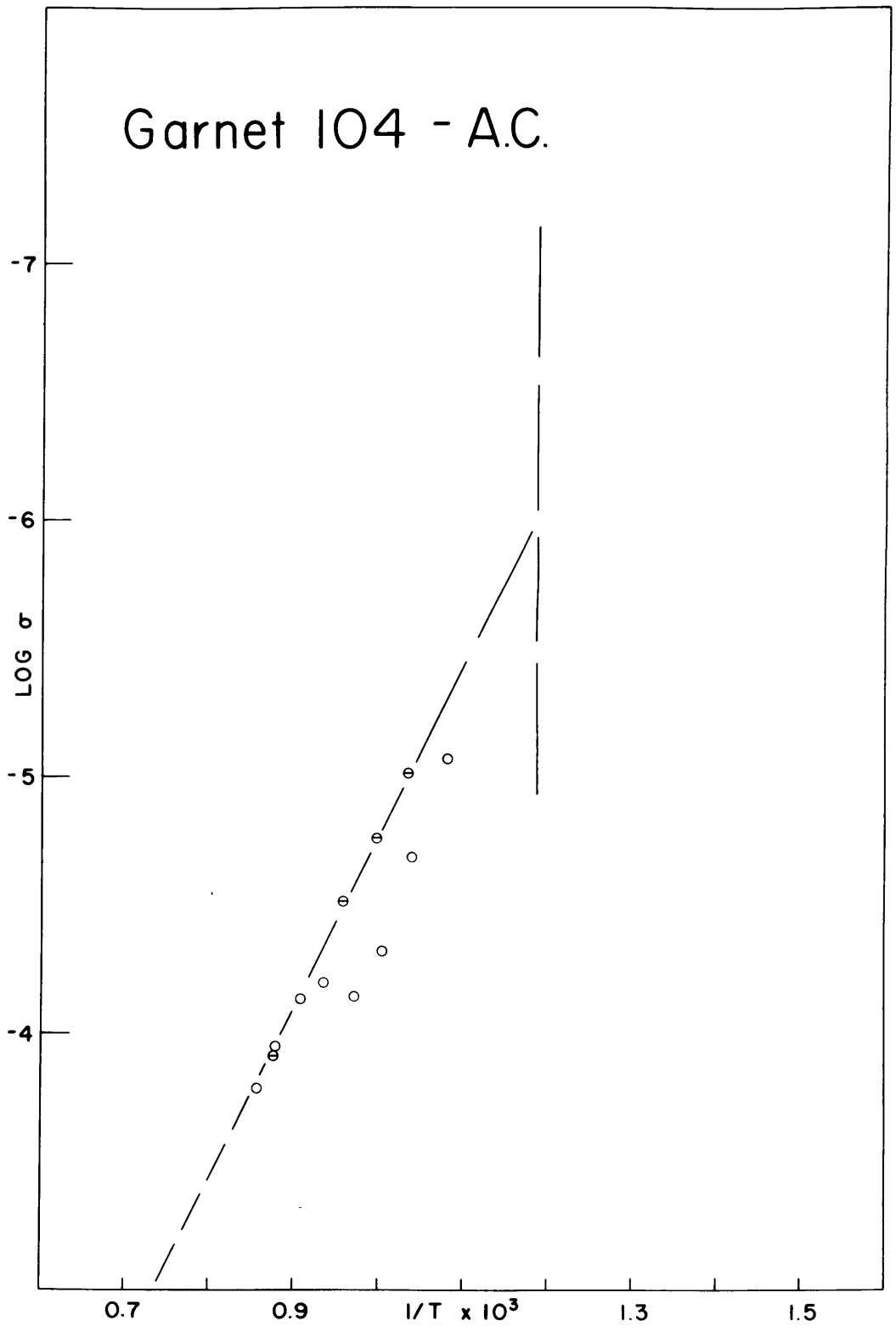

Fig. A-12

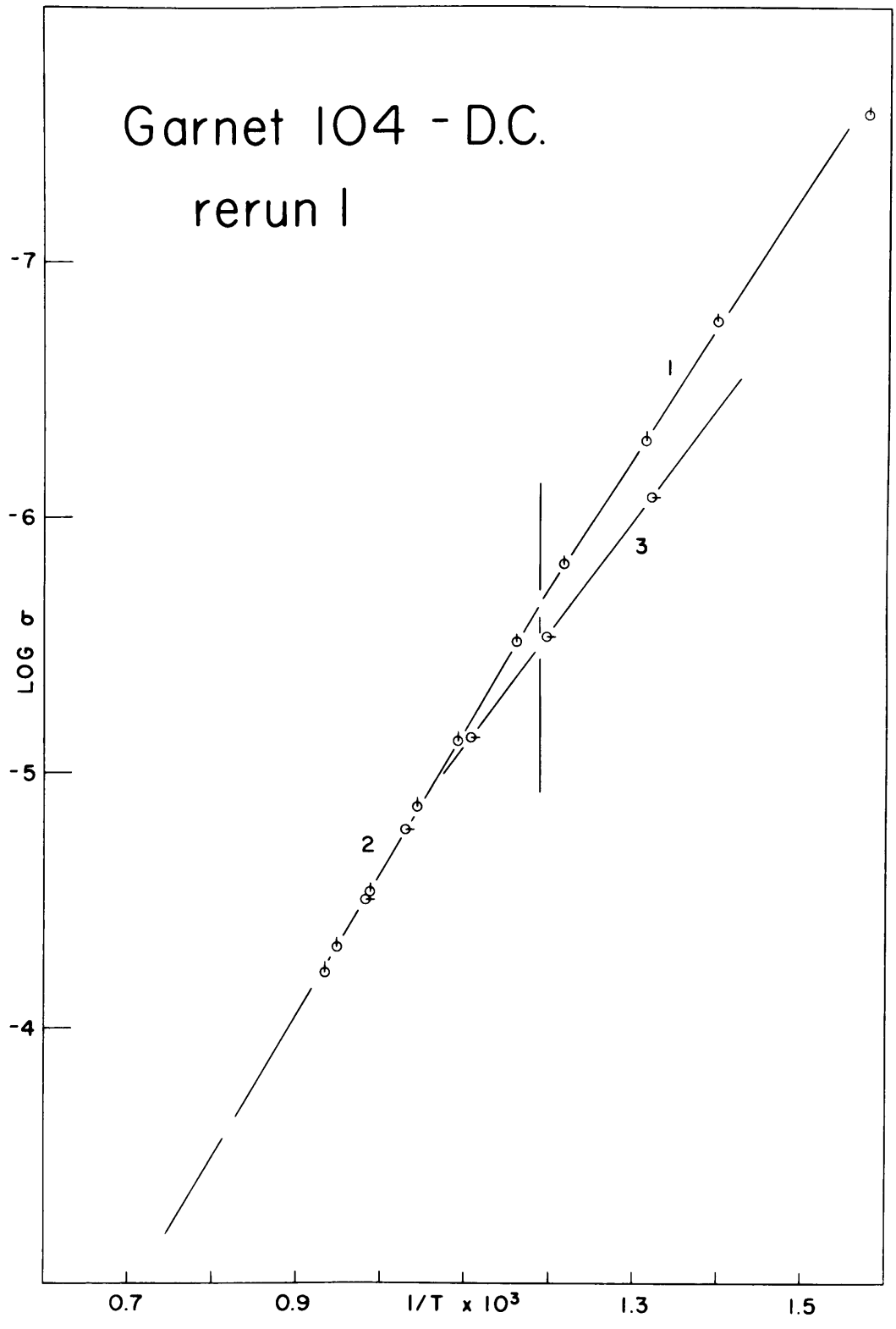

Fig. A-13

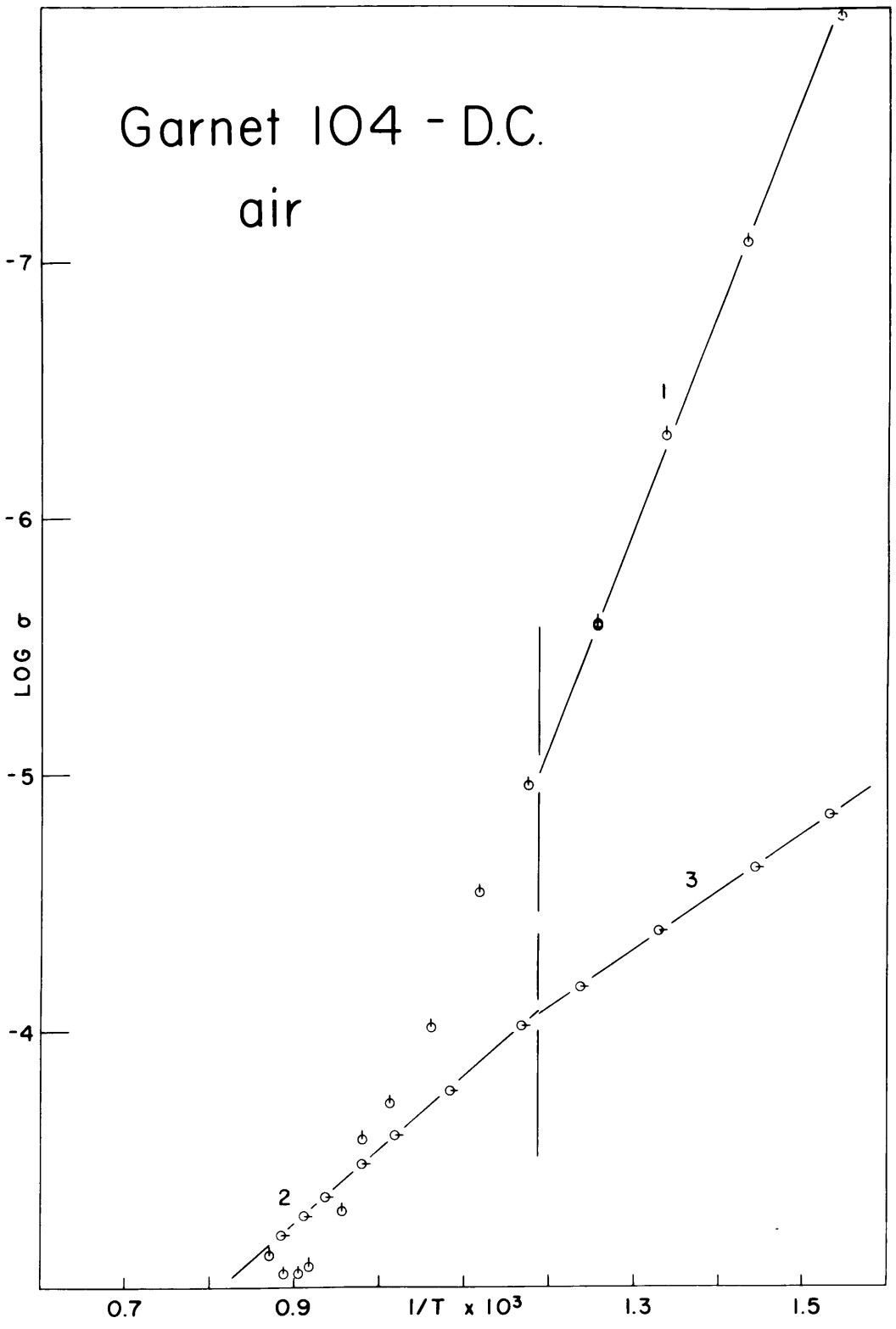

Fig. A-14

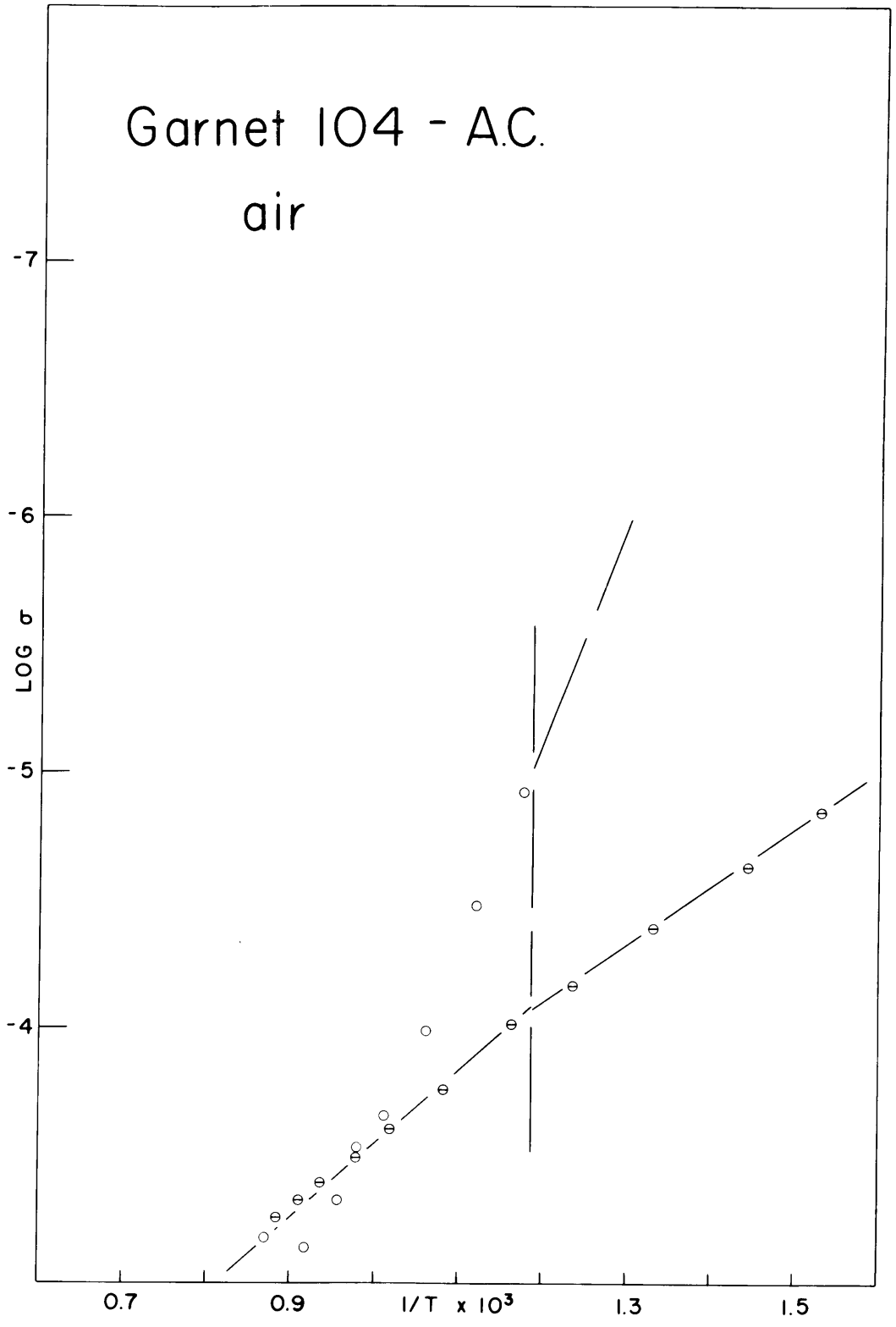

Fig. A-15

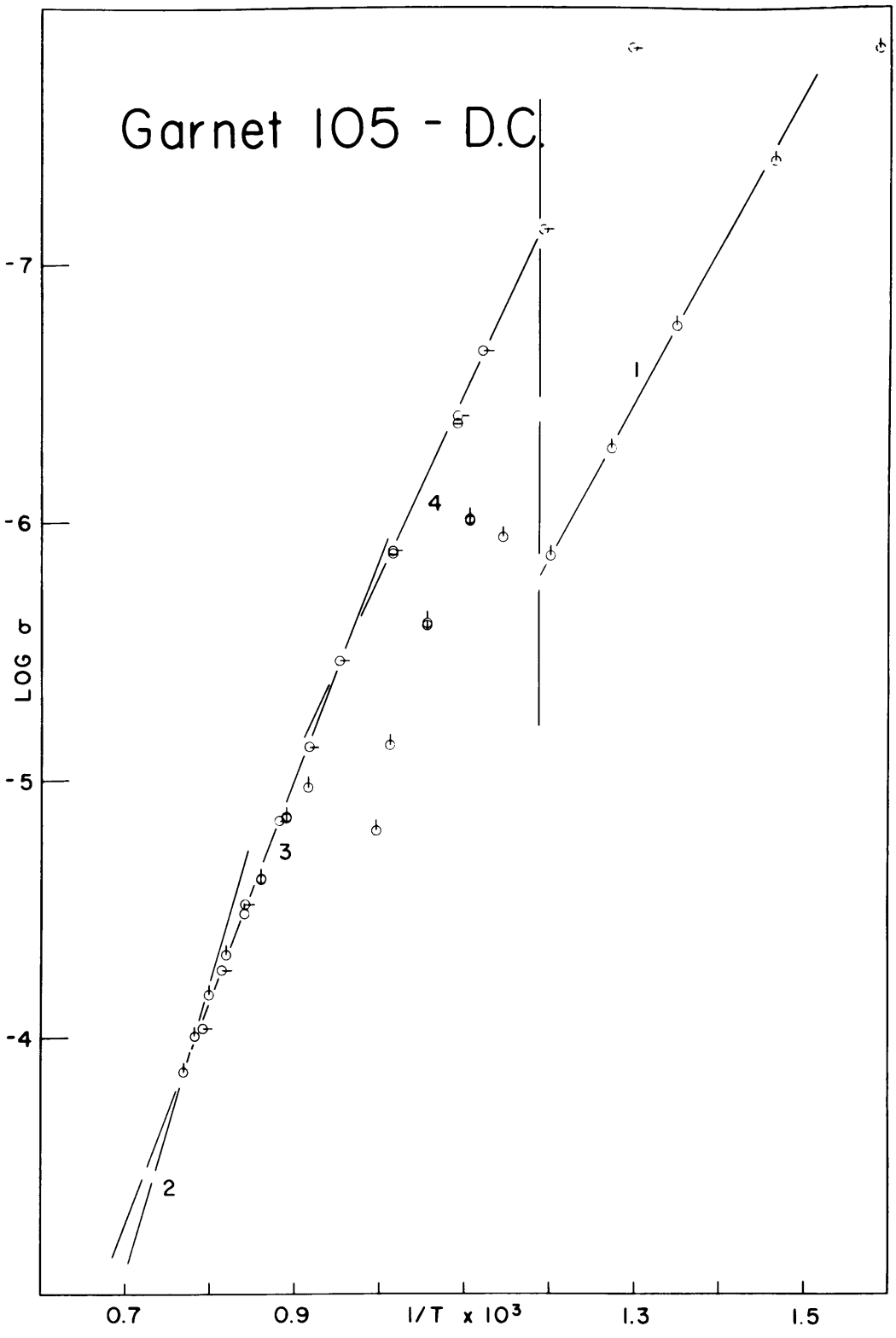

Fig. A-16

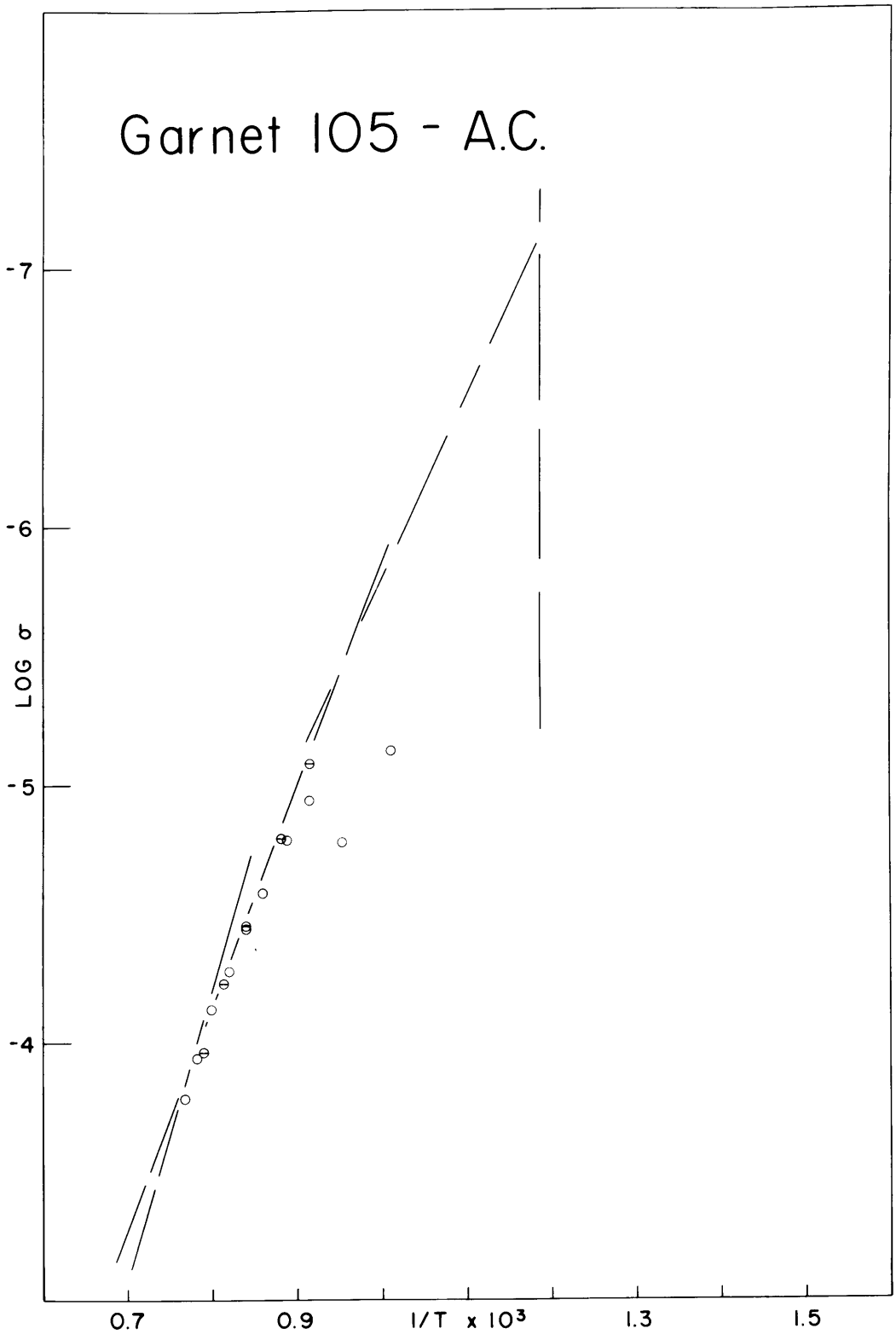

Fig. A-17

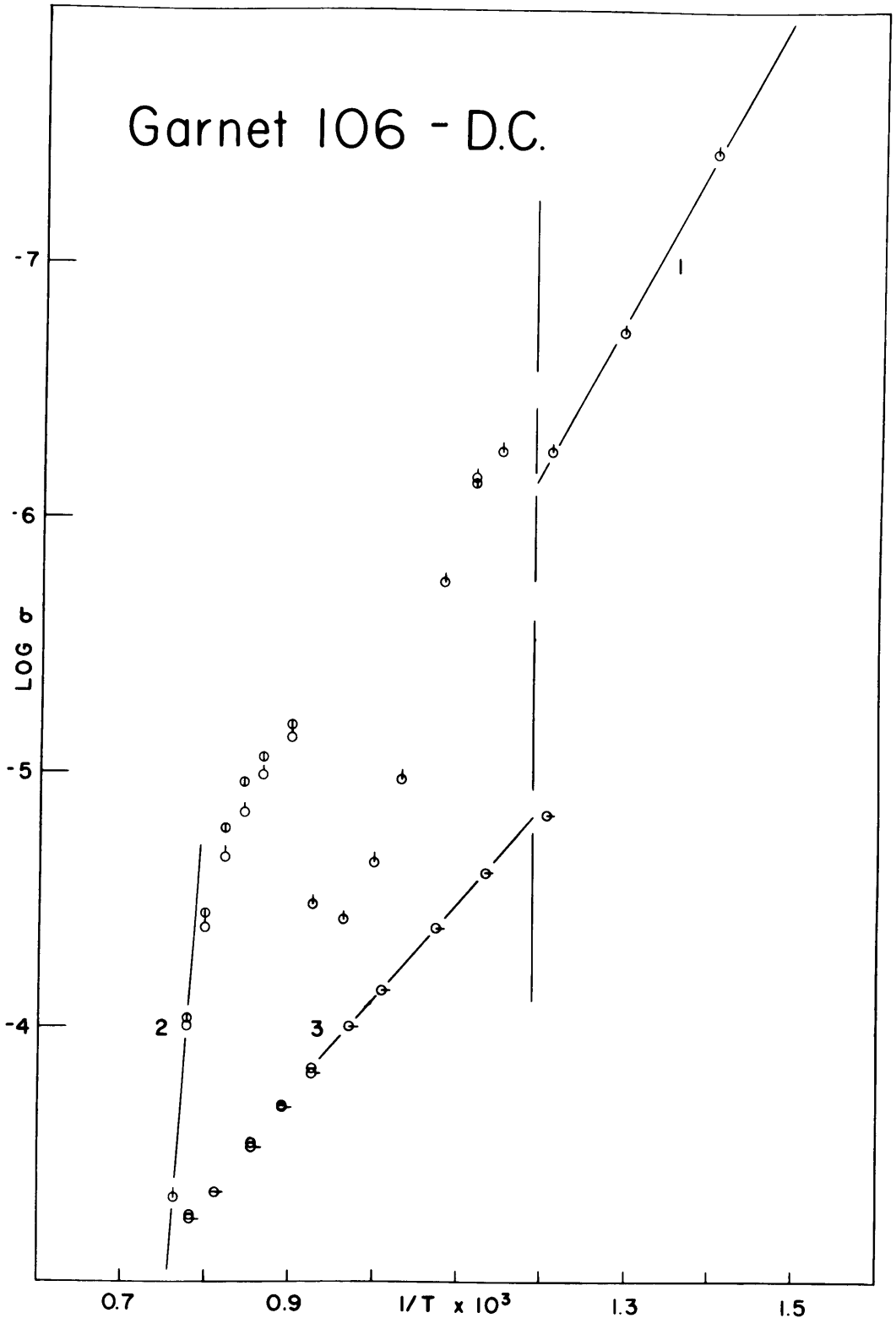

Fig. A-18

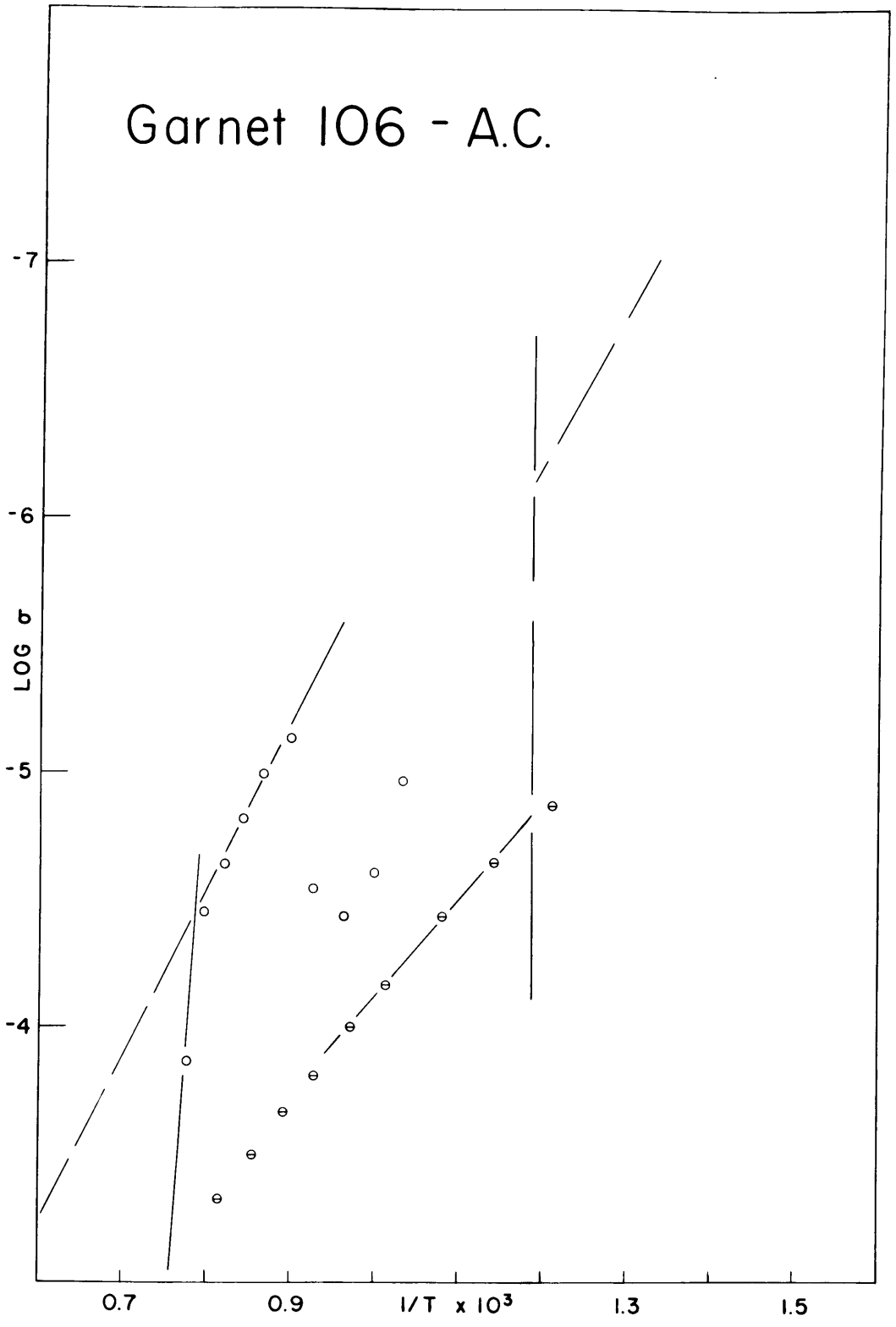

Fig. A-19

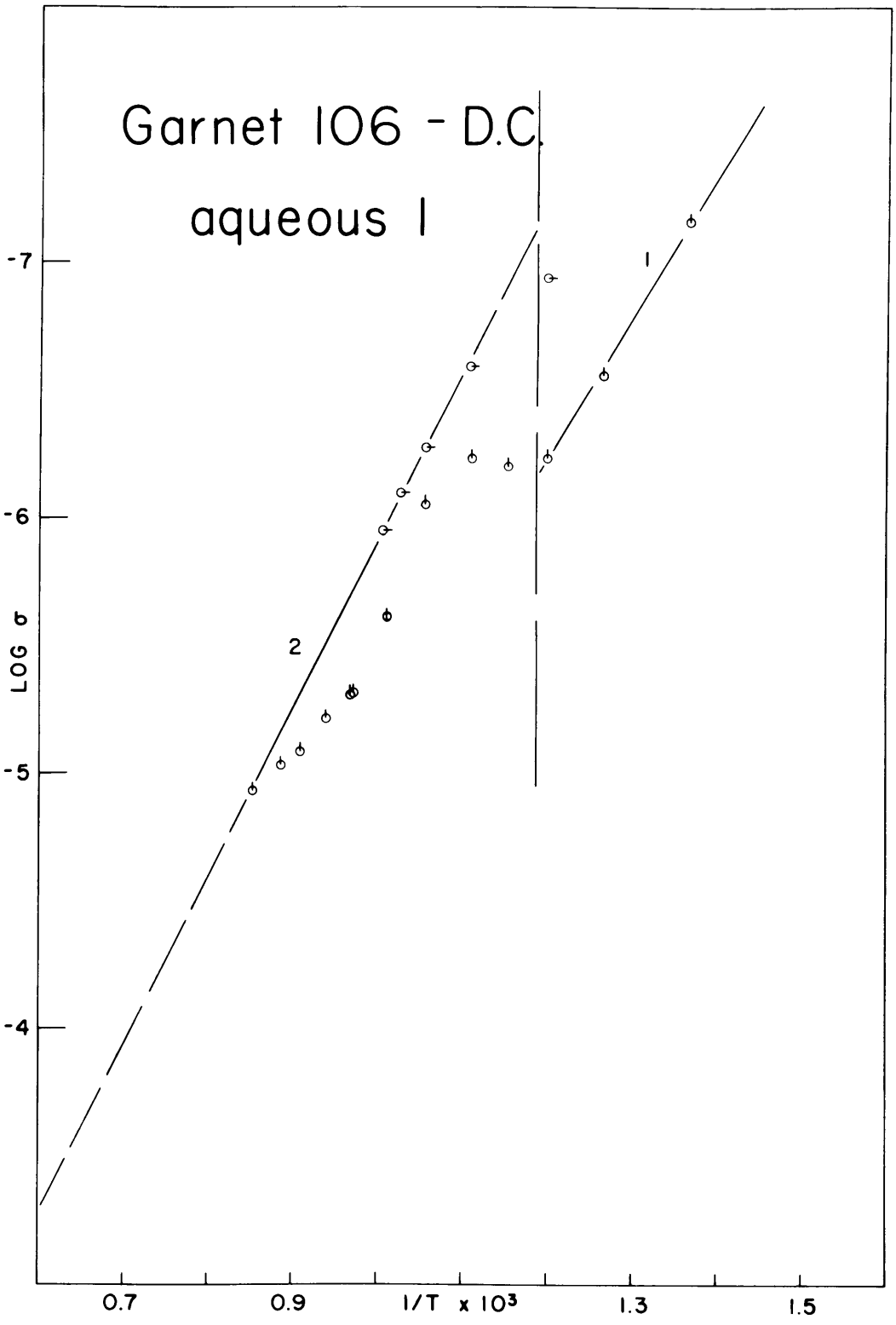

Fig. A-20

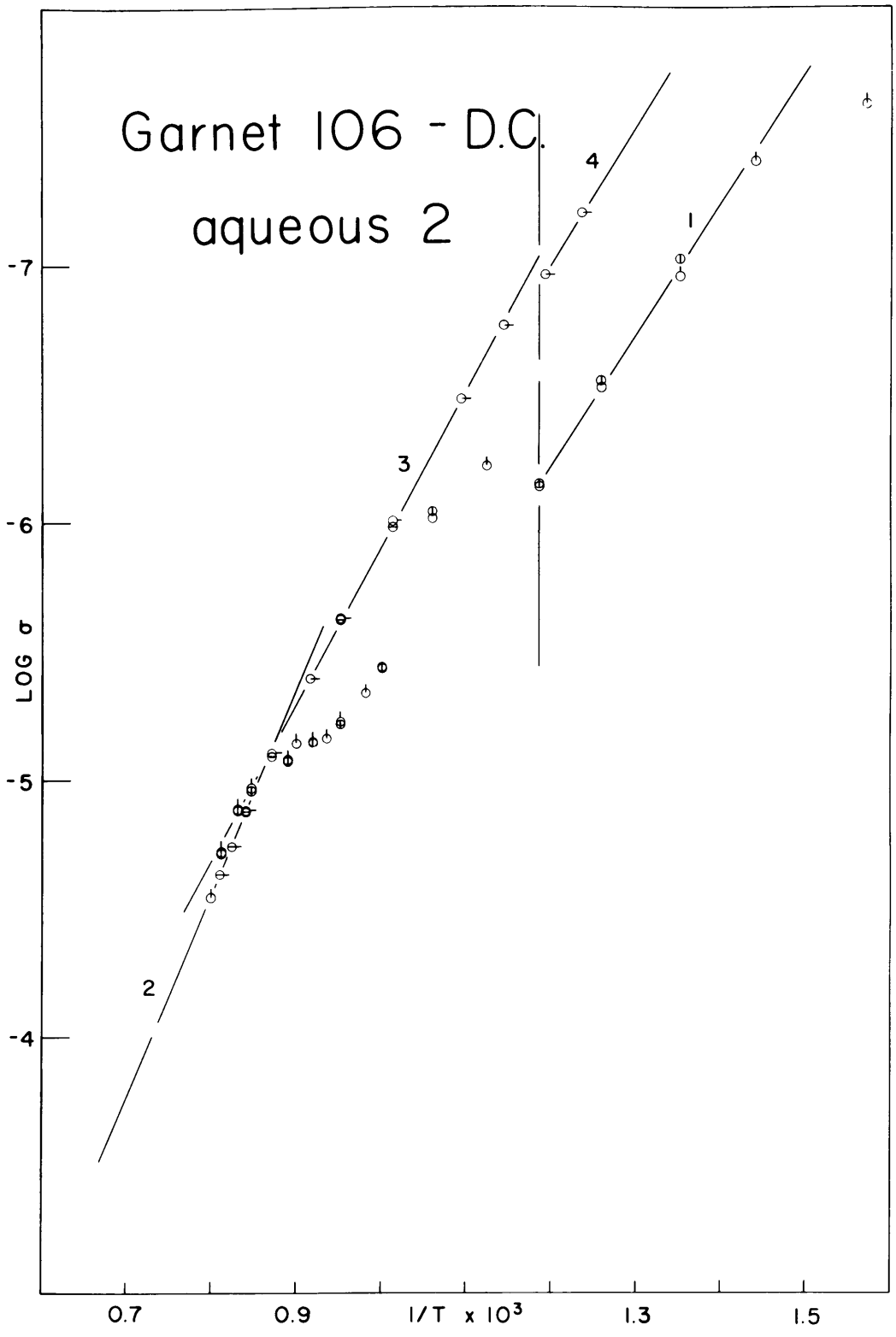

Fig. A-21

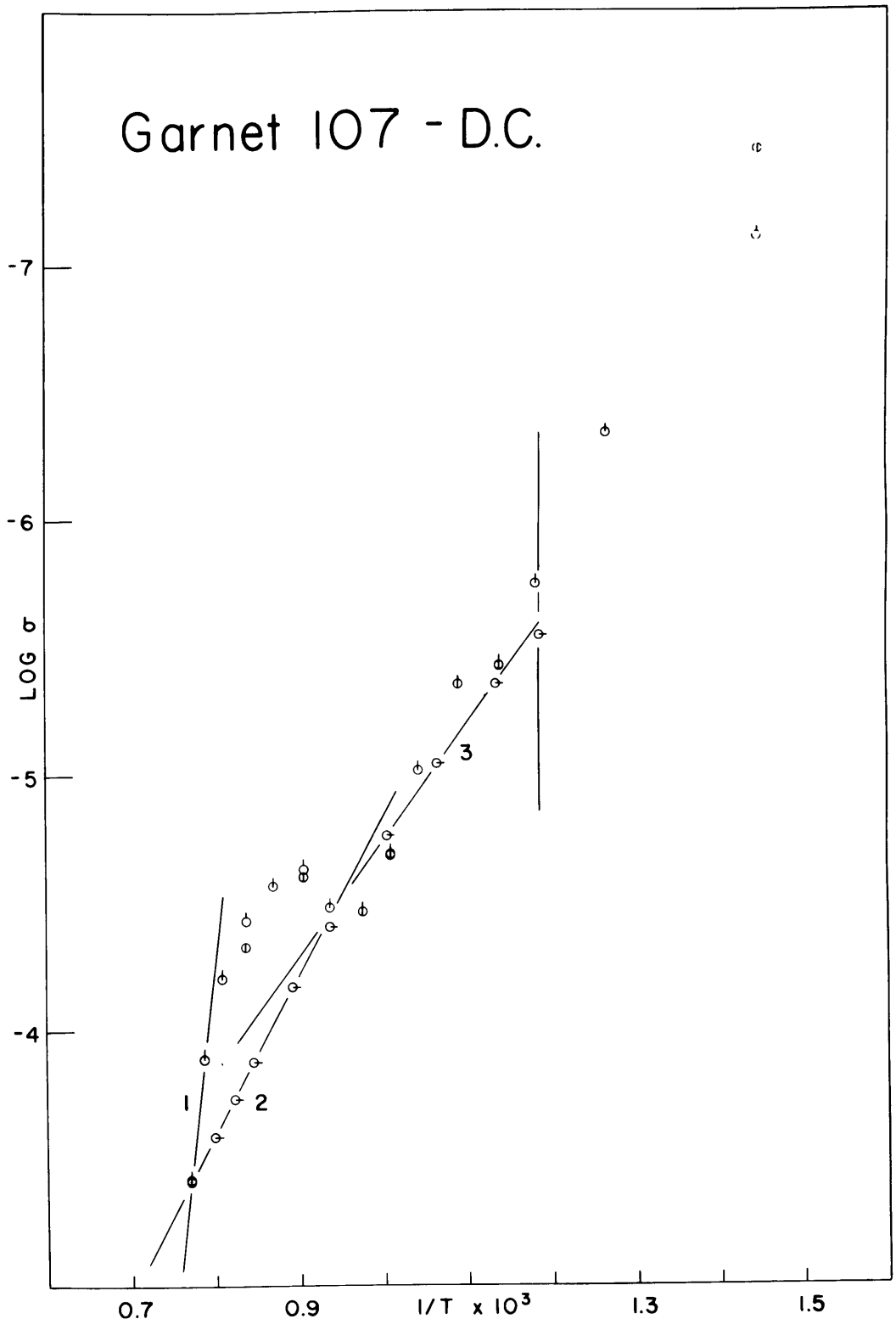

Fig. A-22

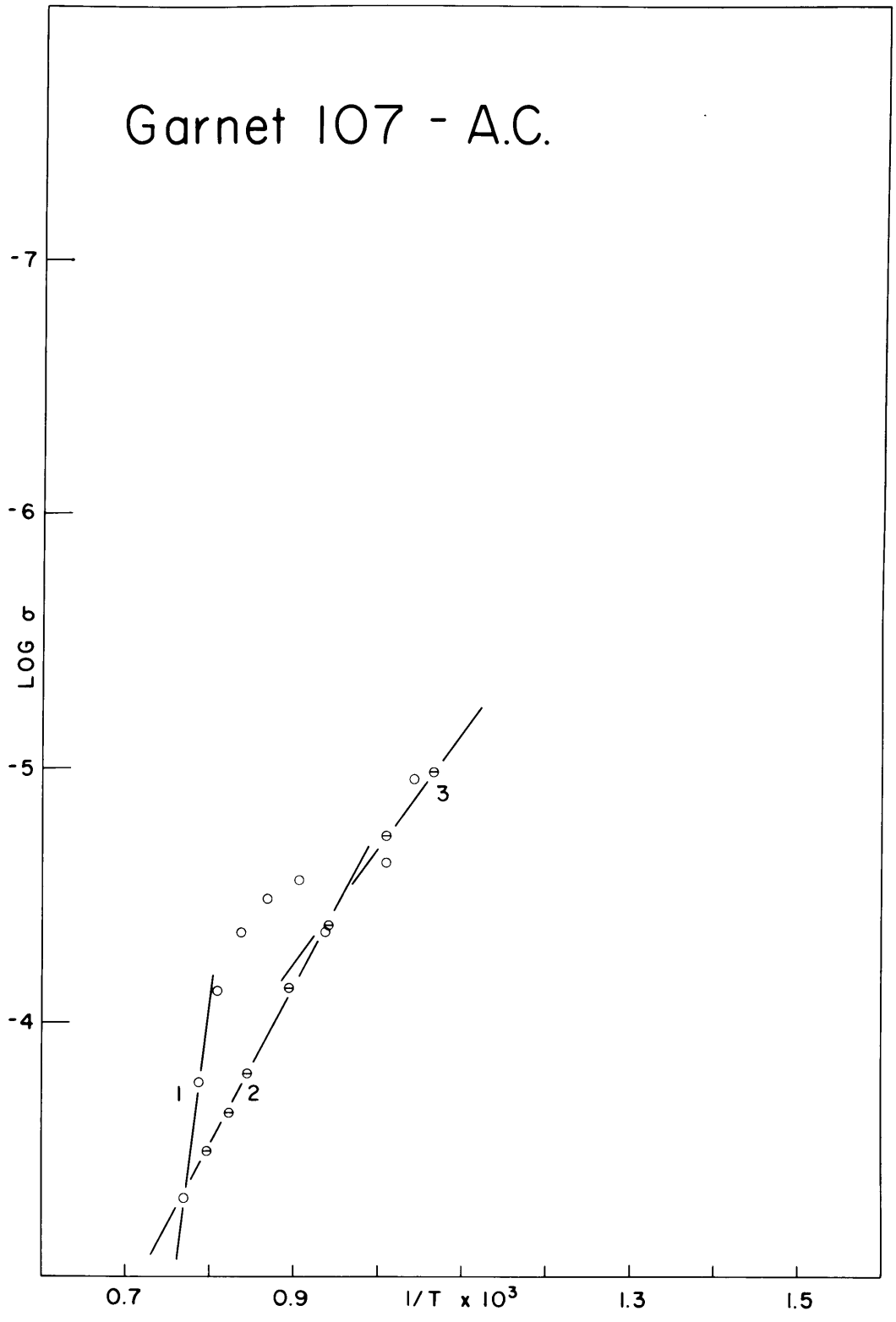

Fig. A-23

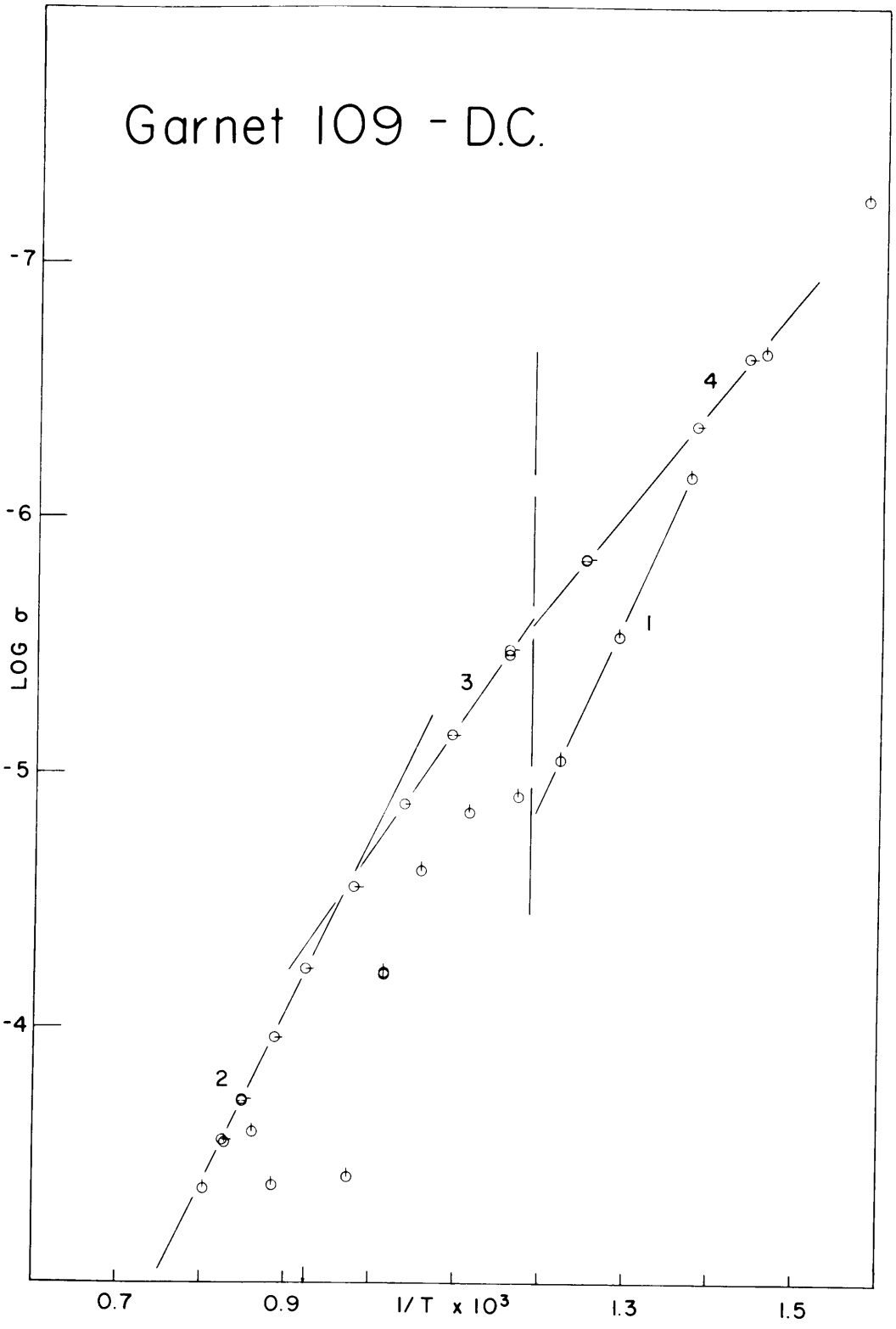

Fig. A-24

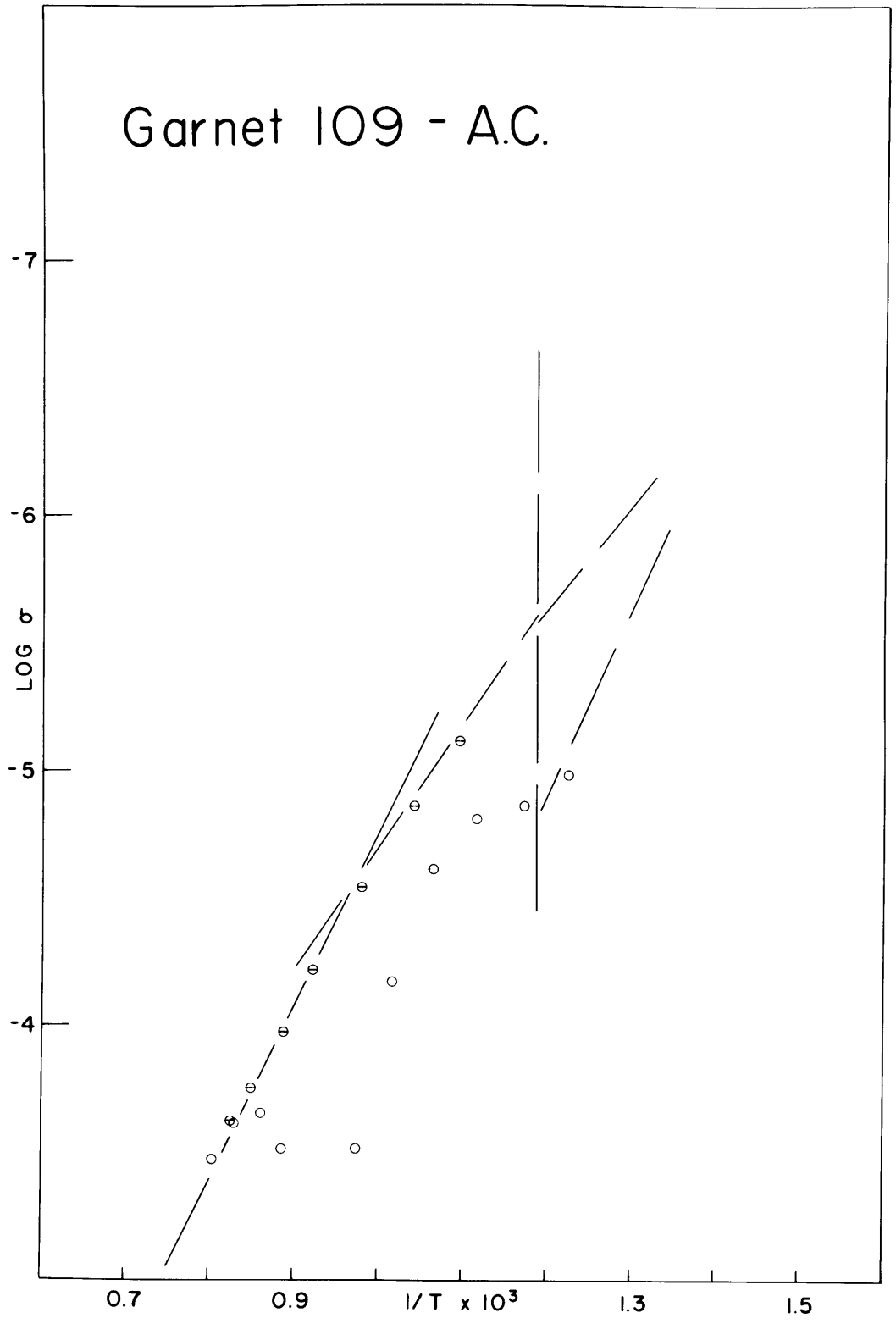

Fig. A-25

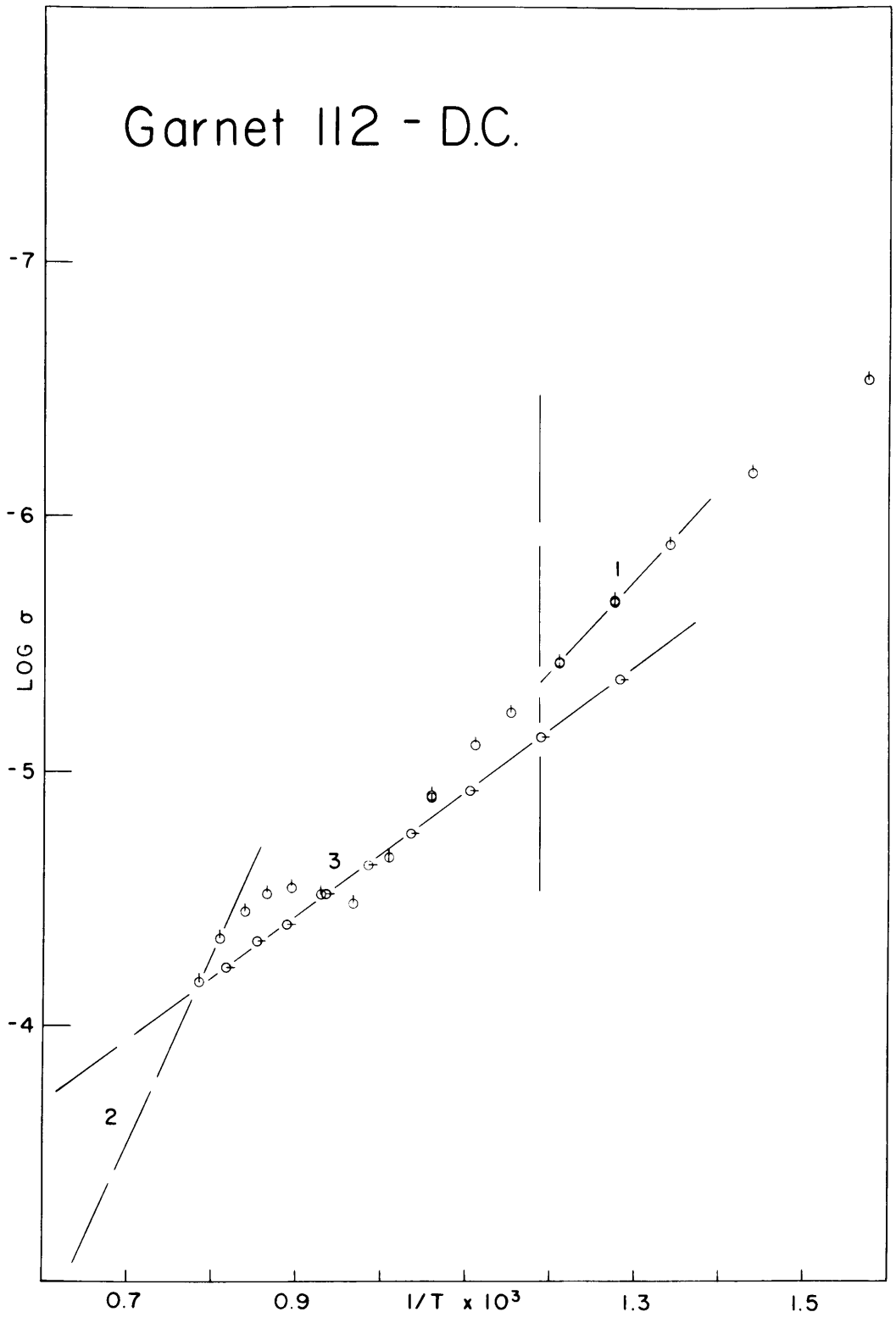

Fig. A-26

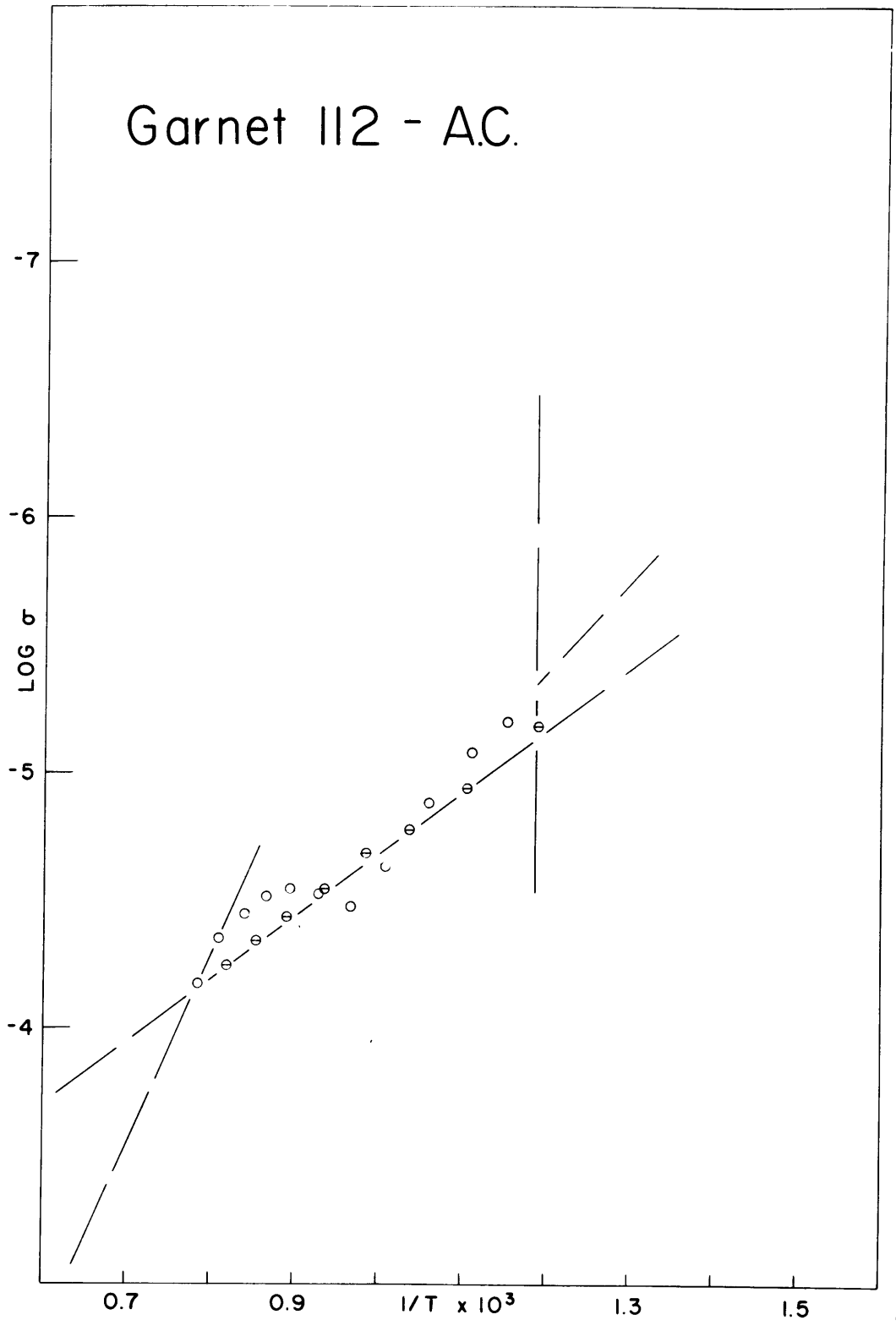

Fig. A-27

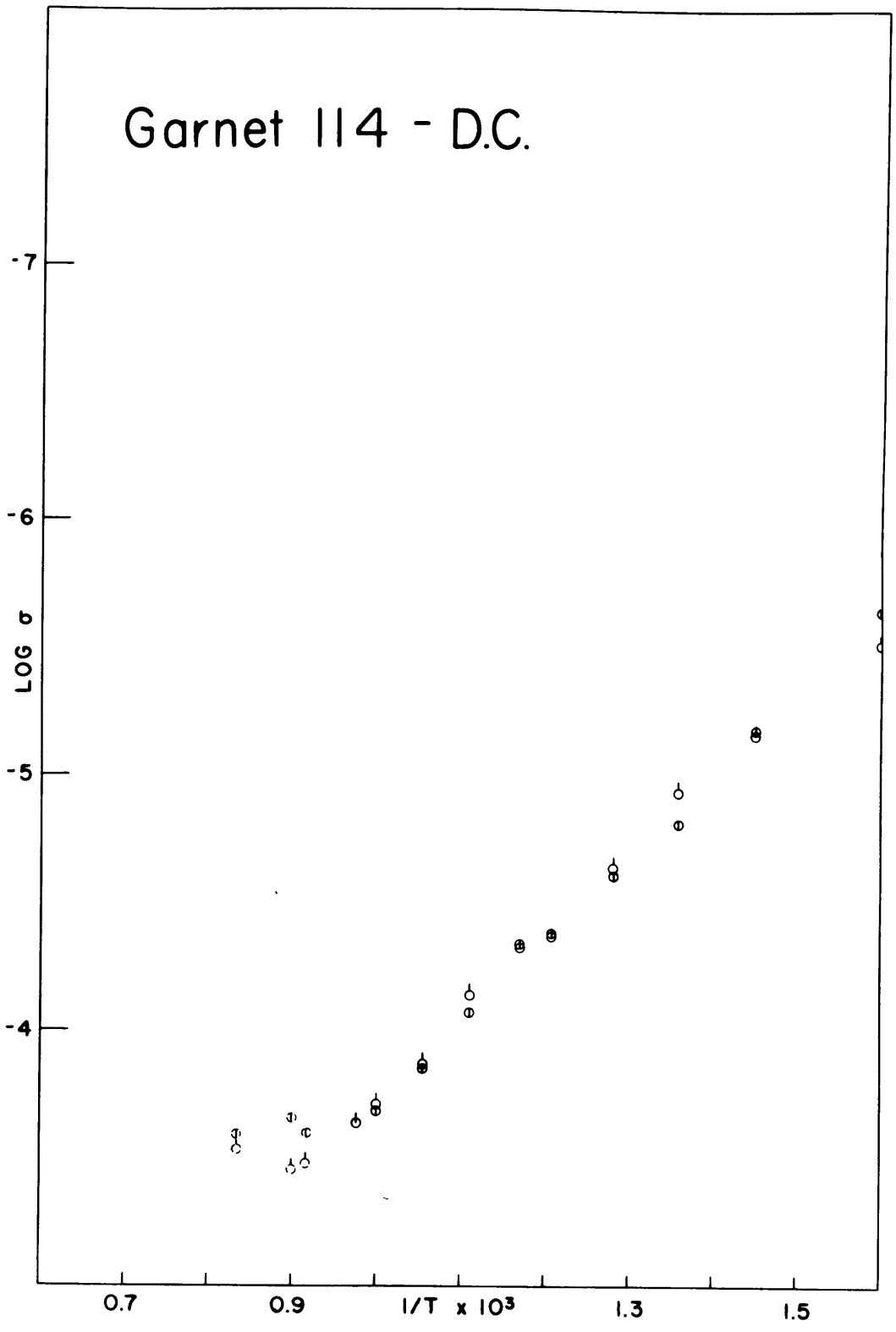

Fig. A-28

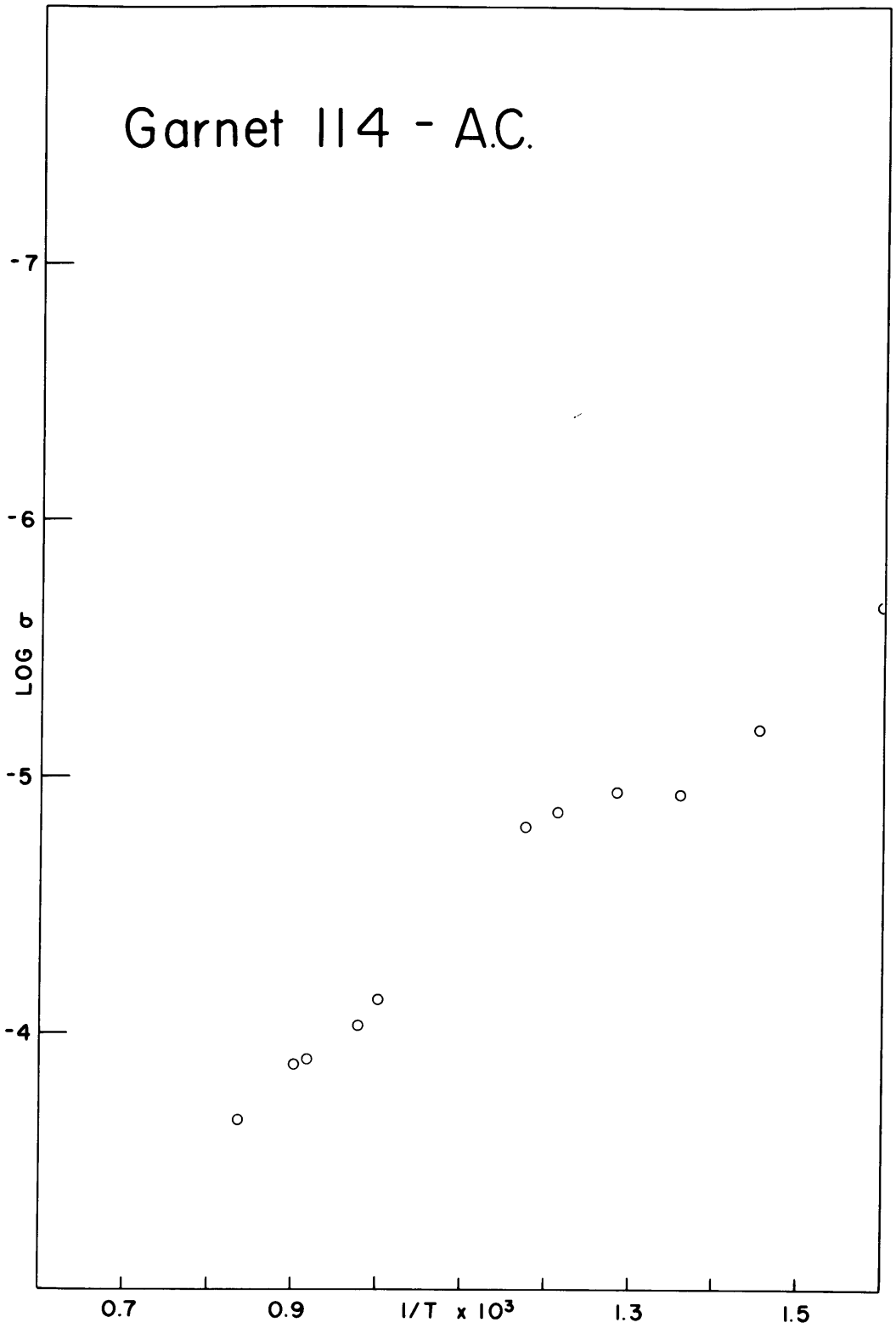

Fig. A-29

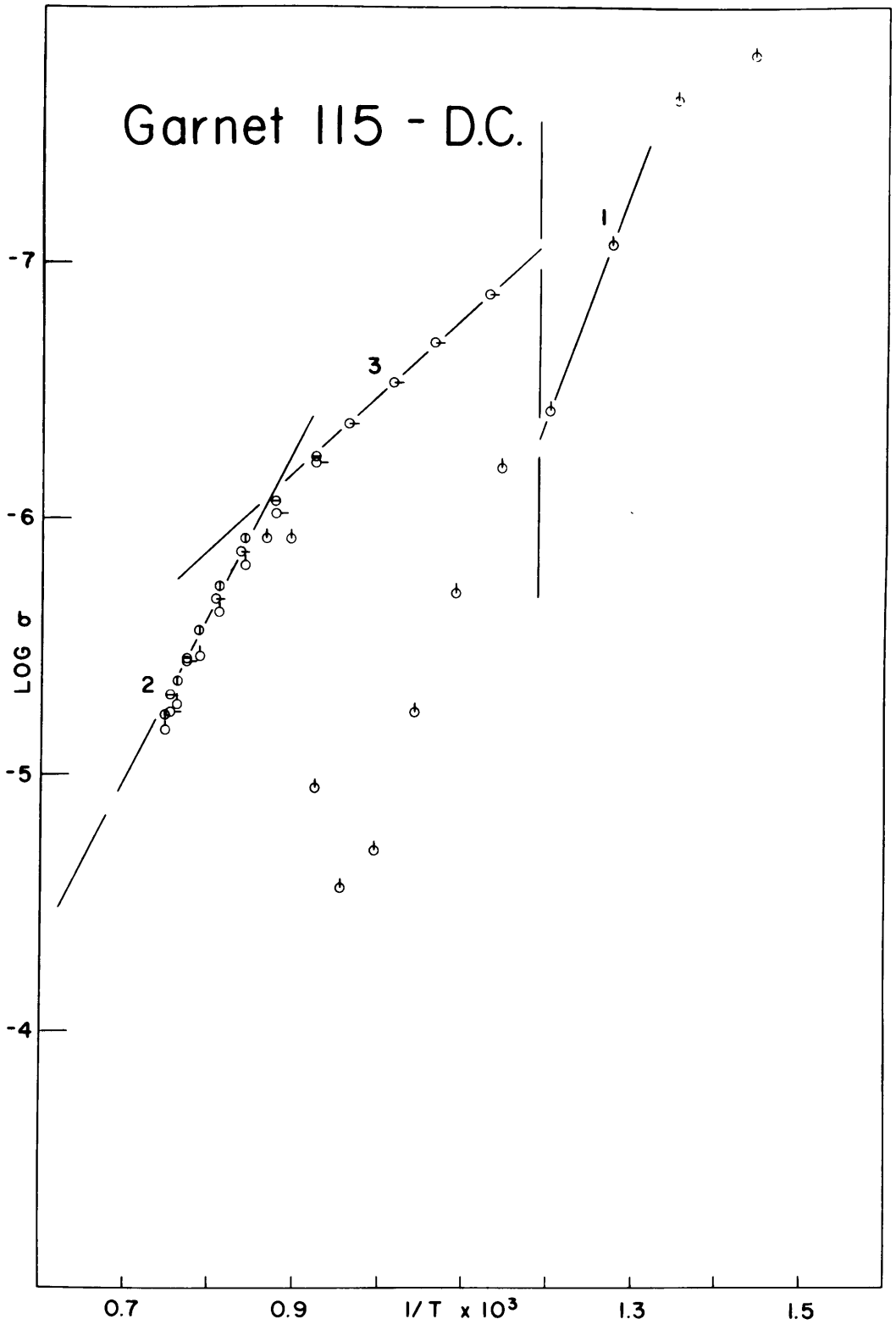

Fig. A-30

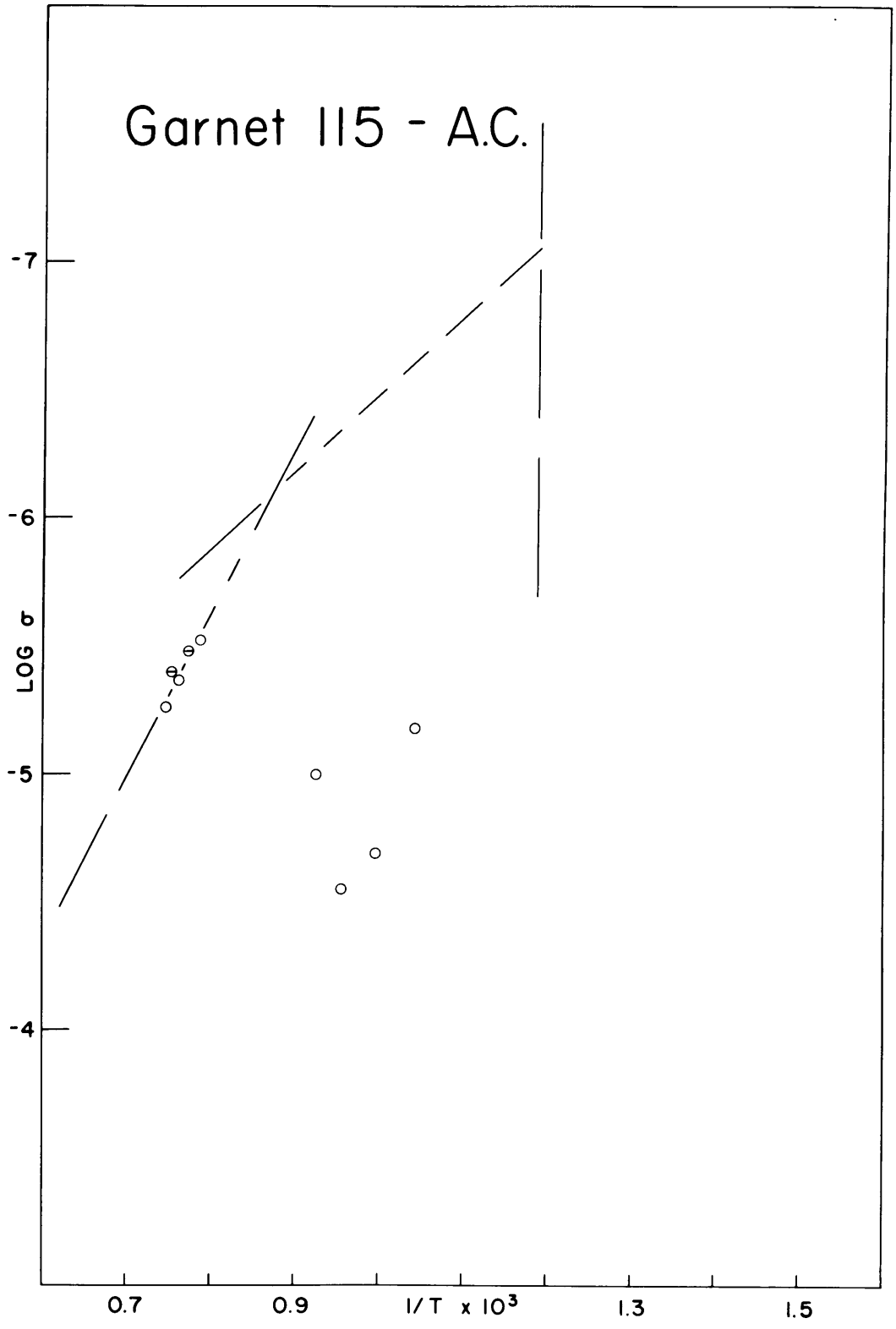

Fig. A-31

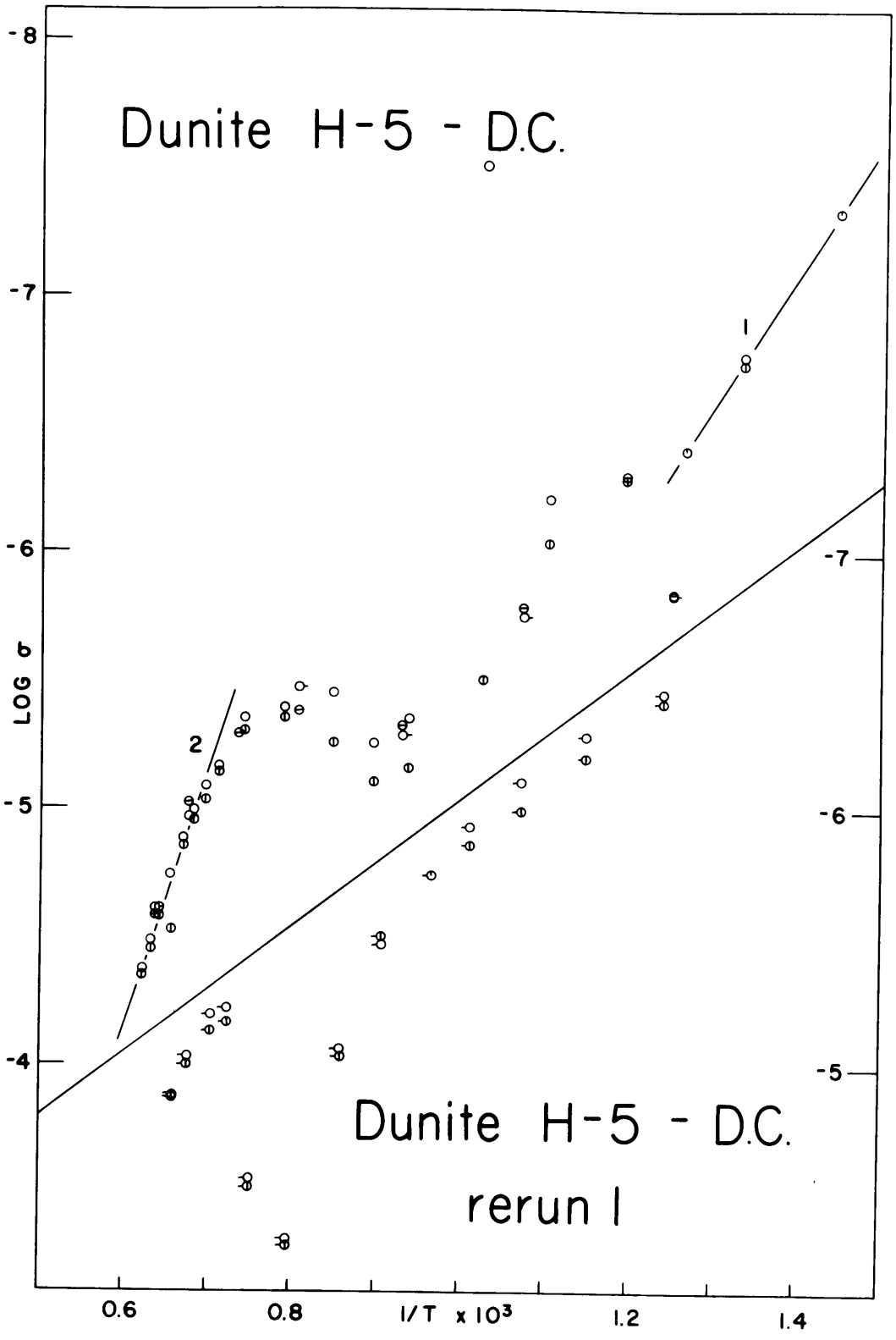
Dunite H-5 - D.C.
-8
-7
-6
-5
-4
LOG σ
1
2
-7
-6
-5
Dunite H-5 - D.C.
rerun 1
0.6
0.8
1/T x 10³
1.2
1.4

Fig. A-32

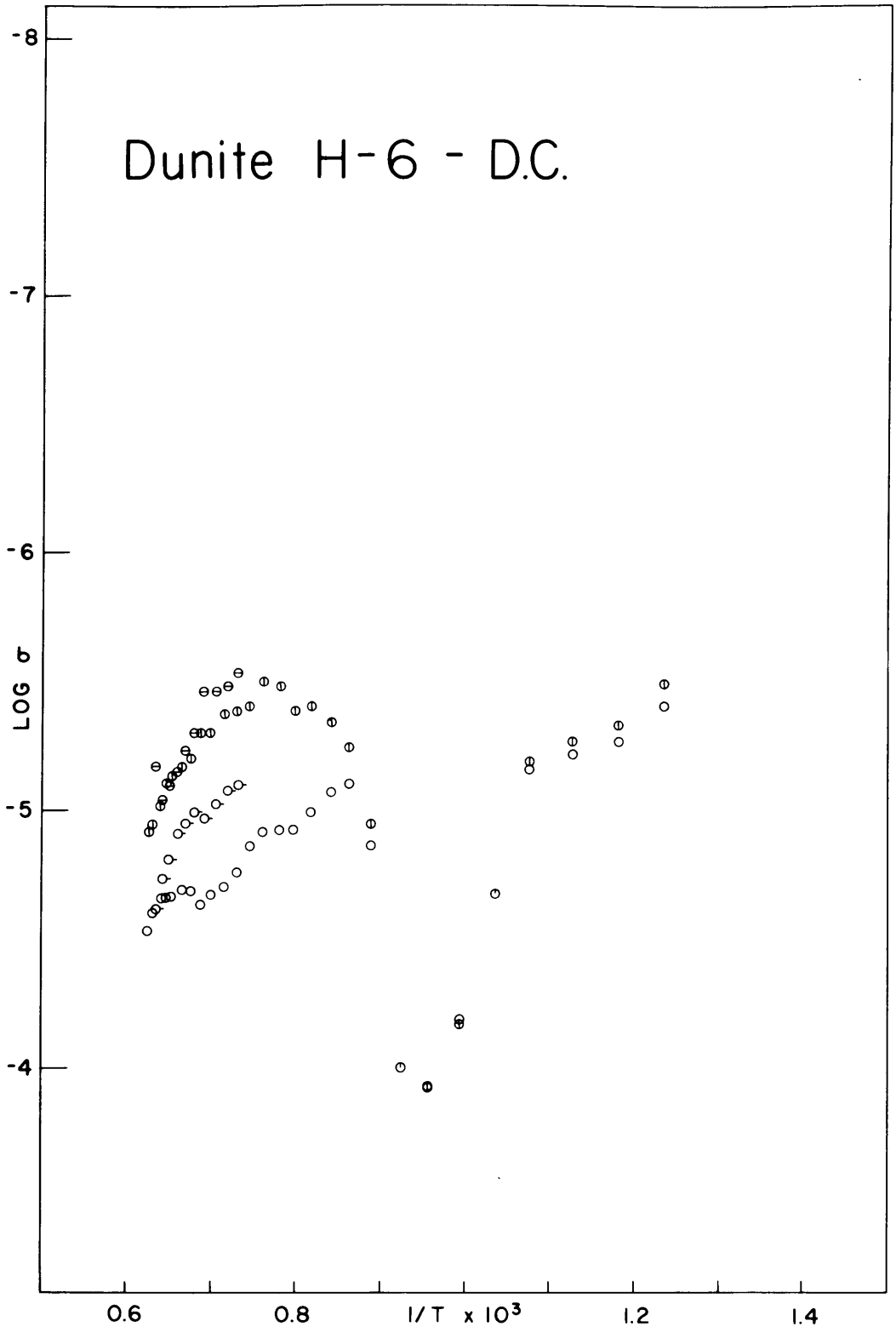

Fig. A-33

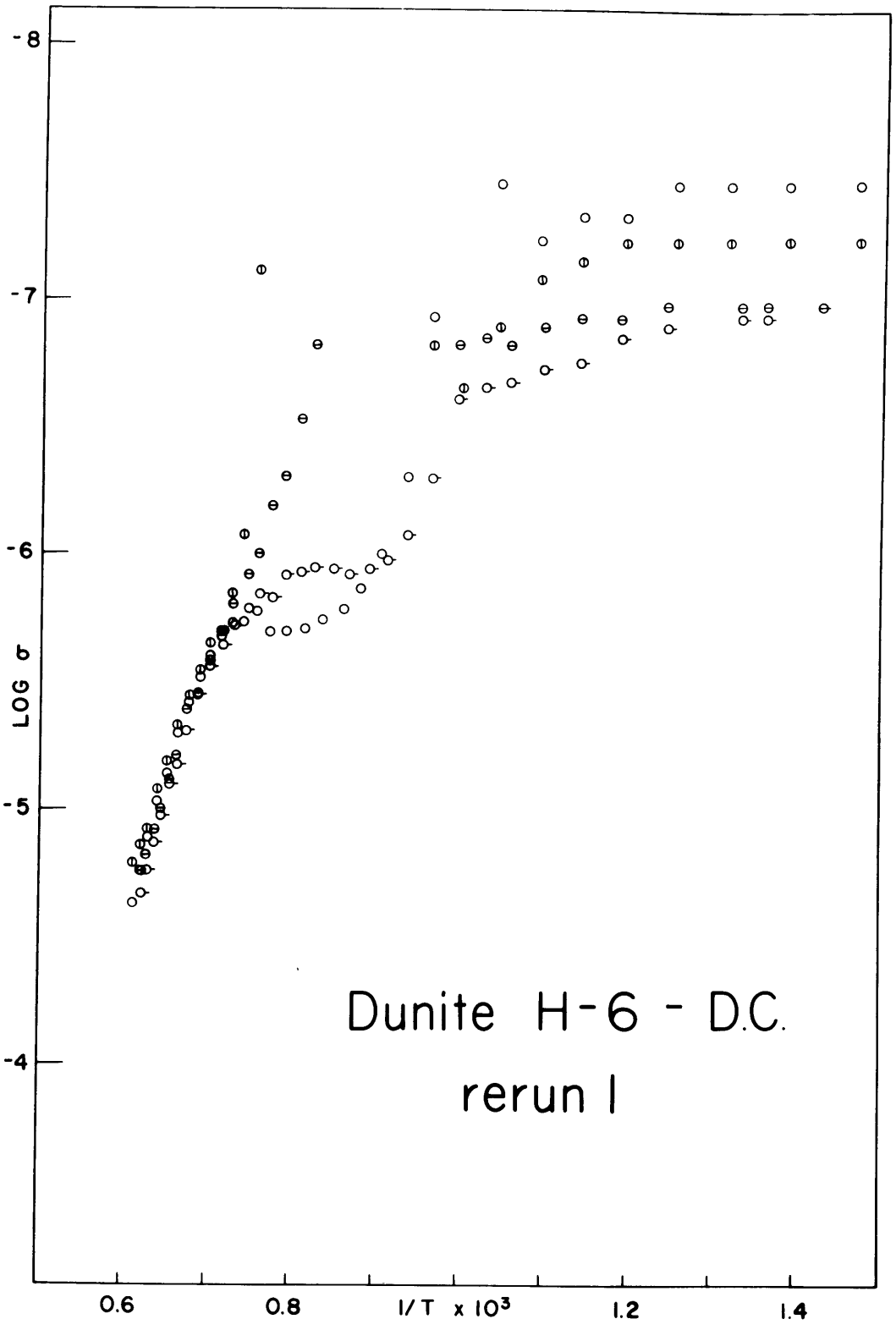

Fig. A-34

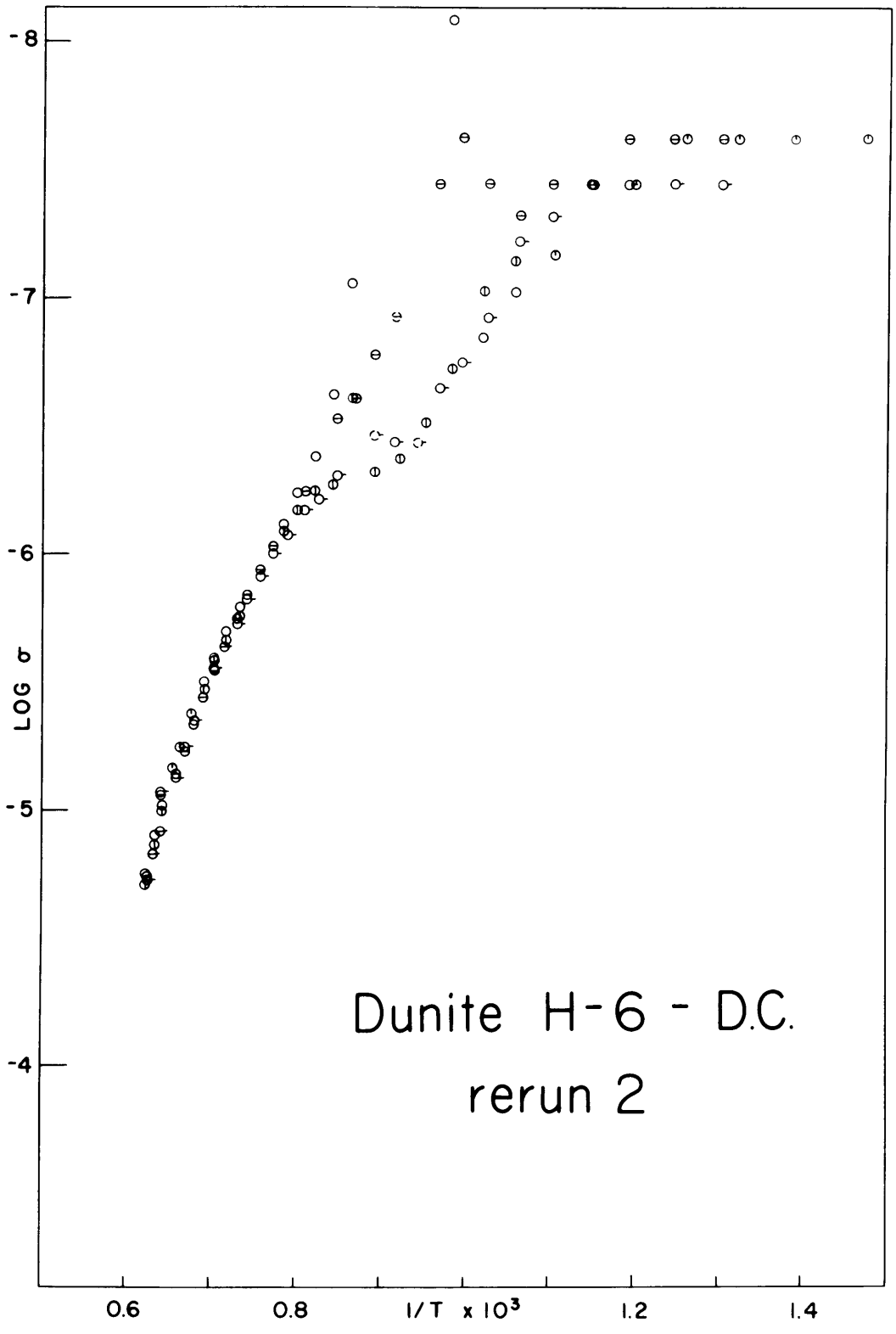

Fig. A-35

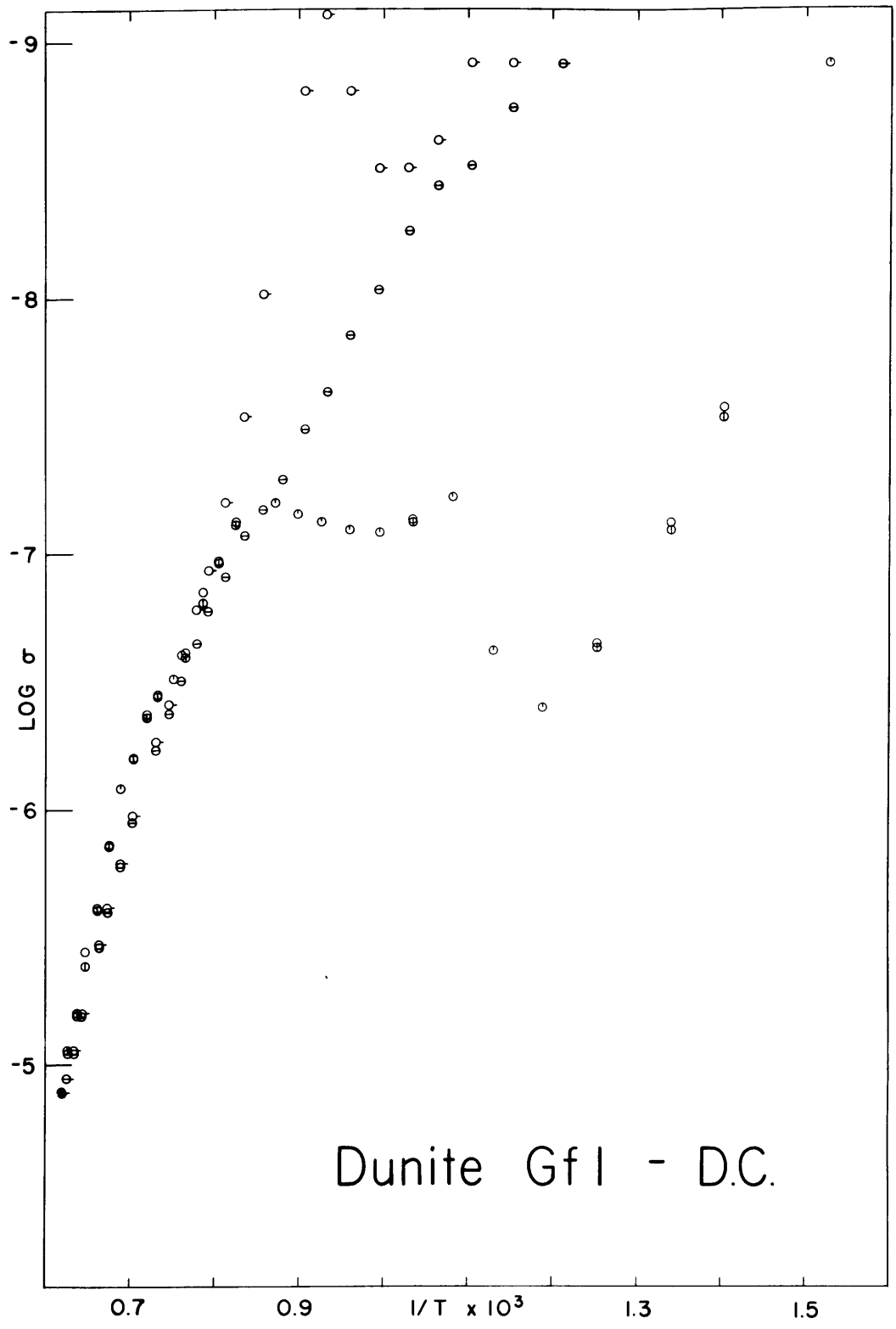

Fig. A-36

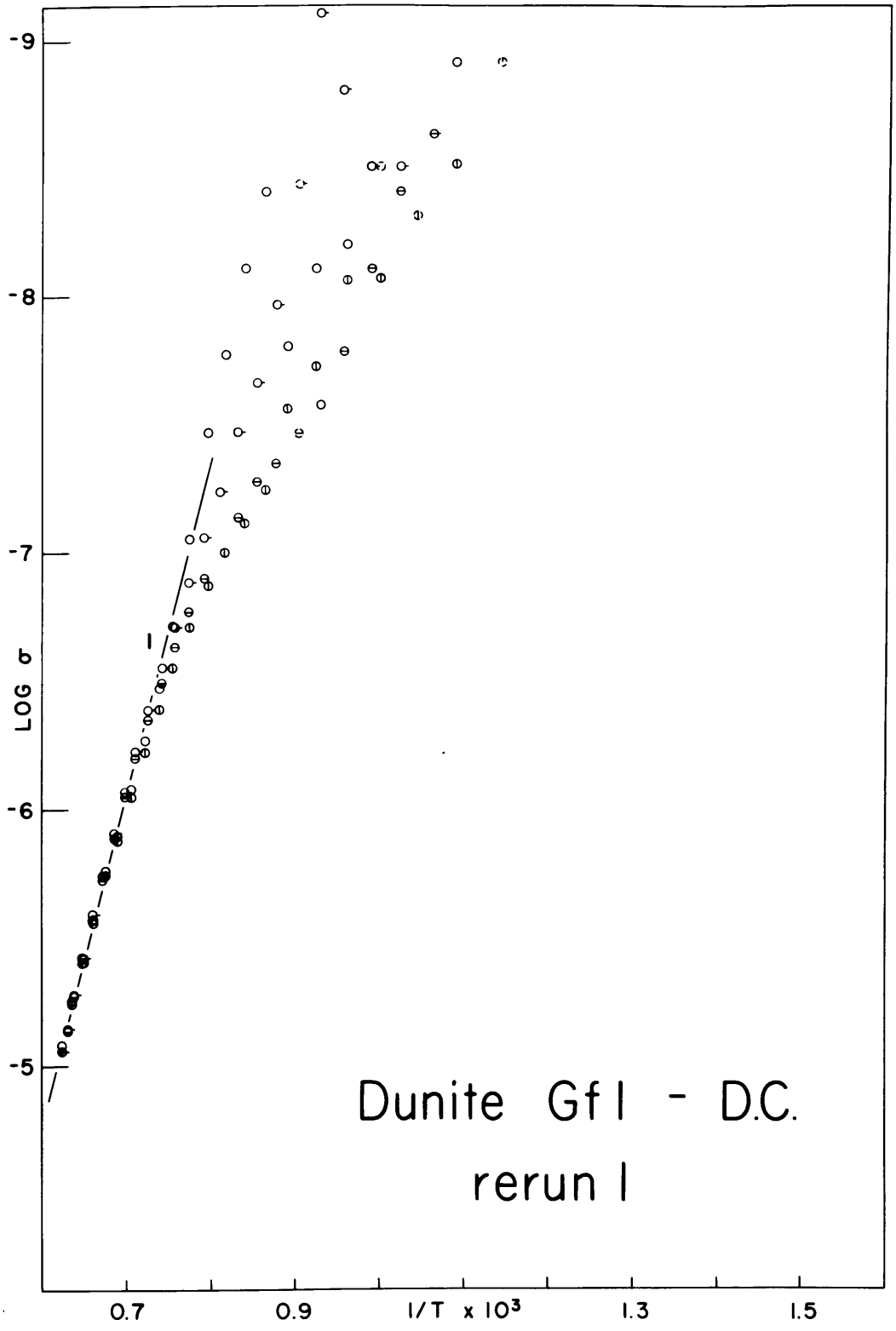

Fig. A-37

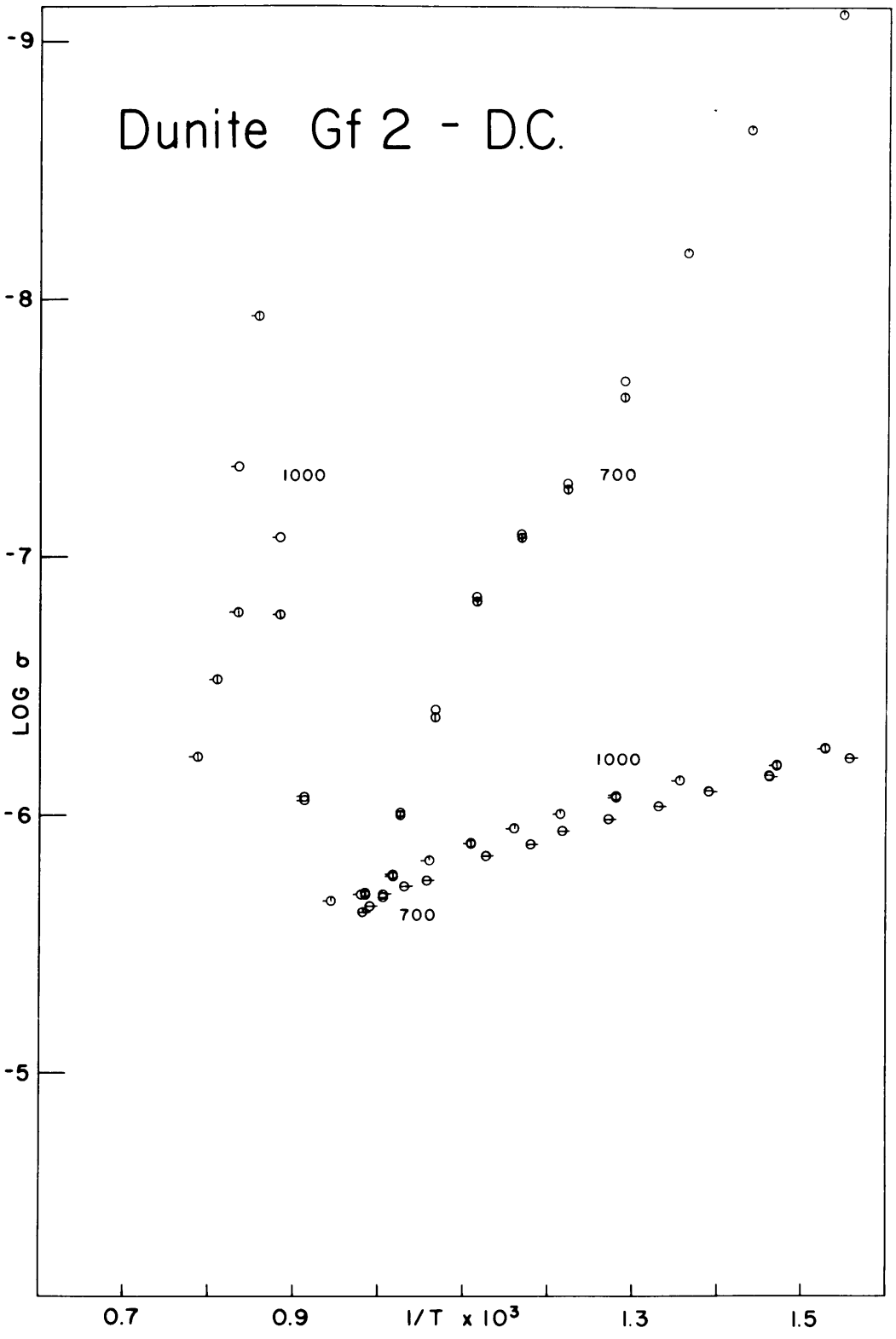

Fig. A-38

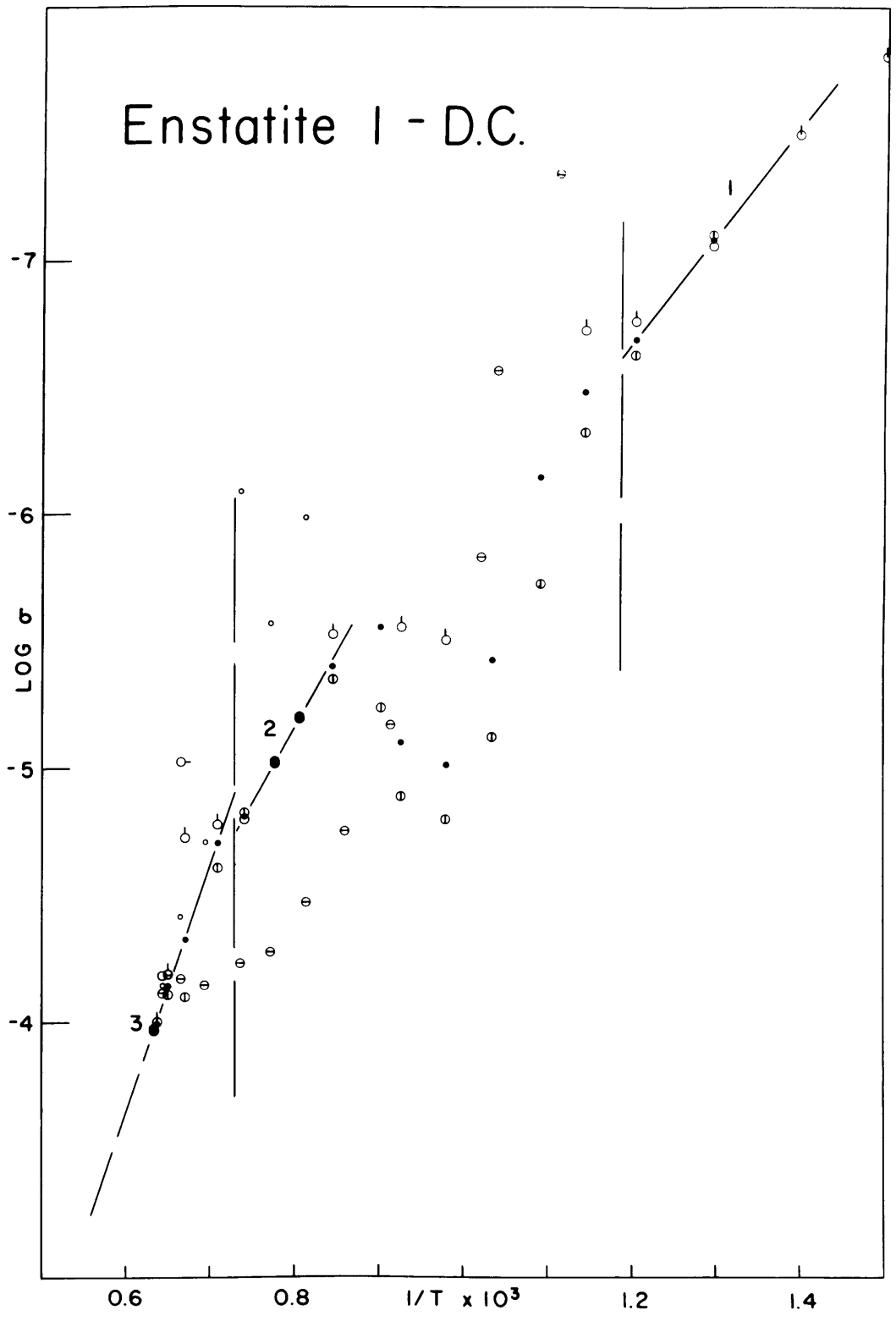

Fig. A-39

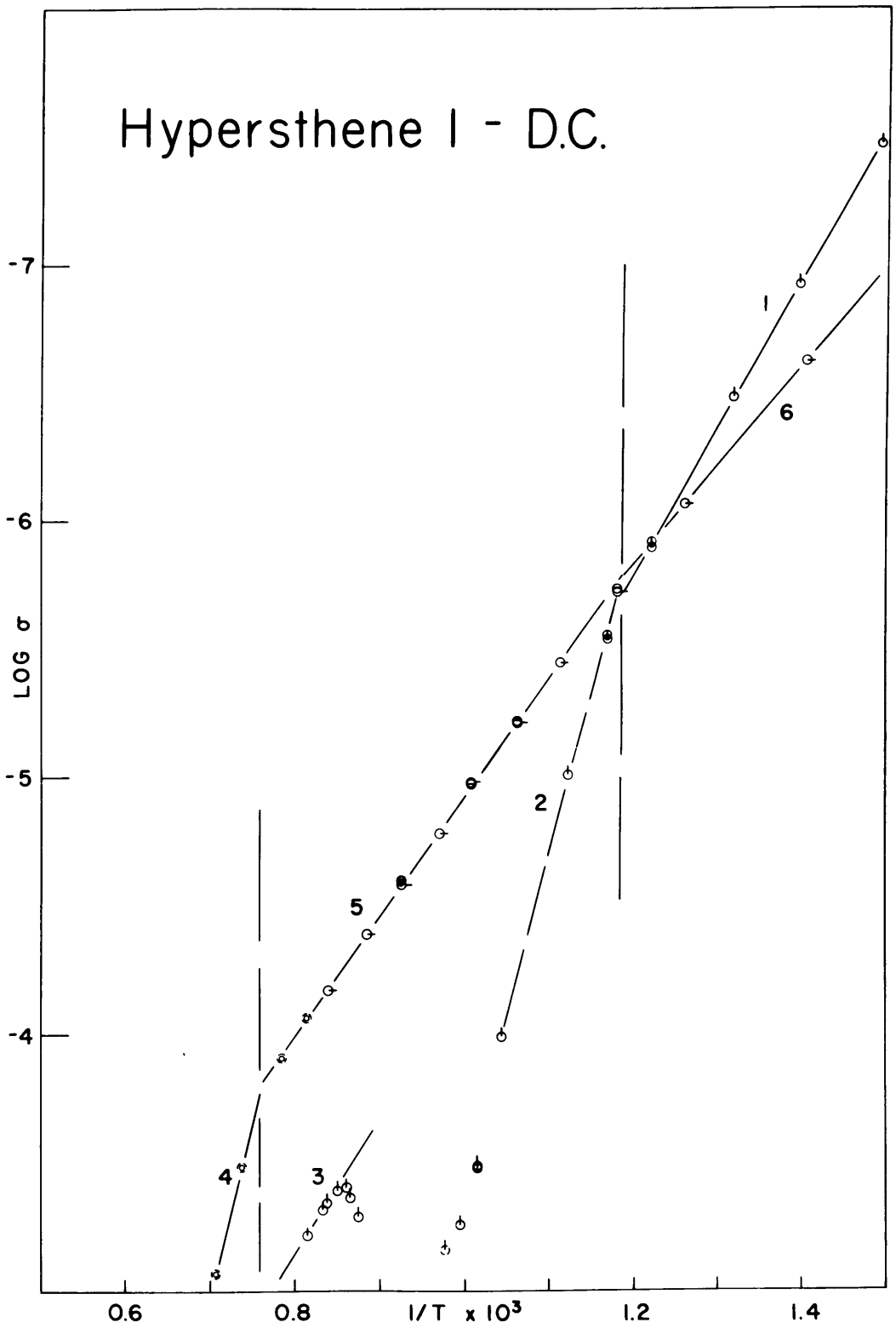

Fig. A-40

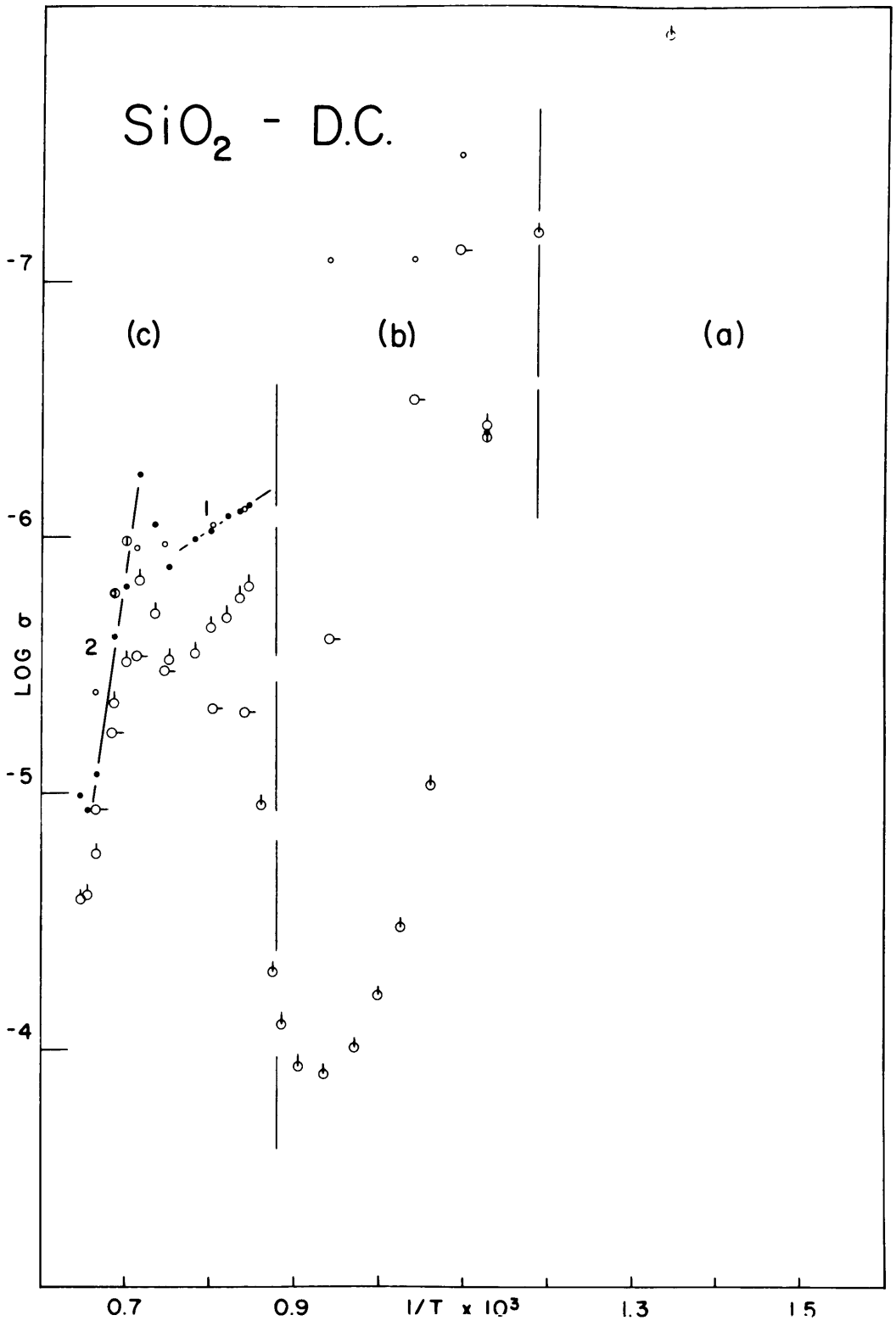

Fig. A-41

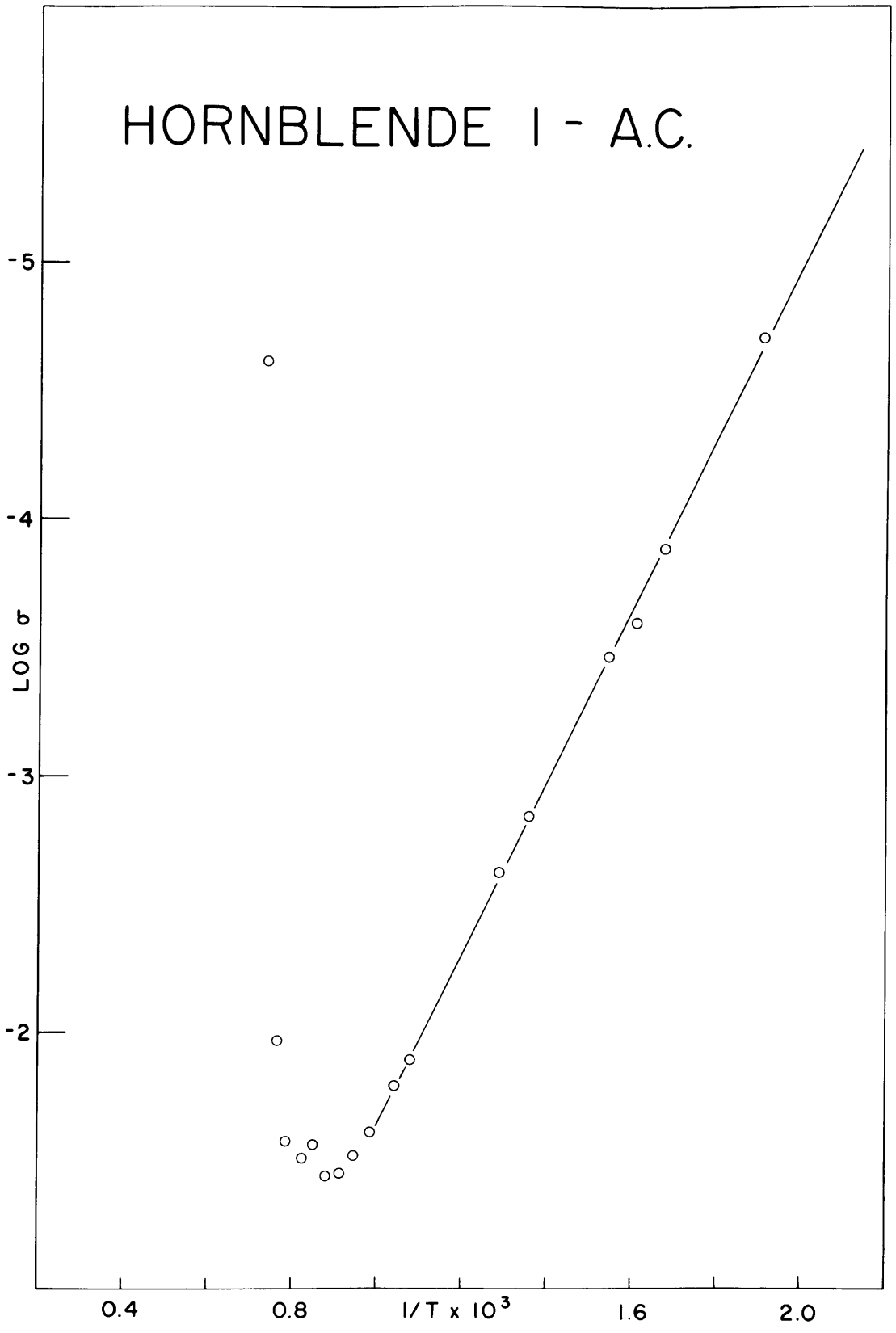

Fig. A-42

APPENDIX B

DERIVATION OF THE EQUATIONS FOR TEMPERATURES AT DEPTH

The equations resulting in the temperature disbributions of Figure XI-1 may be derived in a straightforward manner. The steady-state heat conductivity equation for a half-bounded region is given by (Carslaw and Jaeger, 1959):

$$\frac{d}{dx}\left(K\frac{dT}{dx}\right) = A'$$

where A^1 is the heat generation and K is the thermal conductivity. If we let the subscript "i" designate a particular layer, then:

$$K_i \frac{dT_i}{dx_i} = -A_i' + C_i = -\rho_i A_i + C_i$$

where ρ_i is the density, A_i is the heat generation per unit mass, and C_i is a constant of integration determined by the boundary conditions:

$$K_1 \frac{dT_1}{dx} = H_1 \qquad \text{(at the surface)}$$

where H_1 is the heat flow at the surface, and

$$K_{i-1} \left.\frac{dT_{i-1}}{dx}\right|_{x=x_{i-1}} = K_i \left.\frac{dT_i}{dx}\right|_{x=x_{i-1}}$$

Therefore, for the interior of the first layer, we have:

$$\frac{dT_1}{dx} = \frac{H-\rho_1 A_1 x}{K_1}$$

for the second layer:

$$\frac{dT_2}{dx} = \frac{H-\rho_2 A_2 x - (\rho_1 A_1 - \rho_2 A_2)x_1}{K_2}$$

and so on to the n^{th} layer:

$$\frac{dT_n}{dx} = \frac{H - \rho_n A_n x - \sum_{i=2}^{n} (\rho_{i-1} A_{i-1} - \rho_i A_i) x_{i-1}}{K_n}$$

Assuming that the surface temperature is zero, and integrating again, we obtain the temerature at any given depth in a particular layer. For a layered medium, the temperature in the first layer is given by:

$$T_1 = \frac{(H - \tfrac{1}{2}\rho_1 A_1 x)x}{K_1}$$

the temperature in the second layer by:

$$T_2 = \frac{(H - \tfrac{1}{2}\rho_1 A_1 x_1)x_1}{K_1} + \frac{(H - \rho_1 A_1 x_1)(x - x_1)}{K_2} - \frac{\tfrac{1}{2}\rho_2 A_2 (x - x_1)^2}{K_2}$$

and the temperature in the third layer by:

$$T_3 = \frac{(H - \tfrac{1}{2}\rho_1 A_1 x_1)x_1}{K_1} + \frac{(H - \rho_1 A_1 x_1)(x_2 - x_1)}{K_2} - \frac{\tfrac{1}{2}\rho_2 A_2 (x_2 - x_1)^2}{K_2} + \frac{[H - (\rho_1 A_1 - \rho_2 A_2)x_1 - \rho_2 A_2 x_2](x - x_2)}{K_3} - \frac{\tfrac{1}{2}\rho_3 A_3 (x - x_2)^2}{K_3}$$

BIOGRAPHICAL NOTE

The author was born in Niagara Falls, New York on June 29, 1930. After graduating from Niagara Falls High School in 1948, he was employed for a year by Auto-Lite Battery Corporation before entering Michigan State University in 1949. There, he received the B.S. degree in Geology in 1953 and proceeded through Graduate School. In 1954, Michigan State University awarded him the M.S. degree in Geology and upon graduation, he was employed as a petroleum geologist in the Oklahoma City District of Magnolia Petroleum Company. After serving in the employ of this company for approximately two years, he was awarded one of their generous fellowships and entered the Graduate School at M.I.T. in the fall of 1956. Since October, 1960, he has been employed as a Senior Research Technologist in the Reservoir Mechanics and Rock Properties Section at the Field Research Laboratories of Socony-Mobil Oil Company in Dallas, Texas (the parent company of the former Magnolia Petroleum Company).

BIBLIOGRAPHY

Adams, L. H., Temperatures at moderate depths within the earth, J. Washington Acad. Sci., 14, 459, 1924.

Ahrens, L. H., Spectrochemical Analysis, Addison-Wesley, Cambridge, 1950.

Balchan, A. S., and H. G. Drickamer, The effect of pressure on the spectra of olivine and garnet, J. Appl. Phys., 30, 1446, 1959.

Birch, F., Elasticity and constitution of the earth's interior, J. Geophys. Res., 57, 227, 1952.

Birch, F., and H. Clark, The thermal conductivity of rocks and its dependence upon temperature and composition, Am. J. Sci., 238, 529, 613, 1940.

Birch, F., J. F. Schairer, and H. C. Spicer, Handbook of Physical Constants, Geol. Soc. Amer., Spec. Paper, 36, 243, 1942.

Bowen, N. L., and J. F. Schairer, The system MgO - FeO - SiO_2, Am. Jour. Sci., 5th Ser., 29, 174, 1935.

Bullard, E. C., C. Freedman, H. Gellman, and J. Nixon, The Westward drift of the earth's magnetic field, Phil. Trans. Roy. Soc., A, 243, 67, 1950.

Bullard, E. C., A. E. Maxwell, and R. Revelle, Heat flow through the deep sea floor, in Advances in Geophysics, 3, H. E. Lansberg, editor, Academic Press, New York, 1956.

Cantwell, T., Detection and analysis of low frequency magnetotelluric signals, Ph. D. thesis, Massachusetts Institute of Technology, 1960.

Carslaw, H. S., and J. C. Jaeger, Conduction of Heat in Solids, 2nd Ed., Oxford University Press, 1959.

Clark, S. P., Radiative transfer in the earth's mantle, Trans. Am. Geophys. Union, 38, 931, 1957.

Coster, H. P., The electrical conductivity of rocks at high temperatures, Monthly Notices Roy. Astron. Soc., Geophys. Suppl., 5, 193, 1948.

Coughlin, J. P., E. G. King, and K. R. Bonnickson, High temperature heat contents of ferrous oxide, magnetite, and ferric oxide, J. Amer. Chem. Soc., 73, 3891, 1951.

Cronemeyer, D. C., Electrical and optical properties of rutile single crystals, Phys. Rev., 87, 876, 1952.

Dana, E. S., A Textbook of Mineralogy, 4th ed., revised by W. E. Ford, John Wiley and Sons, New York, 1951.

Darken, L. S., and R. W. Gurry, The system iron-oxygen, II, Equilibrium and thermodynamics of liquid oxide and other phases, J. Amer. Chem. Soc., 68, 798, 1946.

Darken, L. S., and R. W. Gurry, Physical Chemistry of Metals, McGraw-Hill, New York, 1953.

Engelhard, E., Electrical and optical behaviors of semiconductors (IX), Ann. d. Physik, 17, 501, 1933.

Eugster, H. P., Annual Report of the Director of the Geophysical Laboratory, 1956-1957, Carnegie Inst. Wash. Year Book, 56, 161, 1957.

Eugster, H. P., Reduction and oxidation in metamorphism, in Researches in Geochemistry, P. H. Abelson, editor, John Wiley and Sons, New York, 1959.

Fairbairn, H. S., and others, A cooperative investigation of precision and accuracy in chemical, spectrochemical, and modal analysis of silicate rocks, U. S. Geol. Survey Bull., 176, 1951.

Frondel, C., and C. S. Hurlburt, Determination of the atomic weight of Si, J. Chem. Phys., 23, 1215, 1955.

Gutenberg, B., Internal Constitution of the Earth, 1st ed., McGraw-Hill, New York, 1939.

Gutenberg, B., Crustal layers of the continents and oceans, Bull. Geol. Soc. Amer., 62, 427, 1951.

Hess, H. H., and E. P. Henderson, The Moore County meteorite: A further study with a comment on its primordial environment, Amer. Min., 34, 494, 1949.

Hughes, H., The electrical conductivity of the earth's interior, Ph. D. thesis, University of Cambridge, 1953.

Hughes, H., The pressure effect on the electrical conductivity of peridot, J. Geophys. Research, 60, 187, 1955.

Hughes, H., The conductivity mechanism in the earth's mantle (abstr.), J. Geophys. Research, 64, 1108, 1959.

Humphrey, G. L., E. G. King, and K. K. Kelley, Thermodynamic values of FeO, U. S. Bur. Mines Rept. of Investigation, 4870, 1952.

Jacobs, J. A., The earth's interior, Encyl, Phys., 47, (Geophysics, v. 1), Springer-Verlag, Berlin, 364, 1956.

Jaycox, E. K., Spectrochemical analysis of ceramics and other non-metallic materials, J. Opt. Soc. Amer., 37, 162, 1947.

Jeffreys, H., The Earth, 2nd ed., Cambridge University Press, 1929.

Juse, W. P., and B. W. Kurtschatow, Electrical conductivity of Cu_2O, Phys. Zeits. d. Sowjetunion, 2, 453, 1933.

Keith, M. L., and J. F. Schairer, Stability field of sapphirine in the system $MgO - Al_2O_3 - SiO_2$, Jour. Geol., 60, 182, 1952.

Kelley, K. K., U. S. Bur. Mines Bull., 393, 1936.

Kelley, K. K., Specific heats of low temperatures of Mg orthosilicate and Mg metasilicate, J. Amer. Chem. Soc., 65, 339, 1943.

Kelley, K. K., U. S. Bur. Mines Bull., 476, 1949.

Kelley, K. K., Theoretical metallurgy (x), high temp. heat content, heat capacity, and entropy data for inorg. compounds, U. S. Bur. Mines Bull., 477, 1950.

Kraus, E. H., W. F. Hunt, and L. S. Ramsdell, Mineralogy, 4th ed., McGraw-Hill, New York, 1951.

Kuhn, W., and A. Rittmann, Uber den Zustand des Erdinnern und seine Enstehung aus einem homogenen Urzustand, Geol, Rundschau, 32, 215, 1941.

Lahiri, B. N., and A. T. Price, Electromagnetic induction in non-uniform conductors, and the determination of the conductivity of the earth from terrestrial magnetic variations, Phil. Trans. Roy. Soc. London, Ser. A, 237, 509, 1939.

Long, D., Effects of pressure on the electrical properties of semi-conductors, Phys. Rev., 101, 1256, 1956.

Lovering, J. F., Temperatures and pressures within a typical parent meteoric body, Geochim, Cosmochim. Acta, 12, 253, 1957.

Lovering, J. F., The nature of the Mohorovicic discontinuity, Trans. Am. Geophys. Union, 39, 947, 1958.

Lubimova, H. A., Thermal history of the earth with consideration of the variable thermal conductivity of the mantle, Geophys. J. Roy. Astron. Soc., 1, 115, 1958.

Lyubimova, E. A., On the temperature gradient in the upper layers of the earth and on the possibility of an explanation of the low-velocity layers, Bull, Acad, Sci.,.U.S.S.R., Geophysics series, AGU English Translation, 1300, 1959.

MacDonald, G. J. F., Calculations on the thermal history of the earth, J. Geophys. Research, 64, 1967, 1959.

Mason, B., Principles of Geochemistry, John Wiley and Sons, New York, 1952.

Mott, N. F., and R. W. Gurney, Electronic Processes in Ionic Crystals, Clarendon Press, Oxford, 1953.

Muan, A. F., J. Amer. Ceramic Soc., 40, 420, 1957.

Muan, A., and E. F. Osborn, Phase equilibria at liquidus temperatures in the system MgO - FeO - Fe_2O_3 - SiO_2, J. Amer. Ceram. Soc., 39, 121, 1956.

Norton, F. J., Dissociation pressures of iron and copper oxides, General Electric Report 55 - R1 - 1248, 1955.

Orr, R. L., High temperature heat contents of Mg orthosilicate and ferrous orthosilicate, J. Amer. Chem. Soc., 75, 528, 1953.

Paul, W., and G. L. Pearson, Pressure dependence of the resistivity of silicon, Phys. Rev., 98, 1755, 1955.

Poldervaart, A., Chemistry of the earth's crust, Geol. Soc. Amer., Spec. Paper, 62, 119, 1955.

Richardson, F. D., and J. H. E. Jeffes, The thermodynamics of substances of interest in iron and steel making from o° C to 2400° C, I, Oxides, J. Iron Steel Inst. (London), 160, 261, 1948.

Rikitake, T., Electromagnetic shielding within the earth and geomagnetic secular variation, Bull, Earthquake Research Inst., Tokyo Univ., 29, 263, 1951.

Rikitake, T., Electrical conductivity and temperature in the earth, Bull. Earthquake Res. Inst., Tokyo Univ., 30, 13, 1952.

Robertson, E. C., F. Birch, and G. J. F. MacDonald, Experimental determination of jadeite stability relations to 25,000 bars, Am. Jour. Sci., 255, 115, 1957.

Runcorn, S. K., and D. C. Tozer, The electrical conductivity of olivine at high temperatures and pressures, Ann. geophys., 11, 98, 1955.

Shapiro, L., and W. W. Brannock, Rapid analysis of silicates rocks, U.S. Geol. Survey Bull., 1036-C, 19, 1956.

Spenke, E., Electronic Semiconductors, Translated with additions by D. A. Jenny et al., McGraw-Hill, New York, 1958.

Stull, D. R., and G. C. Sinke, Thermodynamic Properties of the Elements, Amer. Chem. Soc. Washington, 1956.

Torgeson, D. R., and T. G. Sahama, HF solution calorimeter and the determination of the heats of formation of Mg_2SiO_4, $MgSiO_4$, and $CaSiO_3$, J. Amer. Chem. Soc., 70, 2156, 1948.

Tozer, D. C., The electrical properties of the earth's interior, in Physics and Chemistry of the Earth, III, Ahrens et al., editors, Pergamon Press, London, 1959.

Turner, F. J., and J. Verhoogen, Igneous and Metamorphic Petrology, McGraw-Hill, New York, 1951.

Urey, H. C., The Planets, Yale University Press, 1952.

Verhoogen, J., Temperatures within the earth, in Physics and Chemistry of the Earth, I, Ahrens et al., editors, Pergamon Press, London, 1956.